

Charles University

Faculty of Science

Study programme: Biology

Branch of study: Experimental Plant Biology



Bc. Božena Klodová

Studying dimer formation and effectors of *Arabidopsis thaliana*
nascent polypeptide-associated complex

Studie tvorby dimerů komplexu asociovaného s nascentním polypeptidem
a jeho efektorů v huseníčku rolním

Diploma thesis

Supervisor: RNDr. Jan Fíla, Ph.D.

Consultant: Assoc. Prof. David Honys, Ph.D.

Prague, 2019

Declaration

I hereby declare that I completed this master thesis independently. It documents my own work if not explicitly otherwise mentioned. I have properly acknowledged and cited all resources used. The thesis is not subject of any other defending procedure.

Prohlášení

Prohlašuji, že jsem závěrečnou práci zpracovala samostatně a že jsem uvedla všechny použité informační zdroje a literaturu. Tato práce ani její podstatná část nebyla předložena k získání jiného nebo stejného akademického titulu.

V Praze, 8. 8. 2019

.....

The presented work was carried out at the Laboratory of Pollen Biology, Institute of Experimental Botany ASCR, v.v.i., Prague 6, Czech Republic.

Acknowledgements

I would like to acknowledge my supervisor RNDr. Jan Fíla, Ph.D. for patient guidance during the experimental work and endless discussion thorough my thesis preparation. Many thanks belong to my consultant Assoc. Prof. David Honys Ph.D. for meaningful comments to my research. I would also like to thank Said S. Hafidh, Ph.D. and Ljudmilla Timofejeva, Ph.D. for introducing me to Bimolecular fluorescence complementation assay. Also, many thanks belong to Ing. Miloslav Juříček, CSc. for assistance on transcriptomic data analyses by providing basic scripts. Further, I would like to acknowledge Ing. Kateřina Malínská, Ph.D. for introduction to confocal microscopy and Ing. Karel Müller, PhD. for assistance on qRT-PCR procedure. I would like to thank all members of Laboratory of Pollen Biology for persistent help in the laboratory.

Finally, I would also like to gratefully acknowledge the financial support from the Czech Ministry of Education, Youth and Sports (LTC18043) and the Czech Science Foundation (19-01723S). Further, the work was supported from European Regional Development Fund-Project “Centre for Experimental Plant Biology” (No. CZ.02.1.01/0.0/0.0/16_019/0000738).

Abstract

The development of plant flowers represents a complex process controlled by numerous mechanisms. The creation of double homozygous mutant of both β subunits (sometimes also referred to as *basic transcription factor 3*) of nascent polypeptide associated complex in *Arabidopsis thaliana* (further referred to as *nacB1 nacB2*) caused quite a strong defective phenotype including abnormal number of flower organs, shorter siliques with a reduced seed set, and inferior pollen germination rate together with a lower ovule targeting efficiency. Previously, NAC complex was described to be formed as a heterodimer composed of an α - and β -subunit, which binds ribosome and acts as a chaperone in *Saccharomyces cerevisiae*. In plants, NACB is connected to stress tolerance and to plant development as a transcription regulator. However, little is known of NAC heterodimer function in plants. In this thesis, yeast two hybrid system (Y2H) and bimolecular fluorescence complementation (BiFC) assays were used to verify the NAC heterodimer formation in *A. thaliana* and to establish any potential interaction preferences between both NACB paralogues and five NAC α paralogues.

To deepen the understanding about molecular mechanisms behind the *nacB1 nacB2* phenotype, flower bud transcriptome of the *nacB1 nacB2* double homozygous mutants was analysed resulting in 1965 differential expressed genes (DEG) when compared to Columbia-0 (Col-0) wild type flower bud transcriptome. Two notable groups of genes emerged from the obtained DEGs list. The first one was represented by genes connected to stress response, consisting of upregulated heat shock proteins and downregulated drought responsive genes. The second group consisted of downregulated genes connected to male germ-line development, namely sperm cell differentiation and pollen tube growth and regulation.

Key words:

Pollen, male gametophyte, *Arabidopsis thaliana*, flower development, Y2H, BiFC, nascent polypeptide-associated complex, flower bud transcriptome, chaperone

Abstract in Czech language

Vývoj rostlinných květů představuje dynamický proces regulovaný řadou rozličných mechanismů. V předchozí studii se podařilo získat dvojitého homozygotního mutanta huseníčku rolního (*Arabidopsis thaliana*) v genech kódujících obě β -podjednotky komplexu asociovaného s nascentním polypeptidem (NAC). Tento mutant se vyznačoval docela výrazným defektním fenotypem; byly pozorovány odchylky od standardního počtu květních orgánů, kratší šesule s nižším počtem semen a zhoršená klíčivost pylu spolu s nižší efektivitou cílení pylové láčky do zárodečného vaku. Komplex NAC byl původně popsán v kvasince *Saccharomyces cerevisiae* jako heterodimer složený z α - a β -podjednotky, který se váže na ribozom a vykazuje chaperonovou funkci. NAC β podjednotka se v rostlinách podílí na regulaci stresové odpovědi, rozmnožování a regulaci vývoje, a to pravděpodobně mechanismem transkripční regulace. Role NAC heterodimeru v rostlinách ale zatím nebyla příliš prozkoumána. Tato diplomová práce si tak klade za cíl ověřit tvorbu NAC komplexu v huseníčku rolním a případně ustanovit vazebné preference mezi dvěma paralogy NAC β podjednotky a pěti paralogy NAC α podjednotky. Využity byly dvě metody studia proteinových interakcí - kvasinkový dvouhybridní systém (Y2H) a bimolekulární fluorescenční komplementace (BiFC).

V rámci porozumění molekulárnímu mechanismu způsobujícímu fenotyp *nacB1 nacB2* rostlin byl analyzován transkriptom květních pupat tohoto mutanta a porovnán s transkriptomem divoké rostliny Columbia-0 (Col-0). Následná analýza odhalila 1965 genů se změněnou expresí v pupatech mutantních rostlin. Mezi tyto geny patří dvě skupiny s výrazným zastoupením. První z nich byly geny spojené se stresovou odpovědí, například zvýšená exprese chaperonů a snížená exprese genů spojených se stresovou resistencí. Druhou skupinou byly geny ovlivňující vývoj samčí zárodečné linie, hlavně pak v diferenciaci spermatické buňky a růstu pylové láčky.

Klíčová slova:

pyl, samčí gametofyt, *Arabidopsis thaliana*, huseníček rolní, vývoj květu, Y2H, BiFC, komplex asociovaný s nascentním polypeptidem, transkriptom květních pupat, chaperon

Abbreviations

3AT	3-amino-1,2,4-triazole
5FoA	5-fluoroorotic acid
aeNAC	archeal NAC α homologue
BiFC	Bimolecular fluorescence complementation
BTF3	basal transcription factor 3
CLIPS	chaperones linked to protein synthesis
<i>Col-0</i>	Columbia-0
DE	differentially expressed
DEG	differentially expressed gene
ER	endoplasmic reticulum
FRET	Förster resonance energy transfer
GFP	green fluorescence protein
GO	gene ontology
NAC	nascent polypeptide-associated complex
NLS	nuclear localisation signal
PCA	Principal Components Analyses
PCR	polymerase chain reaction
PT	pollen tube
RAC	ribosome-associated complex
RFP	red fluorescence protein
SC	synthetic complete medium
SRP	signal recognition particle
TAE	Tris-acetate-EDTA
TE	Tris-EDTA
WT	wild type
x-gal	5-bromo-4-chloro-3-indolyl-B-D-galactopyranoside
Y2H	Yeast two hybrid system
YFP	yellow fluorescence protein

Contents

DECLARATION	3
ACKNOWLEDGEMENTS	5
ABSTRACT	7
ABSTRACT IN CZECH LANGUAGE	9
ABBREVIATIONS	11
INTRODUCTION	14
GOALS	16
CURRENT KNOWLEDGE	17
DE NOVO PROTEIN FOLDING ACROSS SPECIES	17
NAC SUBUNITS - STRUCTURE AND FUNCTIONS.....	18
NASCENT POLYPEPTIDE ASSOCIATED COMPLEX IN YEAST	21
NASCENT POLYPEPTIDE ASSOCIATED COMPLEX IN PLANTS.....	22
NACB1 NACB2 DOUBLE HOMOZYGOUS MUTANT.....	26
MATERIALS AND METHODS	30
YEAST TWO-HYBRID SYSTEM.....	30
<i>Introduction to the method:</i>	30
<i>Yeast strain MaV203</i>	30
<i>RNA extraction and cDNA preparation</i>	31
<i>Construct preparation</i>	32
<i>GatewayTM cloning</i>	34
<i>Interaction partners and design of controls</i>	39
<i>Yeast transformation</i>	40
<i>The preparation of yeast selective media</i>	41
<i>Auxotrophic selection and observation</i>	42
<i>LacZ assay</i>	43
BIMOLECULAR FLUORESCENCE COMPLEMENTATION	44
<i>Introduction to the method</i>	44
<i>BiFC construct preparation</i>	45
<i>Gateway cloning</i>	46
<i>Transformation of Agrobacterium tumefaciens by electroporation</i>	48
<i>Tobacco leaf infiltration</i>	48
TRANSCRIPTOME ANALYSIS	49
<i>RNA extraction and sequencing</i>	49
<i>Mapping and assembly of reads</i>	50
<i>Annotation and enrichment analyses</i>	51
<i>Confirmation of DEGs expression by qRT-PCR</i>	51
RESULTS	53

YEAST TWO-HYBRID SYSTEM.....	53
<i>Cloning</i>	53
<i>Interaction results</i>	53
BIMOLECULAR FLUORESCENCE COMPLEMENTATION	57
<i>Construct preparation</i>	57
<i>Confocal microscopy of transformed leaves</i>	57
TRANSCRIPTOME ANALYSES	62
<i>Sample preparation and raw data processing</i>	62
<i>Differential expression analyses</i>	62
<i>DEG list analyses</i>	64
<i>qRT-PCR data validation</i>	71
DISCUSSION	72
THE FORMATION OF NAC COMPLEX IN PLANTS	72
ANALYSES OF NACB1 NACB2 FLOWER BUD TRANSCRIPTOME	74
CONCLUSION	80
CITATIONS	81
SUPPLEMENT	89

Introduction

The development of *Arabidopsis thaliana* flowers is a complex process regulated by number of mechanisms. Nascent polypeptide-associated complex (NAC) is a heterodimer with ribosome-binding domain and was proved to be essential for development of higher eukaryotes (Wiedmann *et al.*, 1994; Markesich *et al.*, 2000; Wang *et al.*, 2014). It is necessary to emphasize, that the NAC abbreviation is also used for a family of transcription factors. In this case, the abbreviation consists of first letters of several members of this family, namely NAM (*no apical meristem*), ATAF1 and ATAF2, and CUC2 (*cup-shaped cotyledon*) (Aida *et al.*, 1997). However, NAC complex is not related to this family in any way, it is only unfortunate selection of used abbreviations.

NAC consists of two subunits, β and α and as a heterodimer is responsible for *de novo* folding of nascent polypeptides emerging from the ribosome exit tunnel site (Wiedmann *et al.*, 1994). NAC was also reported to play a potential role in protein sorting to endoplasmic reticulum (ER) or mitochondria (Ponce-Rojas *et al.*, 2017; Wiedmann *et al.*, 1994). Apart from its functions as complex, the sole NAC subunits were discovered in various organisms to play their own distinguished roles. In plants, NAC β subunits were reported to be involved in stress tolerance and development regulation, most likely as transcription activators of responsive genes (Kang, Ma, *et al.*, 2013; Wang *et al.*, 2014). However, up to date, there is lack for a direct proof of NAC heterodimer function in plants.

The genome of our model plant *A. thaliana* codes for two genes of NAC β subunit and five genes of NAC α subunit. The first aim of this thesis was to establish whether all paralogues were capable of complex formation and whether there were any binding preferences between them. To address this question, Bimolecular fluorescence complementation and Yeast two-hybrid protein-protein interaction methods were used. The results proved NAC heterodimer formation in *A. thaliana* and brought potential functional discrimination between individual subunits and their dimers.

The second part of the thesis focused on flower bud transcriptomic analyses of previously acquired double homozygous mutant of *A. thaliana* NAC β subunit (*nac β 1 nac β 2*). The mutant exhibited a strong phenotype like abnormal number of flower organs, shorter siliques with a reduced seed set, and inferior pollen

germination rate together with a lower ovule targeting efficiency. Differential expression analyses between *nacβ1 nacβ2* and Col-0 WT flower bud transcriptome resulted in 1965 DEGs. According to Gene ontology, 87 downregulated genes were connected to male germ-line development. Among these genes, regulators of sperm cell differentiation and pollen tube growth were present. These genes could be responsible for the observed *nacβ1 nacβ2* phenotype and could represent potential effectors of NACB transcriptional regulation. There were also 20 upregulated chaperones, which could potentially cover reduced presence of NAC heterodimer. Last but not least, several stress-connected gene families were observed in the mutant, possibly representing the effectors of NACB subunit.

Goals

This Master thesis is a part of the larger project which aims to annotate the nascent polypeptide-associated complex (NAC) and function of its subunits in *Arabidopsis thaliana*. This thesis should address particularly three questions:

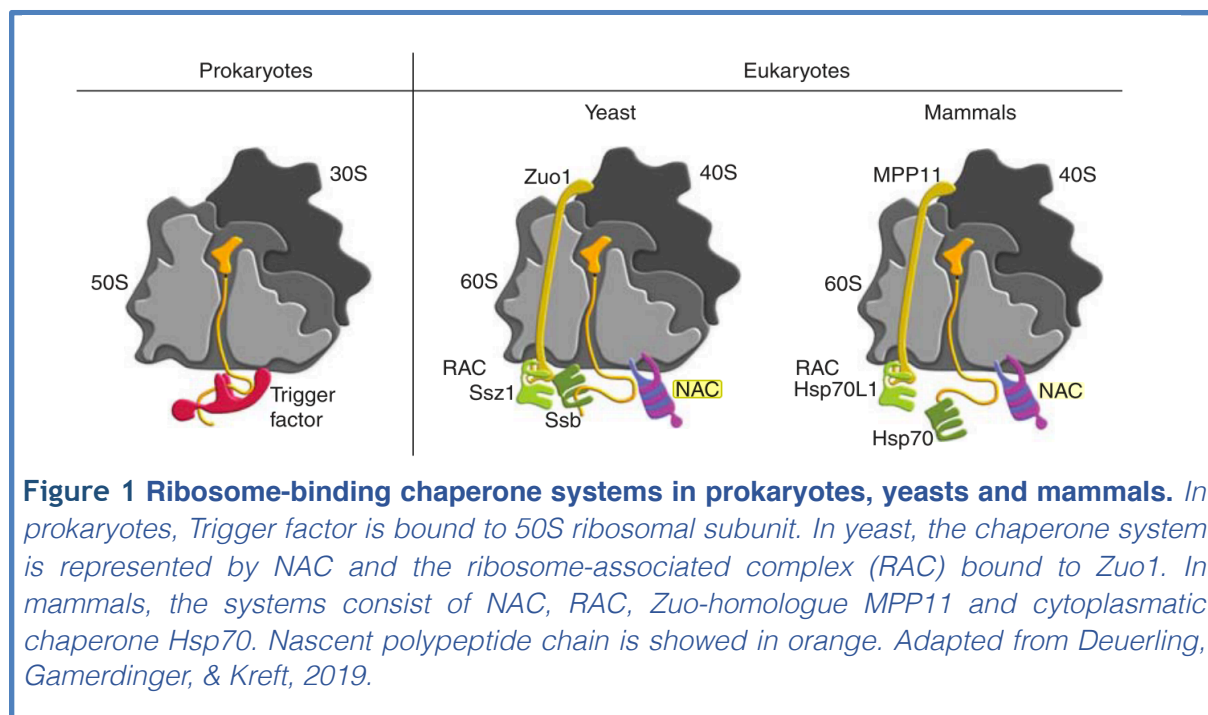
1. Are NAC heterodimers formed in *A. thaliana* and are some of them preferentially formed compared to the others?
2. Are NAC homodimers formed in *A. thaliana*?
3. Which genes are influenced by the knock down of both NACB subunits in *Arabidopsis thaliana* flower buds?

Answering these questions will broaden the up-to-date knowledge and help in planning future experiments for the continuation of the project.

Current knowledge

De novo protein folding across species

Molecular chaperones are key players in guarding cell proteome by assisting protein folding, preventing mis-folded protein aggregation and helping in stress tolerance. Several proteins including chaperones and various other processing enzymes bind to ribosome to assist folding and promote modifications of newly synthesized polypeptide chains, promoting so called *de novo* folding (Albanèse *et al.*, 2006). This group of chaperones can be referred to as chaperones linked to protein synthesis (CLIPS). On the other hand, cytoplasmatic heat shock chaperones are connected to stress protection and re-folding or quality control of existing proteins (Albanèse *et al.*, 2006). CLIPS are presented across species with structural and mechanistical variations (fig. 1). In yeast, there are ATP-dependent Hsp70 chaperone Ssb and ribosome-associated complex (RAC) comprised of Zuotin from Hsp70 family and Ssz from Hsp40 family (Koplin *et al.*, 2010). RAC homologs are conserved in mammals as MPP11 and Hsp70L1. Also, cytosolic Hsp70 is recruited to nascent polypeptides in mammals (Jaiswal *et al.*, 2011). Conserved from *Archea* through yeast to human, nascent polypeptide associated complex (NAC) serves as another assistant for *de novo* protein folding. Bacteria possess their own, well annotated, chaperone protein called Trigger factor (Deuerling *et al.*, 1999). Group of cytosolic *de novo* folding chaperones is represented by Hsp70/40 and Hsp60/10



families in both prokaryotes and eukaryotes. Together with the ribosomal-bound chaperones, complex multicomponent network is formed to assure the correct *de novo* folding of nascent polypeptides.

Although distant and not sharing sequence homology, the functional mechanism of bacterial Trigger factor can help for understanding the functional essentials of less understood NAC or other eukaryotic CLIPS. For instance, Trigger factor is accompanied with cytosolic HSP60/10 family chaperone system GroEL/GroES and DnaK (Hsp70) chaperone (Preissler and Deuerling, 2012). Connection and cooperation between these chaperone systems proved to be crucial for cell survival and the individual chaperones showed a partial functional redundancy. Simultaneous deletion of genes encoding both Trigger factor and DnaK caused protein aggregations and led to cell death under higher temperature (above 30°C) (Deuerling *et al.*, 1999; Teter *et al.*, 1999). On the contrary, overexpression of GroEL/GroES reduced the lethality in the DnaK and Trigger factor double mutant (Vorderwülbecke *et al.*, 2004; Genevaux *et al.*, 2004). Trigger factor associates with L23 ribosome protein via conserved motif at N'-terminal domain. It forms a structural cavity with several hydrophobic side chains serving as contact sites for polypeptides and it can accommodate proteins with various lengths and unrelated functions (Patzelt *et al.*, 2002). Trigger factor binds the ribosome as monomer, yet it was proved to form dimers, which could help with refolding proteins in cytoplasm (Patzelt *et al.*, 2002).

NAC subunits - structure and functions

NAC was first reported in eukaryotes as heterodimer-forming complex of α and β subunit, which associate with the ribosome near the exit tunnel site (Wiedmann *et al.*, 1994). A homologue of eukaryotic NAC α was found in Archeal genome (further referred to as aeNAC), yet no NAC β orthologues seem to be present (Makarova *et al.*, 1999; Macario and Conway De Macario, 2001). Later, the aeNAC was experimentally proved to be expressed in *Methanothermobacter marburgensis* and its ribosome and nascent polypeptide binding abilities were observed (Spreter *et al.*, 2005). Also, competition between human NAC and aeNAC in nascent polypeptide chain binding was observed in the same study, showing a partial functional redundancy. Spreter *et al.* (2005) also managed to acquire Δ 1-18aeNAC crystal structure revealing the residues 25-117 of aeNAC. The structure

consisted of 6-stranded β -barrel-like structure at the N-terminus. This domain seemed to be conserved among all NACs and is referred to as NAC domain. This conserved sequence is likely responsible for homodimer formation in *Archea* and heterodimer formation in Eukaryotes (Spreter *et al.*, 2005). On the C-terminus of aeNAC, there is a UBA domain, which implies a possible NAC regulation by ubiquitination. Based on these data, Spreter *et al.* (2005) suggested similar function for aeNAC homodimers and eukaryotic heterodimers and also potential later evolutionary development of two distinguished α and β subunits in eukaryotes with a more precise functional distribution. Another group discovered that aeNAC shares sequence similarity of 28% with human NAC α and 26% with NAC β (BTF3) and they revealed conserved crystal structure of NAC domain in both human NAC β and NAC α as well as UBA domain presented in the NAC α (Liu *et al.*, 2010). Liu *et al.* (2010) also discovered that human NAC α homodimers exhibit different amino acids to the surface of the complex, and as such can bind the nucleic acids. Since NAC α has also nucleic acid binding affinity and was previously reported to play its role in transcription activation, another hypothesis for the function of NAC α homodimers was proposed. The authors suggest that the NAC α homodimers, which show their affinity to nucleic acid, move to nuclei to work as transcription regulators (Liu *et al.*, 2010). However, their abundance depends on stoichiometric equilibrium between β and α subunits. Heterodimer formation is considered to be preferential, enabling homodimer formation only under excessive concentration of NAC α subunits. Beatrix *et al.* (2000) described NAC heterodimer as one of the most abundant cytosolic complexes in different cell lines and discovered that NAC heterodimer is the only detectable variant. Though, it is possible, that the minority of NAC complex localised to the nucleus or the individual subunits present in the cytoplasm were masked by the notably higher abundance of NAC heterodimer. Other crystal structure analyses of human NACs also proved NAC heterodimer as a dominant form due to electrostatic interaction, but also proposed the possibility of both β and α homodimers formation via the conserved NAC domain (Wang *et al.*, 2010).

Both NAC subunits were predicted to be in contact with the nascent polypeptide chain, however differences were observed in ribosome binding capacity (Beatrix *et al.*, 2000). NAC complex binds ribosomes in 1:1 stoichiometry

by N-terminal domain of NACB as a crucial place for the first contact with ribosome at uL23 (Wegrzyn *et al.*, 2006) or eL31 (Pech *et al.*, 2010) site with possible binding flexibility (Nyathi and Pool, 2015). NAC α was proposed to dock at the uL21 ribosome protein, which is also in the site of exit tunnel (Nyathi and Pool, 2015). Since the discovery of NAC heterocomplex, its mutual regulation with ER-targeting signal recognition particle (SRP) was proposed and this hypothesis was strengthened after the discovery of NAC ribosome binding sites. These could be shared with SRP particle and could negatively regulate its binding to nascent polypeptide chains and thus modify SRP binding specificity (Wiedmann *et al.*, 1994; del Alamo *et al.*, 2011). Yet some of these results remain controversial, since there is not any *in vivo* evidence that SRP-mediated targeting is affected in NAC absence (del Alamo *et al.*, 2011; Gamerdinger *et al.*, 2015). An alternative regulation of ER sorting was proposed in *Caenorhabditis elegans* where NAC was reported to function as masking device of high-affinity Sec61-binding site on ribosomes, therefore preventing non-specific protein sorting to ER (Zimmermann *et al.*, 1998; Gamerdinger *et al.*, 2015). Furthermore, NAC protein sorting does not have to be exclusive for ER since several studies reported a potential role of NAC complex in mitochondrial co-translational protein sorting. In *C. elegans*, amount of mistargeted mitochondrial proteins raised on NAC depletion (Gamerdinger *et al.*, 2015) and in yeast, NAC was reported to promote interaction of ribosome to mitochondria binding site via OM14 receptor (Walsh *et al.*, 2002; Lesnik *et al.*, 2014). However, no NAC mitochondria receptor was discovered in higher organisms so far.

NAC role as ATP-independent chaperone was studied mainly in yeast and is discussed later. Nevertheless, the NAC structure and binding capacities indicated NAC binding to nascent substrates and shielding them from premature degradation in cytosol similarly to Tigger factor (Wiedmann *et al.*, 1994; Duttler *et al.*, 2013; Wang *et al.*, 2010; Koplin *et al.*, 2010). Finally, the role of NAC in ribosome biogenesis was proposed, since ribosomal proteins and ribosome biogenesis factors were among the most aggregated proteins in *nac* mutant in yeast (Koplin *et al.*, 2010).

Apart from the proposed functions as a heterodimer, the individual subunits were discovered to play their own roles in the cell. Due to its structure, NAC α

homodimers seem to be connected to transcription regulation bearing conserved nucleic acid binding domain (Beatrix *et al.*, 2000; Liu *et al.*, 2010). In human and mouse, the transcription regulation capacity of NAC α homodimer was proved. In mouse, NAC α was observed to recruit repressor complexes to suppress expression of myogenin gene in osteoblasts and vice versa osteocalcin gene in myoblast precursors via interaction with histone deacetylases (Yotov and St-Arnaud, 1996). Briefly, NAC α worked as tissue specific co-repressor. In human, NAC α was found to work as transcription co-activator in bone tissue and regulator of erythroid cell differentiations (Lopez *et al.*, 2005). In both cases, NAC α was involved in crucial developmental processes.

NAC β , before its discovery as part of NAC complex, was first observed as basal transcription factor 3 (BTF3) in HeLa cells, representing an essential factor for RNA polymerase II-dependent transcription (Zheng *et al.*, 1987). An alternative role of nematode BNAC/ICD-1 subunit was reported in suppression of apoptosis, during which it binds caspase 3 (Bloss *et al.*, 2003; Creagh *et al.*, 2009). BTF3 and its paralogues have further functions in plant transcription regulation as discussed later.

Nascent polypeptide associated complex in yeast

In yeast (*Saccharomyces cerevisiae*), three genes encode NAC subunits - NAC α (*EGD2*), NACB1 (*EGD1*, *BTF3*), NACB3 (*BTT1*) (Shi *et al.*, 1995). The NAC subunits exhibit chaperone activity in both heterodimer and homodimer formations, yet NACB1 and NACB3 differ significantly in their abundances and substrate specificity (Reimann *et al.*, 1999; del Alamo *et al.*, 2011). More abundant NACB1/NAC α complex was reported to associate preferentially with nascent metabolic enzymes or mRNAs encoding membrane or secretory pathway proteins, whereas minor NACB3/NAC α complex primary associated with nuclear-encoded mitochondrial and ribosomal proteins (del Alamo *et al.*, 2011). Also, NAC α homodimer formation with association affinity similar to NACB1/NAC α was proposed (del Alamo *et al.*, 2011). The effect of knock-out of individual NAC subunits on cell growth and viability were studied by several experiments (Koplin *et al.*, 2010; del Alamo *et al.*, 2011; Reimann *et al.*, 1999). In general, single mutants had no or little effects whereas the double *nacB1 nacB3* mutant showed an impaired growth only under elevated temperature of 37°C (Reimann *et al.*, 1999).

The overexpression of NAC α subunit also resulted in slower growth under elevated temperature. Furthermore, *naca* mutation reverted the phenotype in double *nacB1 nacB3* mutant background, implying toxic effect of the excessively accumulated NAC α subunits (Rospert *et al.*, 2002). NAC α was also found as one of the substrates of E3 ubiquitin ligase RSP5 under stress conditions. Mutants of RSP5 were hypersensitive to stress possibly due to NAC α accumulation (Hiraishi *et al.*, 2009). Koplín *et al.* (2010) observed mutant phenotype showing loss of viability caused by protein-folding stress in case of simultaneous deletions of all three genes encoding NAC (*nacB1*, *nacB3*, and *naca*) together with two SSB chaperones encoding genes (*ssb1* Δ and *ssb2* Δ). Similar phenotype was observed in deletion of *Sse1* (yeast HSP110 working as nucleotide exchange factor for multiple Hsp70s) and worsened in *nacB1 nacB3 naca* triple mutant background (Koplín *et al.*, 2010). The authors observed high protein aggregation and lower cell viability under heat stress or under a low concentration of antibiotics. Only NAC with functional ribosome attachment side was able to complement the mutation, showing that NAC cooperates with SSB-RAC exclusively when bound to the ribosome. This is in correspondence with experiments performed by Ott *et al.* (2015) who also observed NAC complementation of *ssb* mutation. They distinguished between two yeast heterodimers and found out that only the abundant NACB1/NAC α complex could suppress *ssb* mutation. They also discovered that the NACB1 and NAC α differ mainly at their C-termini, with only 10.3% amino acid identity, suggesting different functions of individual yeast heterodimer variants. Del Alamo *et al.* (2011) reported similar effects of triple mutant describing cellular compensation for the loss of NAC by induction of stress-inducible chaperones, other CLIPS (*Ssb1*, *Ssb2*) and ribosomal protein assembly factors. To conclude, NAC in yeast is part of highly connected, partially functionally redundant chaperone system.

Nascent polypeptide associated complex in plants

Number of genes coding for α and β subunits differs among individual plant species. Usually, there is high sequence similarity of plant NACB to human NACB (BTF3). Also, the conserved domains of NACB including NAC domain and plant specific putative nuclear localization signal (NLS) sequence are conserved between individual species (fig. 2). According to Peng *et al.* (2017) phylogeny analyses of BTF3, the common ancestor aeNAC differentiated into two clusters - plant and

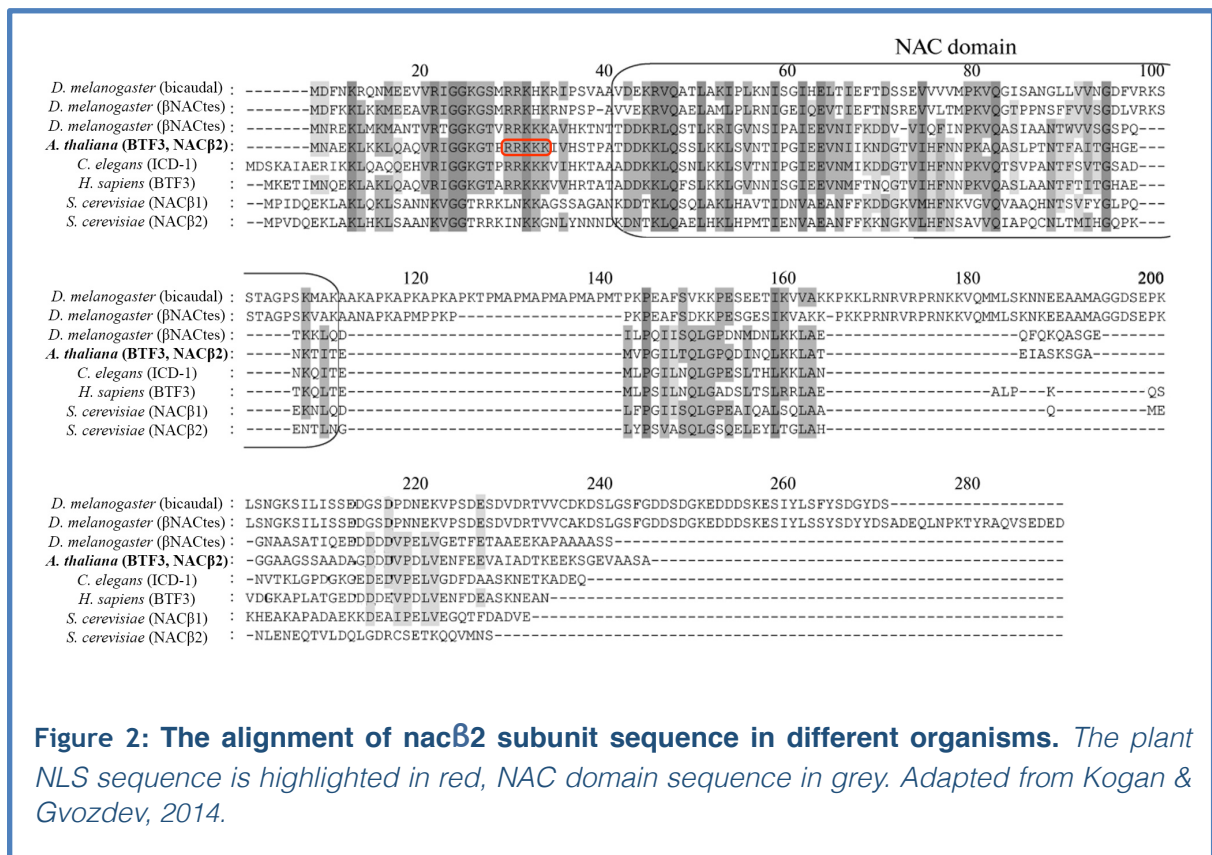


Figure 2: The alignment of nacβ2 subunit sequence in different organisms. The plant NLS sequence is highlighted in red, NAC domain sequence in grey. Adapted from Kogan & Gvozdev, 2014.

animal. Further functional differentiation of BTF3s happened within the individual species resulting in inconsistent number of genes between the plant species. In *Arabidopsis thaliana*, two genes encode for NACβ subunit, NACβ2 (BTF3) and its orthologue NACβ1 (BTF3L) and five genes for NACα subunits named NACα1 to NACα5.

The knowledge about NAC function in plants is still limited. However, several studies aimed to analyse NACβ subunits in different plant species in context of stress tolerance and plant development. In numerous proteomic and transcriptomic studies, NACβ2 expression was reported to respond to various biotic and abiotic stresses across various species as reviewed in table by Jamil et al. (fig. 3).

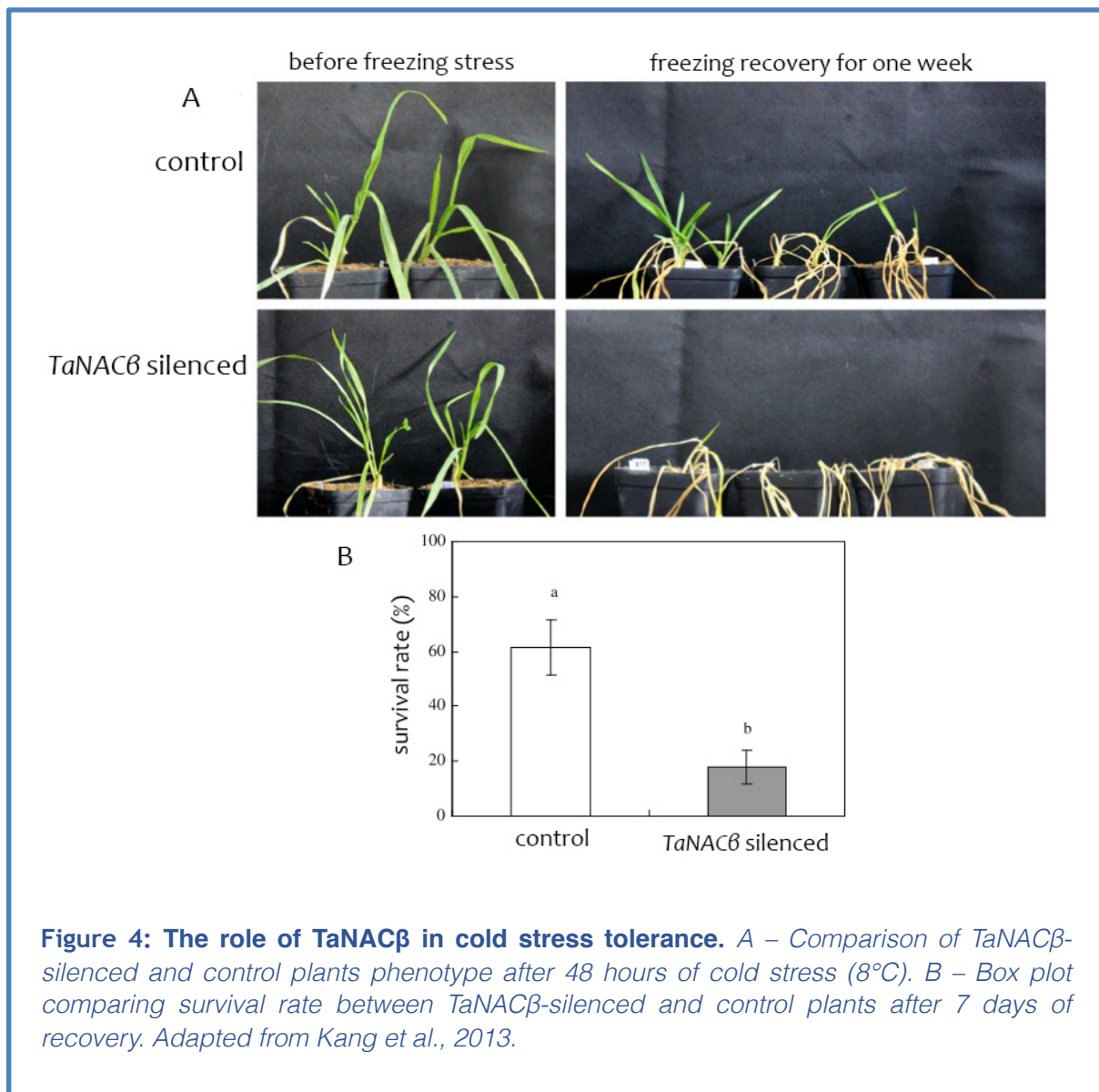
However, only few studies focused on the molecular mechanisms underlying these phenomena. For instance, BTF3 and BTF3L were discovered to be substrates for OST1 kinase and underwent phosphorylation in cold stress environment. The phosphate moiety promoted binding of BTF3L to ribosome, thus BTF3L proteins are responsible for stabilization of newly synthesized cold-induced proteins. Also, phosphorylated BTF3 proteins regulate transcription and stabilise cold-stress response CBF proteins in vascular tissues in *A. thaliana* (Yang et al., 2018). Similar

Figure 3: The regulation of NAC β expression in various plant species under normal, biotic and abiotic stress conditions as reviewed in Jamil, Wang, Xu, & Tu, 2015.

Species	Stress type	Organism part	Expression change
<i>Arabidopsis</i>	Hypoxia	Seed	Up
		Seed embryo	Up
		Endosperm	Down
	Hypoxia UV-B light/drought/cold Mock/osmotic NaCl UV-B light/drought/cold Normoxia/hypoxia Iron deficiency Mock/osmotic Iron deficiency Wounding	Seedling	Down
		Root	Up
		Root	Up
		Root	Up
		Shoot	Down
		Root	Down
		Leaf	Down
		Leaves	Down
		Protoplast	Up
		Leaf	Up
Rice	ABA/MeJA/ETH/SA Bacterial and fungal infection Insect feeding Salt	Endosperm	Up
		Embryo	Down
		Root	Up
		Shoot	Down
		Leaf	Down
		Leaves	Up
		Leaves	Up
		Stem	Down
		Leaves	Down
		Cell culture	Up
Tobacco	Heat/NaCl Heat	Immature	Up
		Silks	Up
Maize	PEG Cold/NaCl/ ABA/SA	Ears	Up
		Immature	Down
		Silks	Down
		Ears	Down
		Root	Up
		Grain	Up
Wheat	Drought Low nitrogen efficiency NaCl Freezing	Root	Up
		Seedling	Up
		Root	Up
Sugar beet		Root	Up
Apple		Fruit	UP
Tomato	Ethylene	Fruit	Up
		Anther	Up
Peanut	NaCl Intercropping with Maize	Root	Down
		Vegetative part	Up
Cucumber	NaCl	Ovary	Down
<i>Suaeda asparagoides</i>		Leaf	Up
<i>Spartina alterniflora</i>	Salt/drought Cold Salt/drought/cold/ABA	Leaf	Up
		Leaf	Down
		Root	Up
<i>Gerbera hybrid</i>		Flower	Up
<i>Salvia aegyptiaca</i>		Young leaf	Up

results were showed in *Jatropha curcas*, where JcBTF3 overexpression in transgenic *A. thaliana* plants led to significant increase in abundance of stress response genes and proline accumulation under cold stress conditions (Peng *et al.*, 2017). Increased levels of BTF3 expression under various abiotic stresses were observed also in wheat (*Triticum aestivum*) (Kang, Li, *et al.*, 2013;). Plants with silenced *TaBTF3* genes showed lower survival rate under freezing or drought stress when compared to control wheat plants (fig. 4). The silencing of the gene was also accompanied with lower free proline and water content in the plants (Kang, Li, *et al.*, 2013). Furthermore, BTF3 of *Capsicum annuum* (*CaBTF3*) was found to be involved in transcription regulation related to hypersensitive response upon the *Tobacco mosaic virus* inoculation (Huh *et al.*, 2012).

In *Nicotiana benthamiana* with silenced *BTF3* (*NbBTF3*), the disruption in leaf morphology and reduction of chloroplast size and chlorophyll content was observed (Yang *et al.*, 2007). On the contrary, in *Nicotiana benthamiana*, a higher tolerance to abiotic stresses accompanied by better reactive oxygen species scavenging and cell membrane stability in plants overexpressing *BTF3* from peanut *Arachis hypogaea* was shown. Under normal conditions, the transgenic plants showed improved growth when compared to WT (Pruthvi *et al.*, 2017). Similarly, transgenic *A. thaliana* plants with overexpressed *SaBTF3* from *Spartina alterniflora* showed enhanced tolerance to drought and salt stress (Karan and Subudhi, 2012). Then, a potential role of *TaBTF3* in wheat chloroplast development was observed by Ma *et al.* (2012). Silencing of *TaBTF3* led to reduction of chlorophyll content and the disruption of mesophyll cells. Moreover, transcription



of mitochondrial and chloroplast genes was reduced in the silenced plants (Ma *et al.*, 2012). Other observed phenotypes were connected to plant growth and reproduction capacity. In *Oryza sativa* var. *japonica*, the inhibition of *Osj10gBTF3* led to delayed germination of mutant plants upon addition of gibberellins, abscisic acid or NaCl (Wang *et al.*, 2014). In another study, modulation of *Osj10gBTF3* expression was observed under salt stress, high temperature and stress caused by addition of exogenous phytochromes. The repression of *Osj10gBTF3* led to dwarfism and total pollen abortion. In connection to that, 4 genes involved in pollen development or plant reproduction were potentially regulated by *Osj10gBTF3* on transcriptional level (Wang *et al.*, 2012). Furthermore, *AtBTF3* was found to interact with translation initiation factor 4E in a yeast two-hybrid system, so the BTF3 was proposed to be involved in regulation of translation initiation (Freire, 2005).

To conclude, BTF3 plays an apparent role in regulation of stress response in plants. Additionally, BTF3 is probably affecting the transcription of other genes with potential role in translation initiation regulation. However, little is known about the function of NAC subunits or NAC heterodimeric complexes in plants.

nacβ1 nacβ2 double homozygous mutant

In previous study in our lab, NAC was selected as a candidate gene from phosphoproteomic profiling study of tobacco (*Nicotiana tabacum*) activated pollen (Fíla *et al.*, 2016). In *Arabidopsis thaliana*, there are 5 genes encoding NAC α subunit (*NAC α 1* At3g12390, *NAC α 2* At3g49470, *NAC α 3* At5g13850, *NAC α 4* At4g10480, *NAC α 5* At1g33040) and two genes for NAC β subunit (*NAC β 1* At1g73230 and *NAC β 2* (also *BTF3*, At1g17880). Firstly, T-DNA insertion lines for each gene were purchased and sown, but no phenotypic differences were observed in any single homozygous mutant. After series of crosses, double homozygous mutants in *NAC β 1* and *NAC β 2* were obtained, referred to hereafter as *nacβ1 nacβ2*. In animals, mutation of all NAC β subunits resulted in embryo lethality (Deng and Behringer, 1995; Markesich *et al.*, 2000). On the contrary, the *A. thaliana nacβ1 nacβ2* mutant survived but showed quite a strong defective phenotype in flowers and siliques when compared to Columbia-0 wild type plants (these and the following data are from manuscript in preparation by Fíla, Klodová, Juříček, Šesták, and Honys 2019).

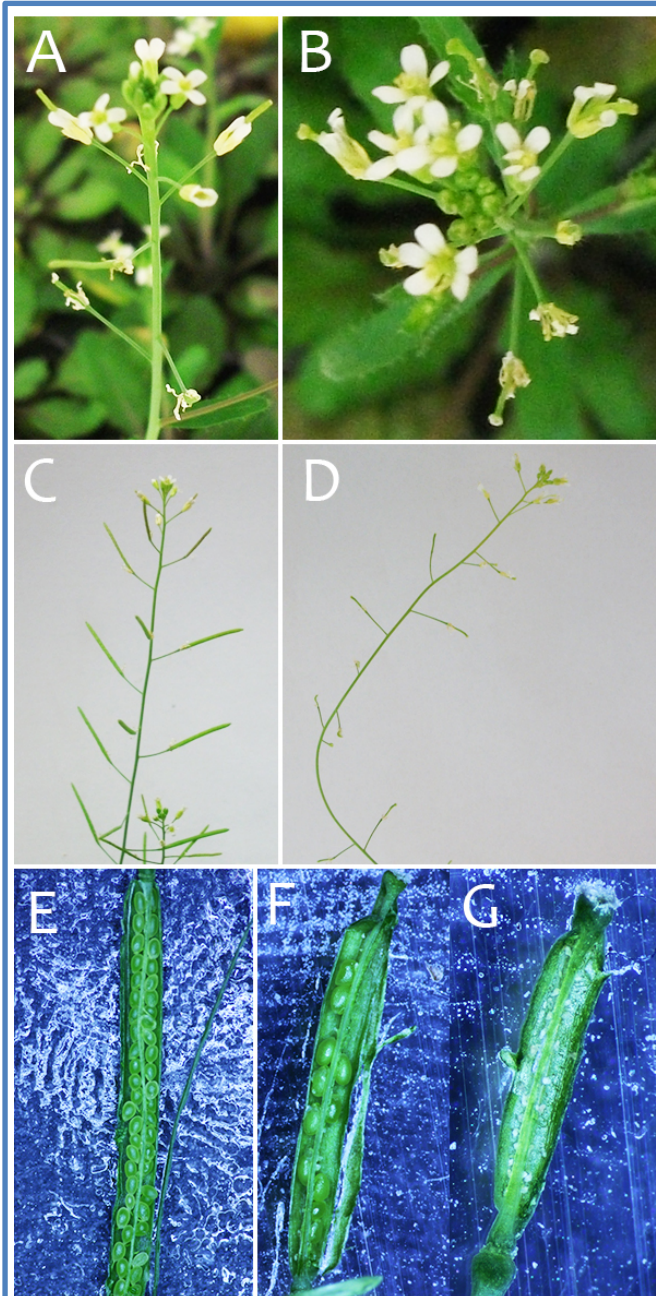
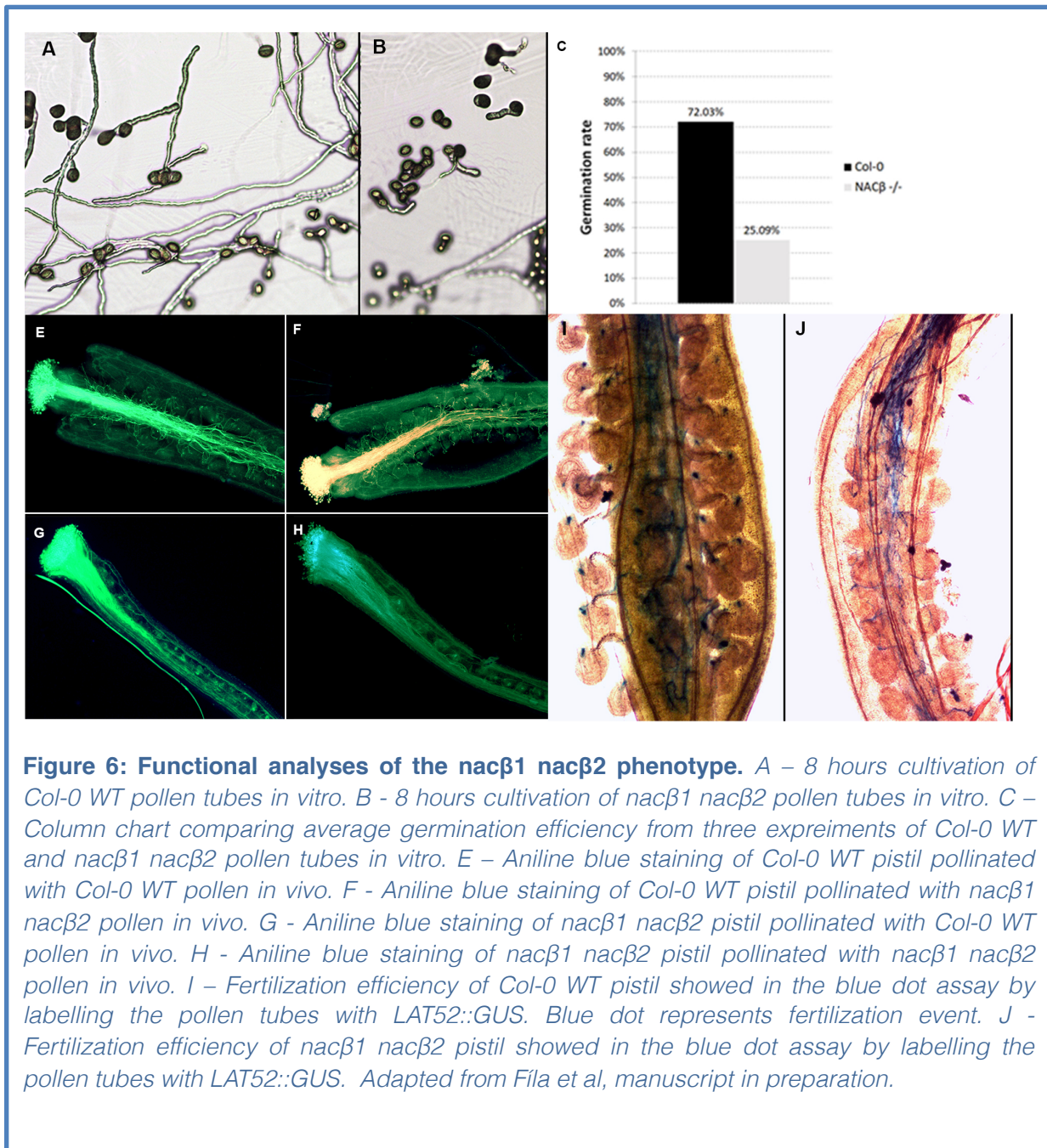


Figure 5: The phenotype of *Arabidopsis thaliana* *nacβ1 nacβ2* mutant. A – *Col-0* WT inflorescences with normal number of flower organs. B – *nacβ1 nacβ2* inflorescences with aberrations in the numbers of petals, sepals and anthers. C – *Col-0* WT normal-sized siliques. D – *nacβ1 nacβ2* shorter siliques. E – *Col-0* WT seeds in silique. F – less severe phenotype of *nacβ1 nacβ2* silique consisting of combination of healthy green normal-sized seeds with aborted ones. G – severe phenotype of *nacβ1 nacβ2* silique with most of the seeds aborted.

In particular, 90% of the *nacβ1 nacβ2* flowers carried abnormal numbers of flower organs (including different number of petals, sepals and anthers) with no distinct regularity (fig. 5). The siliques were remarkably shorter and produced significantly less seeds (median of total seeds per silique reached 15 in mutant, and 53 in WT), with most of the seeds represented by aborted embryo sacks. Furthermore, the differences appeared also in leaf chlorophyll content since only three fifths of the WT chlorophyll content were present in the *nacβ1 nacβ2* leaves.

For the functional analyses of gametophyte function, *in vitro* pollen tube cultivation, blue dot assay and aniline blue staining (staining of callose in the pollen tube cell walls) of the *in vivo* grown pollen tubes were carried out. It was proved that the mutant pollen tubes germinated with a lower efficiency (only 20-30% of *nacβ1 nacβ2* pollen grains germinated compared to 68-75% of the WT, fig. 6C) and grew *in vitro* slower than the wild type did - after 8 hours of cultivation, *nacβ1 nacβ2* PT reached only 142 μm on average, whereas WT PT 252 μm (fig. 6 A, B). Blue dot assay visualized



targeting efficiency of pollen tubes *in vivo*, which was again abnormally low, only 11 % in the mutant compared to 70% in the WT (fig. 6 I, J). In aniline blue staining, the deficiency was revealed in both female and male gametophytes (Fig. 6 E, F, G, H). The *nacβ1 nacβ2* embryo sac failed to attract wild type pollen tubes and on the other hand, the *nacβ1 nacβ2* pollen tube grew inefficiently in the wild type pistils and was not attracted by ovule signals. In case of mutation in both sexes (*nacβ1 nacβ2* pollen grain pollinated *nacβ1 nacβ2* pistils), the targeting efficiency was dramatically diminished. Last but not least, the development of *nacβ1 nacβ2*

plants were delayed for 10-14 days during the stem development when compared to WT. In conclusion, mutation of both β subunits resulted in plants with severe defects in reproduction as well as flower development. Subsequently, one task of this thesis was to analyse the *nac β 1 nac β 2* flower bud transcriptome to potentially uncover molecular mechanisms underlying these phenotypic defects and to settle future study prospects for the function of the NACB subunits in the regulation of *A. thaliana* reproduction.

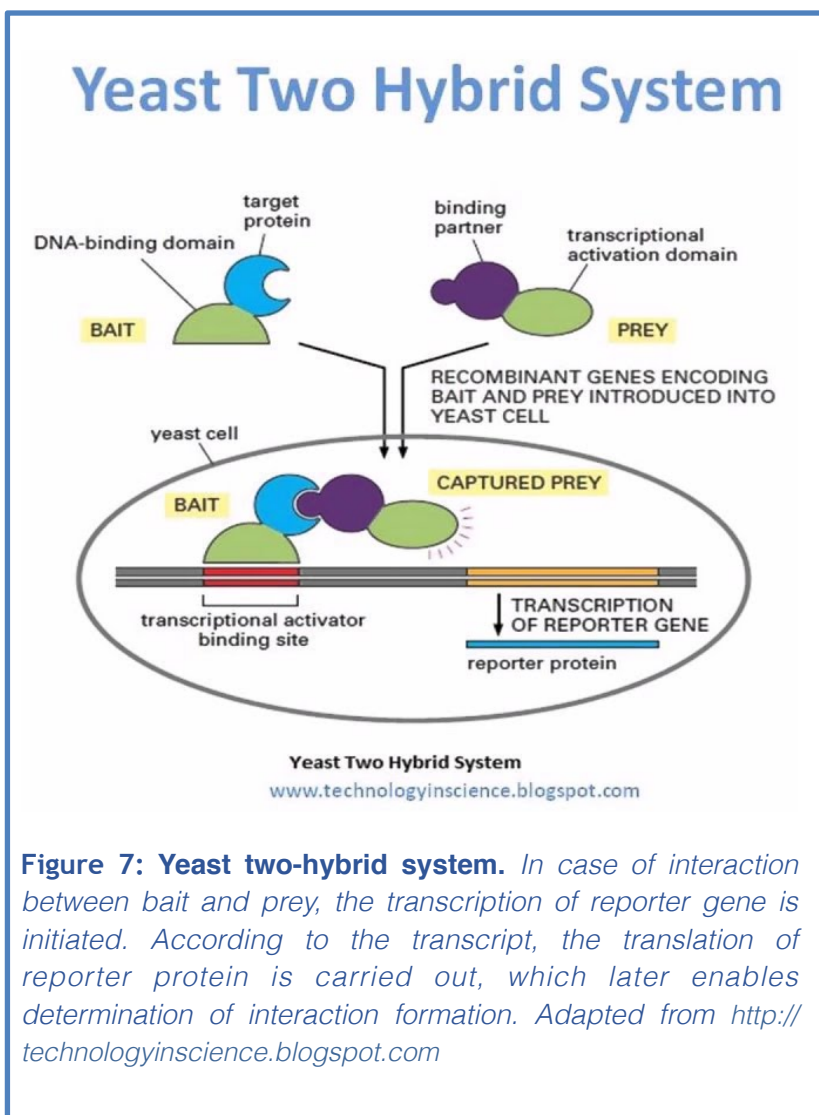
Materials and Methods

Yeast two-hybrid system

Introduction to the method:

Yeast two hybrid system (Y2H) is an *in vivo* method used for detection of protein-protein interactions, where potentially interacting proteins are expressed in yeast nucleus. If their interaction occurs, the transcription of reporter genes inserted into the yeast genome is performed and so the interaction is visualized via auxotrophy selection and enzymatic activity detection during the yeast grow. The first gene to be tested for interaction is fused with GAL4 DNA binding domain, and this construct is also called a bait. The second partner tested for interaction is fused with GAL4 activation domain and is referred to as prey (Fig. 7). When bait and prey interact with each other, the activation domain is approximated to the

DNA binding domain and downstream reporter gene is expressed. Although it is an *in vivo* method, it still represents a heterologous system tested in organism quite distant to *Arabidopsis thaliana*, which may result in both false positive and false negative results. However, multiple controls can be designed to avoid several of these artefacts.



Yeast strain MaV203

MaV203 yeast strain serves as a host for prey and bait plasmids

and bears genomic features to enable detections of formed interactions. There are single copies of three reporter genes included in MAV203 genome - *HIS3*, *URA3* and *LacZ*. Each of them has different promoter featuring GAL activated domain. The genome of MaV203 strain carries also two irreversible auxotrophic mutations *leu2* and *trp3* to provide selection for transformants. On the contrary, *GAL4* and *GAL80* genes encoding GAL4 and its repressor GAL80 are deleted from MaV203 genome, therefore galactose is no longer needed for activation of GAL4 inducible promoters.

RNA extraction and cDNA preparation

Seeds of *Arabidopsis thaliana*, ecotype Columbia-0 were sown on Jiffy tablets, left at 5°C for 2 days to stratify, and then cultivated under the normal long-day conditions (16h light/8h dark) at 21°C in the growth chambers. The plants were pricked to new Jiffy pots after two weeks. RNA was extracted from the leaves of 4 weeks old plants by RNeasy plant mini Kit (Qiagen, Venlo, Netherlands, 74904) according to the manufacturer's instructions. Firstly, 100 mg of leaf tissue was harvested and grinded thoroughly in liquid nitrogen by a mortar in a pestle. 450 µl of RLT Buffer was added to the homogenized sample and transferred to the QIAshredder spin column and centrifuged at 13 000x g for 2 min. The supernatant was transferred to a fresh microtube and 225 µl of 96% ethanol was added. The sample was transferred into the RNeasy Mini spin column and centrifuged at 10 000x g for 30 seconds. The flow-through was discarded, 700 µl of Buffer RW1 was added to the column and spun again. The flow-through was discarded again. This step was repeated twice with 500 µl Buffer RPE. Then, the Rneasy Mini spin column was placed into a new collection tube and spun for another minute. Rneasy Mini spin column was placed into a fresh 1.5 ml Eppendorf tube and 30 µl of RNase-free water was added to the centre of spin column membrane. The tube was centrifuged (13 000x g for 1 min) to elute the RNA. The integrity of RNA was checked on 1.2 % agarose gel electrophoresis in 1× Tris-acetate-EDTA (TAE) Buffer (40mM Tris (MP Biomedicals, 819623), 20mM acetic acid (Merck, 71251-5ML-F), 1 mM EDTA (Merck, E9884), pH 8.0) with ethidium bromide (PanReac AppliChem, A2273). The gel was run at 100 V until the blue line reached the front (approx. 90 min). Concentration and purity of samples was validated on NanoDrop™ One^c (Thermo Fisher Scientific).

Extracted leaf RNA was cleaned of DNA and reverse-transcribed to cDNA using DNA-free™ DNA removal kit (Invitrogen, Waltham, Massachusetts, USA, AM1906) and Reverse Transcription System (Promega, A3500), respectively, both times according to the following manufacturer's instructions. For DNA removal, 1.5 µg RNA in 2.59 µl was mixed with 1 µl 10x DNase I Buffer and 1 µl of rDNase I together with 5.41 µl ddH₂O. The mixture was incubated for 30 minutes at 37°C. 2 µl of resuspended DNase Inactivation Reagent were added and mixed. The tube was incubated for 2 minutes at room temperature and mixed occasionally. The tubes were centrifuged to pellet the DNase inactivation reagent and the solution was transferred to a fresh microtube. Then, the reverse transcription was carried out as follows. 4 µl RNA (150 ng.µl⁻¹) and 1 µl oligo(dT)₁₅ primer (500ng.µl⁻¹) were mixed and put to 70°C block for 5 minutes and then immediately chilled on ice for 5 minutes. Then, reverse transcription reaction master mix consisting of 7.3 µl of nuclease-free water, 4 µl ImProm-II™ 5× Reaction Buffer, 1.2 µl of 25 mM MgCl₂, 1 µl of 10 mM dNTP mix, 0.5 µl of Recombinant Rnasin® Ribonuclease Inhibitor and 1 µl of ImProm-II™ Reverse Transcriptase was prepared and added to each RNA sample in 15 µl aliquots. The tubes were incubated at 25°C for 5 minutes and moved to 42°C for 1 hour. Finally, the samples were incubated at 70°C for 15 minutes. The concentration of the synthesized cDNA was measured on Nanodrop.

Construct preparation

Gateway cloning was selected for the preparation of constructs and was conducted according to Gateway® Technology with Clonase™ II protocol (Invitrogen, Carlsbad, California, USA). Firstly, specific primers for the amplification of two *A. thaliana* NACβ and five *A. thaliana* NACα genes were designed *in silico*. Forward primers started at the start codon of each gene and reverse primers were designed into the 3'UTR (untranslated region) site. For the purposes of Gateway cloning, the primers consisted of gene-specific sequences linked with the attB recombination site - attB1F (forward primer) and attB2R (reverse primer), respectively. The whole set of primers is in the figure 8. Also, attB site-specific primers attB1F and attB2R were designed for the amplification of recombination sites (fig. 8). Specificity of the primers was checked on the leaf cDNA by polymerase chain reaction (PCR) with Taq

Figure 8: Primer pairs used in PCR to synthesize DNA fragments for Gateway cloning for Y2H. *attB* site-specific sequence in the gene-specific primers is highlighted in red.

Primers used in Gateway cloning for Y2H			
gene ID	gene name	primer name	primer sequence
At1g17880	NACbeta2	At1g17880_attB1F	AAAAAGCAGGCTGGATGAATAGGGAGAAGTTGATGAAG
		At1g17880_attB2R	AGAAAGCTGGGTAAAGAAGAAGCAGCAGCAGCT
AT1g73230	NACbeta1	AT1g73230_attB1F	AAAAAGCAGGCTCGATGAATAGGGAAAAAGTTGATGAAG
		AT1g73230_attB2R	AGAAAGCTGGGTAAAGAAGCAGCAGCTTTGGGAGC
At1g33040	NACalpha5	At1g33040_attB1F	AAAAAGCAGGCTACATGCCAGGAGCAATTGTGGAG
		At1g33040_attB2R	AGAAAGCTGGGTGTGTAGTGAGTTCATAATGGCTG
At3g12390	NACalpha1	At3g12390_attB1F	AAAAAGCAGGCTCCATGACTACCGAAGAGAAAGA
		At3g12390_attB2R	AGAAAGCTGGGTGGTGGTAAGCTCCATGATGG
AT3g49470	NACalpha2	At3g49470_attB1F	AAAAAGCAGGCTATATGTCTCCTCCTGCTG
		At3g49470_attB2R	AGAAAGCTGGGTGAGTAGTGAGTTCATTATTGC
At4g10480	NACalpha4	At4g10480_attB1F	AAAAAGCAGGCTCTATGCCAGGTCCAGTTATTGAG
		At4g10480_attB2R	AGAAAGCTGGGTCTGTAGTGAGTTCATAATGGC
At5g13850	NACalpha3	At5g13850_attB1F	AAAAAGCAGGCTCCATGACTGCCGAACAGAAAG
		At5g13850_attB2R	AGAAAGCTGGGTGGTGGTAAGCTCCATGATG
		attB1F	GGGGACAAGTTGTACAAAAAGCAGGCT
		attB2R	GGGGACCACTTTGTACAAGAAGCTGGGT

DNA polymerase (Merciáza, Merci s.r.o, 10005) on the cycler (Eppendorf Mastercycler Nexus, 6331000017). The PCR conditions were as follows 94°C/2 min initial denaturation, 40 cycles: 94°C/30 s denaturation, 55°C/30 s primer annealing, and 72°C/90 s extension; 72°C/5 min final extension, 4°C hold. The reaction was prepared as follows: for one reaction 1µl of template leaf cDNA (concentration 200 ng.µl⁻¹), 2.5 µl of Merci Buffer (10x Merciáza reaction Buffer, Merci s.r.o, 300419, final conc. 1×), 0.5 µl of dNTPs (10 mM stock solution, 0.2 mM final concentration each, Thermo Scientific, R0192), 1 µl of forward primer (10 µM stock solution, final concentration 0.4 µM), 1 µl of reverse primer (10 µM stock solution, final concentration 0.4 µM), 0.15 µl of Taq polymerase (concentration 5U. µl⁻¹; 1.5 U per reaction) and 18.85 µl of ddH₂O. 5 µl of 6x DNA Loading dye (Thermo Scientific, R0611) was added to each sample after amplification and the samples were electrophoresed on 1.2 % agarose (SERVA for DNA electrophoresis, SERVA, 11404.07) gel in 1× TAE with ethidium bromide.

After the primer specificity was checked, preparation of amplified DNA fragments for Gateway cloning proceeded. Phusion High-Fidelity DNA Polymerase (Thermo Fisher, F530S) was used for the double step amplification. In the first step PCR, gene-specific primers were used, the reaction mix was prepared in the following manner: 1 µl of leaf cDNA (concentration 200 ng. µl⁻¹), 0.3 µl of Phusion polymerase (stock solution 2 U. µl⁻¹, final 0.6 U), 5 µl of 5× HF Buffer (Thermo Fisher, F530S), 1 µl of forward primer (10 µM stock solution, final concentration 0.4

μM), 1 μl of reverse primer (10 μM stock solution, final concentration 0.4 μM), 0.5 μl of dNTPs (10 mM stock solution, 0.2 mM final concentration each), 16.2 μl of ddH₂O. The PCR cycling conditions were as follows: 98°C/1 min, 10 cycles: 98°C/20 s, 55°C/30 s, and 72°C/1 min; 72°C/ 10 min; 4°C hold. The first round of PCR was followed by a second PCR run, primed by attB site-specific attB1F and attB2R primers. The reaction components were as follows: 5 μl of 1st PCR, 0.6 μl of Phusion polymerase (stock solution 2 U. μl^{-1} , final 1.2 U), 10 μl of 5× HF Buffer, 4 μl of forward attB1F primer (10 μM stock solution, final concentration 0.8 μM), 4 μl of reverse attB2R primer (10 μM stock solution, final concentration 0.8 μM), 1 μl of dNTPs (10 mM stock solution, 0.2 mM final concentration each), 25.4 μl of ddH₂O. 50 μl of PCR reaction with 10 μl of 6x DNA loading dye were subsequently loaded onto 1.2% agarose gel and electrophoresed (100 V until the blue line reached the front, approx. 90 min) as above. The fragments corresponding to gene length were extracted from the gel using GeneJet gel extraction kit (Thermo Scientific, Waltham, Massachusetts, U.S., K0691). Firstly, the slice containing DNA fragment was excised from the gel under the UV lamp by a razor blade, placed into pre-weighed Eppendorf tube and weighed. 1.5:1 (buffer volume: gel weight) of Binding Buffer was added to each sample and left in 55°C until the gel became completely dissolved. 800 μl of the solubilized gel was then transferred into the GeneJet purification column and centrifuged for 1 min, 13 000 × g. The flow-through was discarded, and 700 μl of Wash Buffer was added into the GeneJET purification column and centrifuged with the same settings. Again, the flow-through was discarded and the tubes were centrifuged for another 1 minute. The DNA was eluted with 30 μl of Elution buffer to a new Eppendorf tube. The procedure resulted in amplified DNA purified into Elution buffer. The purity and integrity of DNA was checked by 1.2% agarose gel electrophoresis with ethidium bromide performed as above. The DNA concentration was measured on NanoDrop™ One^c (Thermo scientific).

Gateway™ cloning

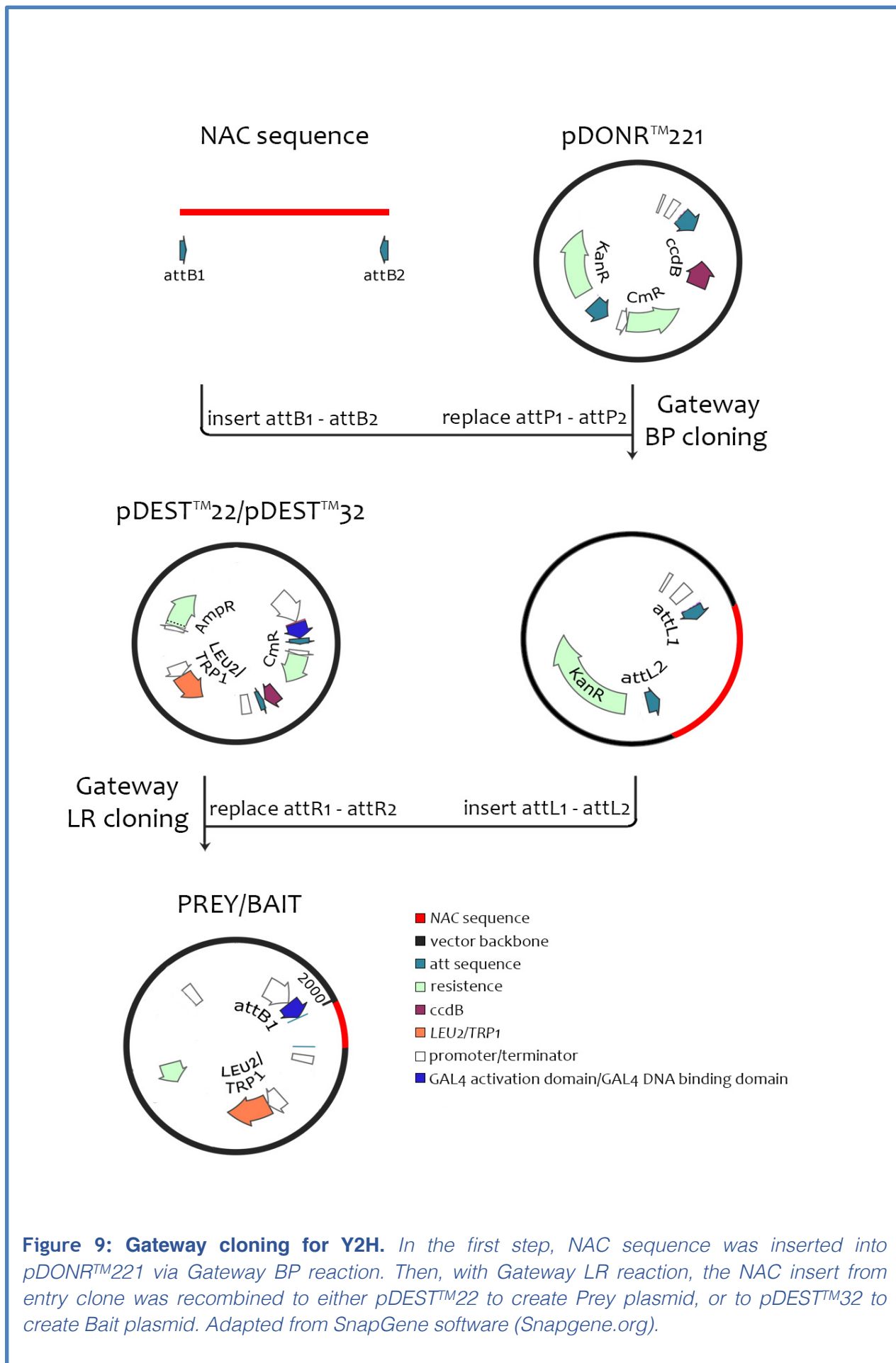
BP reaction and E.coli transformation

Gateway® pDONR™221 (Gateway® pDONR™221 Vector (12536017); Invitrogen) was selected as an entry vector for the cloning. It bears the attP1 and attP2 sites for the homologous recombination with attB1 and attB2 sites on the

amplified DNA fragments (fig.9). The BP recombination reaction was conducted by Gateway BP clonase II enzyme mix (Invitrogen) using 75 ng vector DNA and 75 ng insert DNA. TE Buffer (1mM Tris, 1mM EDTA, pH 8.0) was added to final volume of 5 μ l. One μ l of Gateway BP clonase II enzyme mix was added to each reaction. The samples were incubated at 25°C for 18 hours. Then, 1 μ l proteinase K was added to each sample and incubated for 10 minutes at 37°C.

The constructs were then transformed into the home-made *E. coli* TOP10 chemically competent cells (Invitrogen, C404006) as follows. 2.5 μ l of the terminated BP reaction was mixed with 50 μ l of competent cells in the Eppendorf tube and then incubated on ice for 30 minutes. The mixtures were heat-shocked in 42°C water bath for 30 seconds and placed on ice for another 2 minutes. 250 μ l of S.O.C media (0.5 mM Yeast Extract Powder (MP Biomedicals, 103303), 2.0 mM tryptone (Sigma-Aldrich, 91079-40-2), 10 mM potassium chloride (Serva, 26868), 2.5 mM magnesium chloride (Sigma-Aldrich, 7786-30-3), 20 mM α -D- glucose (SERVA, 50-99-7)) was added to the tubes and incubated for 60 minutes at 37°C, 160 rpm. The cells were then spread on the LB agar (for one litre of medium: 20 g agar (Sigma-Aldrich, 05040-1KG), 10 g NaCl (Sigma-Aldrich, S9888), 10 g tryptone (Sigma-Aldrich, T7293-250G), 5 g yeast extract powder (MP Biomedicals, 103303)) plates including kanamycin 50ng.ml⁻¹ (Kanamycin monosulfate, Duchefa Biochemie, K0126.0010) and left to grow overnight at 37°C.

The identity of the transformants was proved with the colony PCR. Eight colonies of each construct were selected for verification. Taq DNA polymerase and gene-specific primers designed for cloning were used for the colony PCR. Each selected colony was stroked with lab tip and the cells were transferred into the prepared PCR regencies (2.5 μ l 10 \times Merck Buffer, 1 μ l of forward primer (10 μ M stock solution, final concentration 0.4 μ M), 1 μ l of reverse primer (10 μ M stock solution, final concentration 0.4 μ M), 0.15 μ l Taq polymerase (concentration 5U. μ l⁻¹; final 1.5 U), 0.5 μ l of dNTPs (10 mM stock solution, 0.2 mM final concentration each), 19.85 μ l of ddH₂O) and amplified under these conditions: 94°C/5 min; 40 cycles: 94°C/1 min, 55°C/1 min, 72°C/90 s; 72°C/5 min; 4°C hold. 5 μ l of loading dye were then added to the reaction, and subsequently 10 μ l of this mixture were loaded onto the 1.2% agarose gel with ethidium bromide and electrophoresed under the same conditions as above.

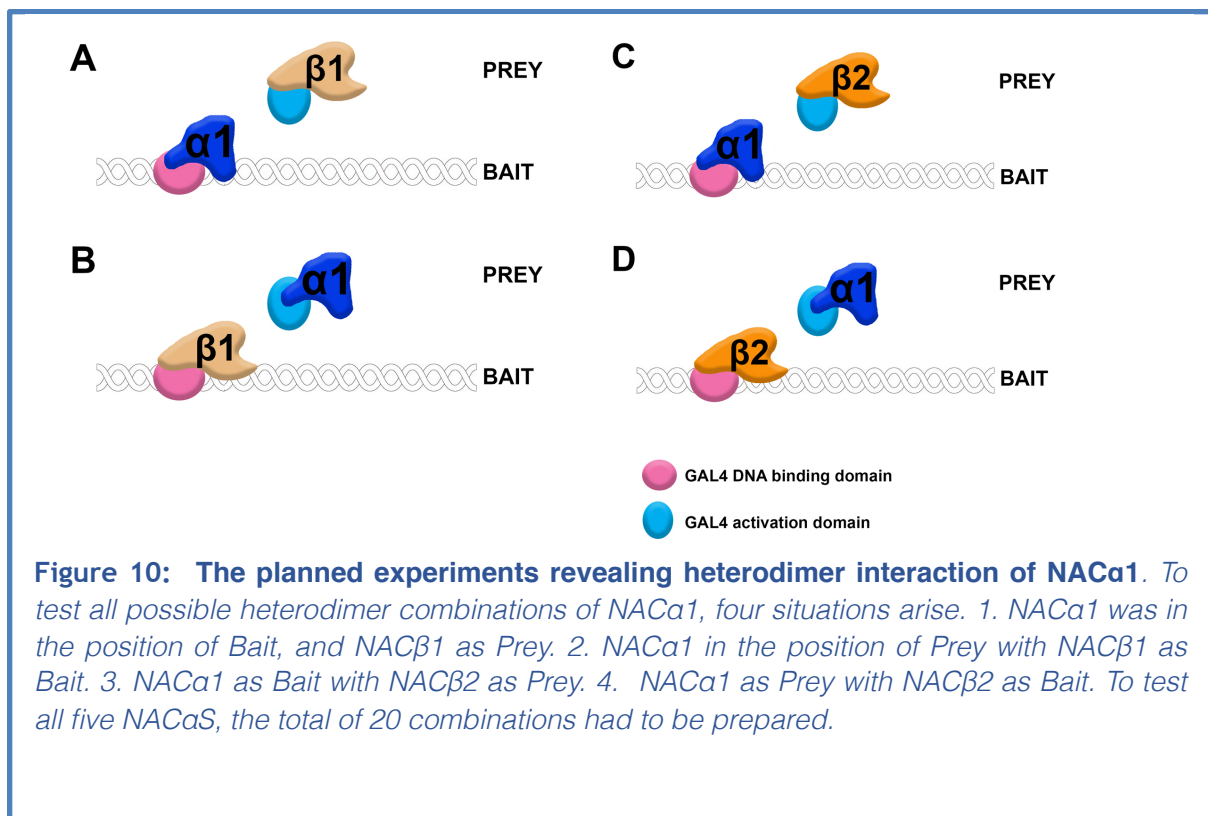


Two verified colonies of each construct were inoculated to the liquid LB media (LB Broth high salt, for one litre of medium: 10 g NaCl, 10 g tryptone, 5 g yeast extract powder) with kanamycin (50ng.ml⁻¹) and cultivated for 16 hours at 37°C with 180 rpm shaking and the grown suspension was used for plasmid extraction with GeneJet plasmid miniprep kit (Thermo Scientific, Waltham, Massachusetts, USA, K0502). Firstly, 5 ml of LB culture was centrifuged (2 mins, 5000× g) to pellet the cells, which were then resuspended in 250 µl Resuspension Solution in the 1.5 ml Eppendorf tube. 250 µl Lysis solution was added, and the tubes were inverted 6 times to mix the solutions. 350 µl Neutralization Solution was added, and the solution was mixed again by inverting the tubes 6 times. The tubes were then centrifuged for 5 mins, 13 000× g. 850 µl of supernatant was transferred into the GeneJET spin columns by pipetting. The tubes were centrifuged for 1 min (same conditions) and the flow-through was discarded. The columns were washed with 500 µl of Wash Solution and spun for another minute. This step was repeated once more with 500 µl of Wash Solution. After the removal of the flow-through, the tubes were spun for another minute. GeneJET spin columns were then transferred into the fresh Eppendorf tubes and the DNA was eluted with 30 µl Elution buffer. The concentration of extracted plasmid DNA was measured by Nanodrop™ One^c. The plasmid integrity was then validated using the 1.2 % agarose gel electrophoresis with ethidium bromide. The sequence of the cloned DNA fragment was verified by Sanger sequencing (Eurofins Genomics, Ebersberg, Germany) and *in silico* alignment of the acquired sequencing data (SnapGene software, from GSL Biotech; available at snapgene.com).

LR reaction

Plasmids pDEST™32 and pDEST™22 were used as destination vectors. They contain attR1 and attR2 sites for recombination with attL1 and attL2 sites on pDONR™221 entry clones with NAC sequences (fig. 9). pDEST™32 bears GAL4 DNA binding domain, thus serves as a bait in the Y2H system and introduces the gene *TRP1*. pDEST™22 with GAL4 activation domain serves as prey and introduces the gene *LEU2*. In MaV203 strain genome, both mentioned genes (*TRP1* responsible for tryptophan synthesis, and *LEU2* taking part in leucin synthesis) bear a deletion, so untransformed cells are unable to grow on medium lacking tryptophan and leucin. After transformation, these genes are introduced to the cells and they are able to

synthesize histidine and uracil. This feature is later used as a marker for successful transformation of yeasts since on the media lacking leucin and tryptophan survive only transformants carrying both plasmids. In our experimental design, all 5 NAC α and both NAC β genes were cloned to both pDESTTM23 and pDESTTM22 destination vectors to be able to check their interaction crosswise. GatewayTM LR ClonaseTM II Enzyme mix (Thermo Scientific, 11791020) was used for the site-specific recombination. The LR recombination reaction was mixed using 50 ng of entry plasmid and 50 ng destination vector and 1 μ l of LR clonase II and incubated at 25°C for 18 hours. *E. coli*, strain TOP10 chemically competent cells were transformed by the LR reaction under the above conditions (see section BP reaction). This time, the antibiotics selection was different, ampicillin 100 ng.ml⁻¹ (ampicillin sodium, Duchefa Biochemie, A0104) for pDESTTM32 and gentamicin 10 ng.ml⁻¹ (gentamicin sulfate, Duchefa Biochemie, G0124.0010) for pDESTTM22. Also, the colony PCR, electrophoresis, cultivation in liquid media, plasmid isolation, and verification of plasmid purity and integrity was executed in the same manner as after the BP recombination reaction (see above).



Interaction partners and design of controls

For the first round of experiments, interaction between NAC heterodimers was tested. Therefore, the combinations of NAC β and NAC α plasmids were transformed into yeast (*Saccharomyces cerevisiae*), strain MaV203. To avoid experimental artefacts caused by random binding of DNA binding domain or activation domain, the combinations were transformed in both constellations - i.e. both β -preys were co-transformed together with every α -bait and on the contrary, both β -baits were co-transformed with every α -prey (fig. 10). Thus, there were in total 20 combinations to be tested. In the second round of experiments, the formation of homodimers was tested. Again, the potential interacting partners were transformed in both directions, resulting in the total of 29 combinations.

To support the results with credible controls, each prey plasmid for either β - or α -NAC was co-transformed with empty pDESTTM32 and each bait plasmid was co-transformed with empty pDESTTM22 to avoid false positive results, caused by random binding of activation domain to DNA or auto-activation of DNA binding domain. Furthermore, commercial controls from Thermo-Fisher Scientific ProQuestTM System (PQ1000101) were performed as described in fig. 11. K1 controls bear no plasmids, so these cells will not grow on SC-Leu-Trp medium. K2 strong positive interaction control represents a combination of plasmids with proved strong interaction designed by the manufacturer, namely pEXPTM32 with Krev1 and

LEU2 Plasmid	TRP1 Plasmid	Purpose
K1 none	none	Negative transformation control
K2 pEXP TM 32/Krev1	pEXP TM 22/RalGDS-wt	Strong positive interaction control
K3 pEXP TM 32/Krev1	pEXP TM 22/RalGDS-m1	Weak positive interaction control
K4 pEXP TM 32/Krev1	pEXP TM 22/RalGDS-m2	Negative interaction control
K5 pDEST TM 32	pDEST TM 22	Negative activation control
K6 Bait plasmid	pDEST TM 22	Negative activation control
K7 pDEST TM 32	Prey plasmid	Negative activation control

Figure 11: Controls for Y2H provided in Thermo-Fisher Scientific ProQuestTM System.

pEXPTM22 with RalGDS-wt. This control should be positive on all selective media. For weak positive interaction control K3, point mutation was introduced to RalGDS sequence, weakening the interaction with Krev1. This control should be positive on all selective media apart from the medium lacking uracil and in x-gal assay. K4 negative interaction control has stronger mutation in RalGDS, which subsequently ceases to interact with Krev1. K5 control consists of empty pDESTTM32 plasmid in combination with empty pDESTTM22 plasmid and serves as negative activation control, proving that DNA binding domain is not activated by DNA activation domain without the formed interaction.

Yeast transformation

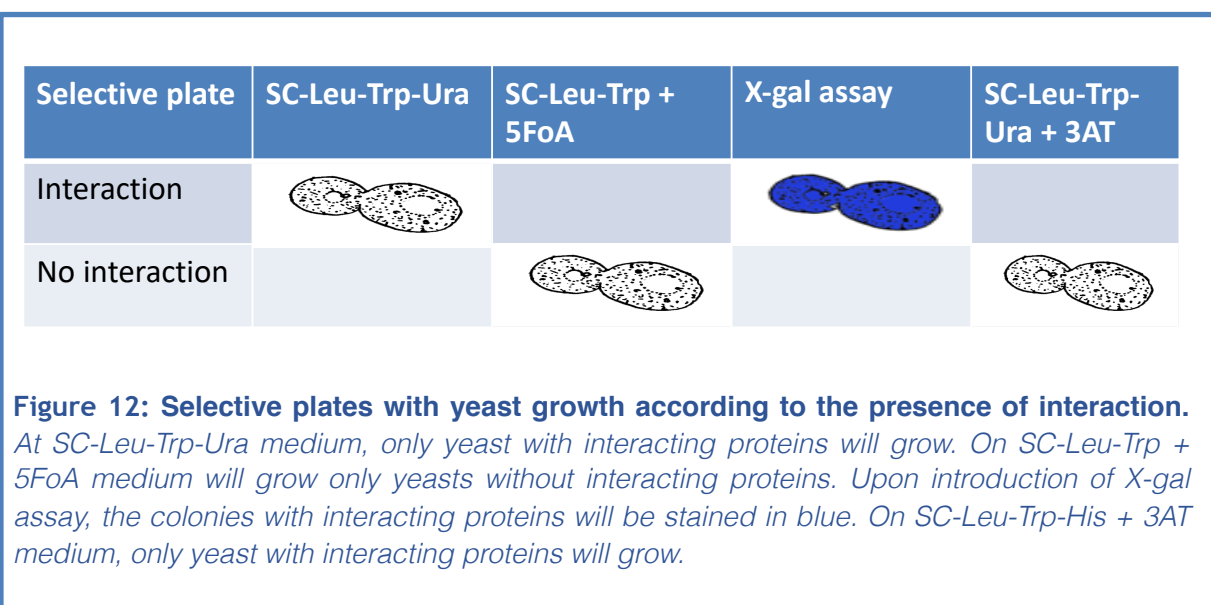
Yeast transformation was performed according to ProQuestTM Two-Hybrid System (Ver. A, Invitrogen, PQ10001-01, PQ10002-01) protocol. Firstly, the competent cells were prepared. Commercially obtained glycerol of the MaV203 strain was spread on plates with YPAD medium (yeast extract powder (1% w/v MP Biomedicals, 103303), 2% w/v peptone (Fluka analytical, 70172-500G), 2% w/v sucrose (Serva, 161135), 0,01% w/v adenine hemisulfate salt (Sigma, A9126-25G), pH adjusted to 6 with HCl, 2% w/v agar (Sigma-Aldrich, 05040-1KG)) and grown overnight at 30°C. One grown colony was transformed to 5ml liquid YPAD media (1% w/v Yeast Extract Powder, 2% w/v peptone (Fluka analytical, 70172-500G), 2% w/v sucrose (Serva, 161135), 0.01% w/v adenine hemisulfate salt (Sigma, A9126-25G), pH adjusted to 6 with HCl) and cultivated at 30°C for 16 hours with shaking at 160 rpm. The overnight culture was diluted to OD₆₀₀ = 0.4 in 50 ml of YPAD and cultivated for another 3 hours at 30°C. The cells were pelleted by centrifugation for 10 minutes at 1125x g and resuspended in 40 ml 1x TE Buffer (10 mM Tris, 1 mM EDTA, pH 7.5). The cells were pelleted once more under the same conditions and resuspended in 1 ml of 1X LiAc/0.5X TE (for 100ml: 10 ml of 1 M lithium acetate (Sigma-Aldrich, 517992-100G), 5 ml of 10x TE (100mM Tris, 10mM EDTA), 85 ml H₂O) and then incubated for 10 minutes at 30°C. For each transformation, 500 ng of both plasmid DNA (bait and prey) and 100 µg of denaturated sheared salmon sperm DNA (Thermo Fisher Scientific, AM9680) were mixed with 100 µl of the prepared yeast suspension. 700µl of 1X LiAC/40% PEG-3350/1x TE (for 100 ml: 10 ml of 1 M

lithium acetate, 10 ml 10xTE, 40 g PEG-3350 (Biogen, 19760)) was added to the mixture and mixed well. The cells were then incubated for 30 minutes at 30°C. 88 µl of sterile dimethyl sulfoxide (DMSO, Roth, 7029.1) was added to the suspension and the yeast cells were heat-shocked at 42°C for 7 minutes. Then the tubes were centrifuged in the microcentrifuge for 10 seconds and the supernatant was removed by pipetting. Finally, the pellet was resuspended in 100 µl TE and plated on synthetic complete (SC) leucin and tryptophan drop out medium (SC-Leu-Trp, 0.67% BD Difco™ yeast nitrogen base without amino acids (Fisher Scientific, DF0919-15-3), 0.135% -Leu/-Trp DO supplement (Clontech, 630417), 2% sucrose, 2% agar) plates. The plates were incubated overnight at 30°C. For the test of heterodimer formation, three independent transformations were carried out, whereas two independent transformations were performed in the case of homodimers.

The preparation of yeast selective media

For the observation of formed interactions, the above-mentioned yeast (*Saccharomyces cerevisiae*) MaV203 strain was used. To test the expression of reporter genes showing protein interaction, the following media were prepared.

To check whether the transformation was successful, the yeast cells were planted on SC-Leu-Trp medium. All yeasts carrying both pDEST™32 and pDEST™22 plasmids should grow on this media regardless of which gene (if any) was inserted



to the plasmid since pDESTTM32 introduces *LEU2* gene (gene responsible of the synthesis of leucine) and pDESTTM22 introduces *TRP1* gene (gene responsible of the tryptophan synthesis) to the yeast strain originally lacking these genes.

The first selection was represented by SC-Leu-Trp-Ura selective plates (0.67% yeast nitrogen base without amino acids (BD DifcoTM, cat. n. DF0919-15-3), 0.064% - Leu/-Trp/-Ura DO supplement (Clontech, cat. n. 630424), 2% agar (Sigma-Aldrich, cat.n. BCBX4391), 2% dextrose, pH adjusted by NaOH to 5.9) where only yeast cells expressing the interacting proteins should grow, since after the interaction, *URA3* begins to be expressed (fig. 12). Secondly, the SC-Leu-Trp plates containing 0.2% 5-fluoroorotic acid (5FoA, Thermo Scientific, R0812) acid were prepared. Inducing *URA3* will cause formation of toxic 5-fluorouracil, so no cells will grow on 5FoA plates in case of interaction formation. For the third verification, x-gal assay (interaction results in accumulation of blue pigment in cells, described later) was used to determine the enzymatic activity of *LacZ* expressed in yeasts bearing the interacting proteins. Last, SC-Leu-Trp-His medium was supplied with 3-amino-1,2,4-triazole (3AT, Fluka, 09540) in the concentrations of 10mM, 50 mM, 75 mM, and 100 mM, resulting with four selective plates. Since 3AT acts as an inhibitor in dose-dependent manner of histidine synthesis, various concentrations will be applied to establish the tolerance threshold. With the tolerance threshold concentration of 3AT, only cells with specific interactions will grow under these conditions. On the contrary, the background unspecific growth under a too low 3AT concentration or unspecific growth suppression due to excessive concentration of 3AT will be excluded. The validation of protein interaction should then be determined more precisely.

Auxotrophic selection and observation

The colonies grown on SC-Leu-Trp media one day after transformation were re-stroked to new SC-Leu-Trp plates to create master plates for replica plating on individual selective plates. 4 strokes of different colonies for each bait-and-prey combination and control with bait and empty pDESTTM32 were done, 2 strokes on the same plate were made for each other control (fig. 13). The master plates were then incubated at 30°C for 24 hours. Then, the master plates were replica-plated on individual selective media - SC-Leu-Trp-His+3AT (four different concentrations:

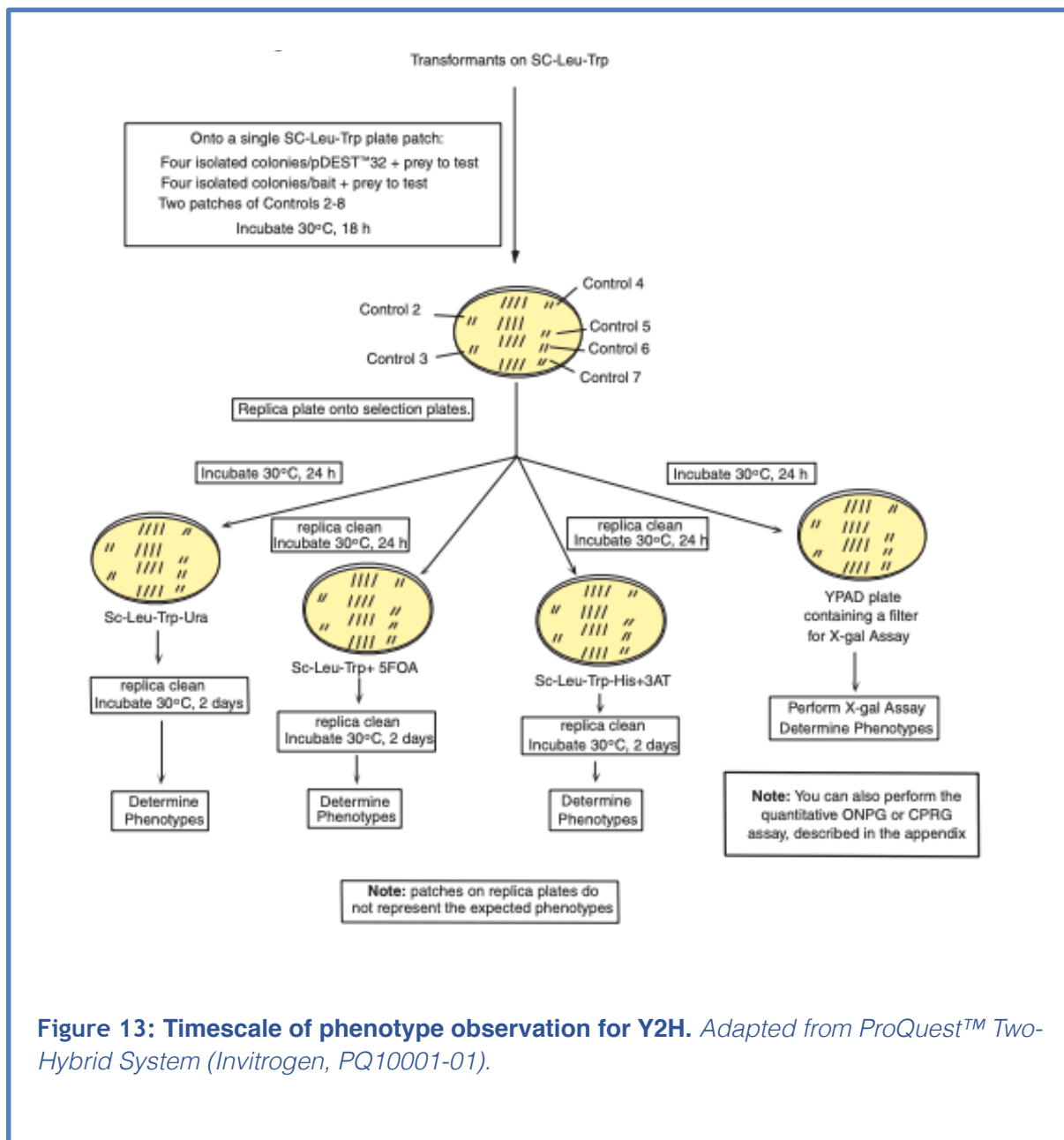


Figure 13: Timescale of phenotype observation for Y2H. Adapted from ProQuest™ Two-Hybrid System (Invitrogen, PQ10001-01).

10 mM, 25 mM, 50 mM, and 100 mM), SC-Leu-Trp-Ura, YPAD for x gal assay and SC-Leu-Trp+5FoA. The colonies on YPAD medium were covered with nitrocellulose membrane. Plates containing 3AT were replica cleaned before incubation. The replicas were then incubated at 30°C for 24 hours. YPAD medium was then analysed by x-gal assay as mentioned later. SC media were replica cleaned and left in 30°C for another two days. After this time, the phenotype of yeast colonies was determined (fig. 13).

LacZ assay

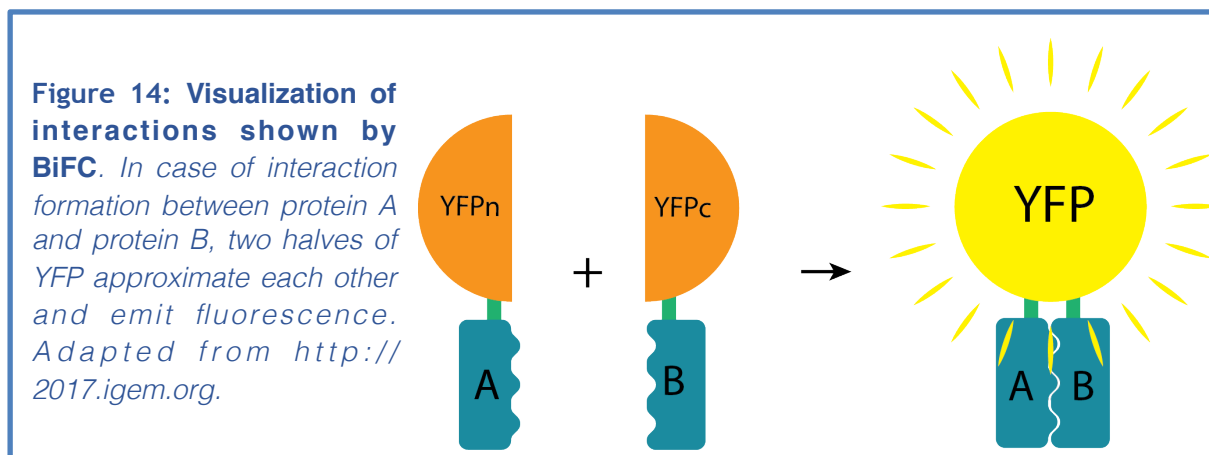
LacZ assay was performed according to manufacturer's instructions as follows. The master plate was replica plated on YPAD plate which was then covered with nitrocellulose membrane (Thermo Scientific, TD2496201). For each reaction,

10 mg X-gal (5-bromo-4-chloro-3-indolyl- β -D-galactopyranoside, MP Biomedicals, 150001) in 100 μ l dimethyl sulfoxide (DMF, Carl Roth GmbH + Co, 7029.1) was mixed with 60 μ l 2-mercaptoethanol and 10 ml Z buffer (60mM $\text{Na}_2\text{HPO}_4 \cdot 7\text{H}_2\text{O}$ (Sigma-Aldrich, 431478), 40mM $\text{NaH}_2\text{PO}_4 \cdot \text{H}_2\text{O}$ (Sigma-Aldrich, S9638), 10mM KCl (Serva, 26868), 1mM $\text{MgSO}_4 \cdot 7\text{H}_2\text{O}$ (MERCK, 1.05886.), pH 7.0). Two 90mm Whatman™ filters were placed into glass Petri dish and saturated with 10 ml X-gal solution. All bubbles were removed by forceps. The nitrocellulose membrane was carefully removed from the plate by forceps and immediately soaked into the liquid nitrogen, where it was held for 30 seconds. Then, it was placed into the Petri dish on top of the filter papers with the colony side up. The plates were covered and incubated at 37°C for 24 hours. The appearance of blue staining was caused by the cleavage of X-gal by β -galactosidase giving rise to 5,5'-dibromo-4,4'-dichloro-indigo. The appearance of blue staining was monitored after 1, 2 and 24 hours of incubation.

Bimolecular fluorescence complementation

Introduction to the method

Bimolecular fluorescence complementation (BiFC) is an *in vivo* detection method revealing protein-protein interactions, which are visualized via fluorescence. The sequence of each tested gene is fused with one half of YFP tag and then transiently expressed in *Nicotiana benthamiana* leaves. Only if the proteins interact, the two halves of YFP can reach the necessary proximity to bind together and emit fluorescence (fig. 14).



BiFC construct preparation

The construct preparation and cloning were performed in the same way as in the Y2H with several modifications. This time, reverse primers were designed to amplify only coding sequence without STOP codon (since the fused tag was localized in the C-terminus of the construct), whereas the forward primers started with the START codon. Two sets of primers for each NAC paralogue were designed (fig. 15). Gateway cloning-specific sites were represented by attB1 and attB3 sites in the forward primers, and attB4 and attB2 in the reverse primers. The forward primer with attB1 sequence and the reverse primer with attB4 site were used for

Primers used in Gateway cloning for BiFC			
gene ID	gene name	primer name	primer sequence
At1g17880	NACβ2	At1g17880_attB1F	AAAAAGCAGGCT GGATGAATAGGGAGAAGTTGATGAAG
		At1g17880_attB4R	TGTATAGAAAAGTTGGGTG AGAAGAAGCAGCAGCAGCTGGTGC
		At1g17880_attB3F	ATAATAAAGTTGCGATGAATAGGGAGAAGTTGATGAAG
		At1g17880_attB2R	AGAAAGCTGGGT AAGAAGAAGCAGCAGCAGCT
AT1g73230	NACβ1	At1g73230_attB1F	AAAAAGCAGGCT CGATGAATAGGGAAAAGTTGATGAAG
		At1g73230_attB4R	TGTATAGAAAAGTTGGGTG AGTTGCAGCAGCTTTGGGAGCC
		At1g73230_attB3F	ATAATAAAGTTGCAATGAATAGGGAAAAGTTGATGAAG
		At1g73230_attB2R	AGAAAGCTGGGT AAGAAGCAGCAGCTTTGGGAGC
At1g33040	NACα5	At1g33040_attB1F	AAAAAGCAGGCT ACATGCCAGGAGCAATTGTGGAG
		At1g33040_attB4R	TGTATAGAAAAGTTGGGTG TGTAGTGAGTTCATAATGGCTG
		At1g33040_attB3F	ATAATAAAGTTGATATGCCAGGAGCAATTGTGGAG
		At1g33040_attB2R	AGAAAGCTGGGTGTGTAGTGAGTTCATAATGGCTG
At3g12390	NACα1	At3g12390_attB1F	AAAAAGCAGGCT CCATGACTACCGAAGAGAAAGA
		At3g12390_attB4R	TGTATAGAAAAGTTGGGTG GGTGTAAGCTCCATG
		At3g12390_attB3F	ATAATAAAGTTGCAATGACTACCGAAGAGAAAGA
		At3g12390_attB2R	AGAAAGCTGGGTTGGTGGTAAGCTCCATGATGG
AT3g49470	NACα2	At3g49470_attB1F	AAAAAGCAGGCT ATATGTCTCCTCCTCTGCTG
		At3g49470_attB4R	TGTATAGAAAAGTTGGGTG AGTAGTGAGTTCATTATTGC
		At3g49470_attB3F	ATAATAAAGTTGACATGTCTCCTCCTCTGCTG
		At3g49470_attB2R	AGAAAGCTGGGTCAGTAGTGAGTTCATTATTGC
At4g10480	NACα4	At4g10480_attB1F	AAAAAGCAGGCT CTATGCCAGGTCCAGTTATTGAG
		At4g10480_attB4R	TGTATAGAAAAGTTGGGTG TGTAGTGAGTTCATAATGGC
		At4g10480_attB3F	ATAATAAAGTTGCGATGCCAGGTCCAGTTATTGAG
		At4g10480_attB2R	AGAAAGCTGGGTCTGTAGTGAGTTCATAATGGC
At5g13850	NACα3	At5g13850_attB1F	AAAAAGCAGGCT CCATGACTGCCGAACAGAAAG
		At5g13850_attB4R	TGTATAGAAAAGTTGGGTG GGTGTAAGCTCCATGATG
		At5g13850_attB3F	ATAATAAAGTTGCCATGACTGCCGAACAGAAAG
		At5g13850_attB2R	AGAAAGCTGGGTTGGTGGTAAGCTCCATGATG
		AttB3F	GGGGACAACCTTTGTATAATAAAGTTGCT
		AttB4R	GGGGACAACCTTTGTATAGAAAAGTTGGGTG

Figure 15: Primer pairs used in Gateway cloning for BiFC. *attB site-specific sequence is highlighted in red.*

amplification of constructs, which will be finally inserted in fusion with N-terminal half of yellow fluorescence protein (further referred to as nYFP). On the other hand, the forward attB3 and the reverse attB2 primer will be used for the amplification of the gene to be inserted in frame with C-terminal half of YFP (further referred to as cYFP). Primer testing, cDNA amplification and fragment gel extraction was carried out in the same way as in Y2H.

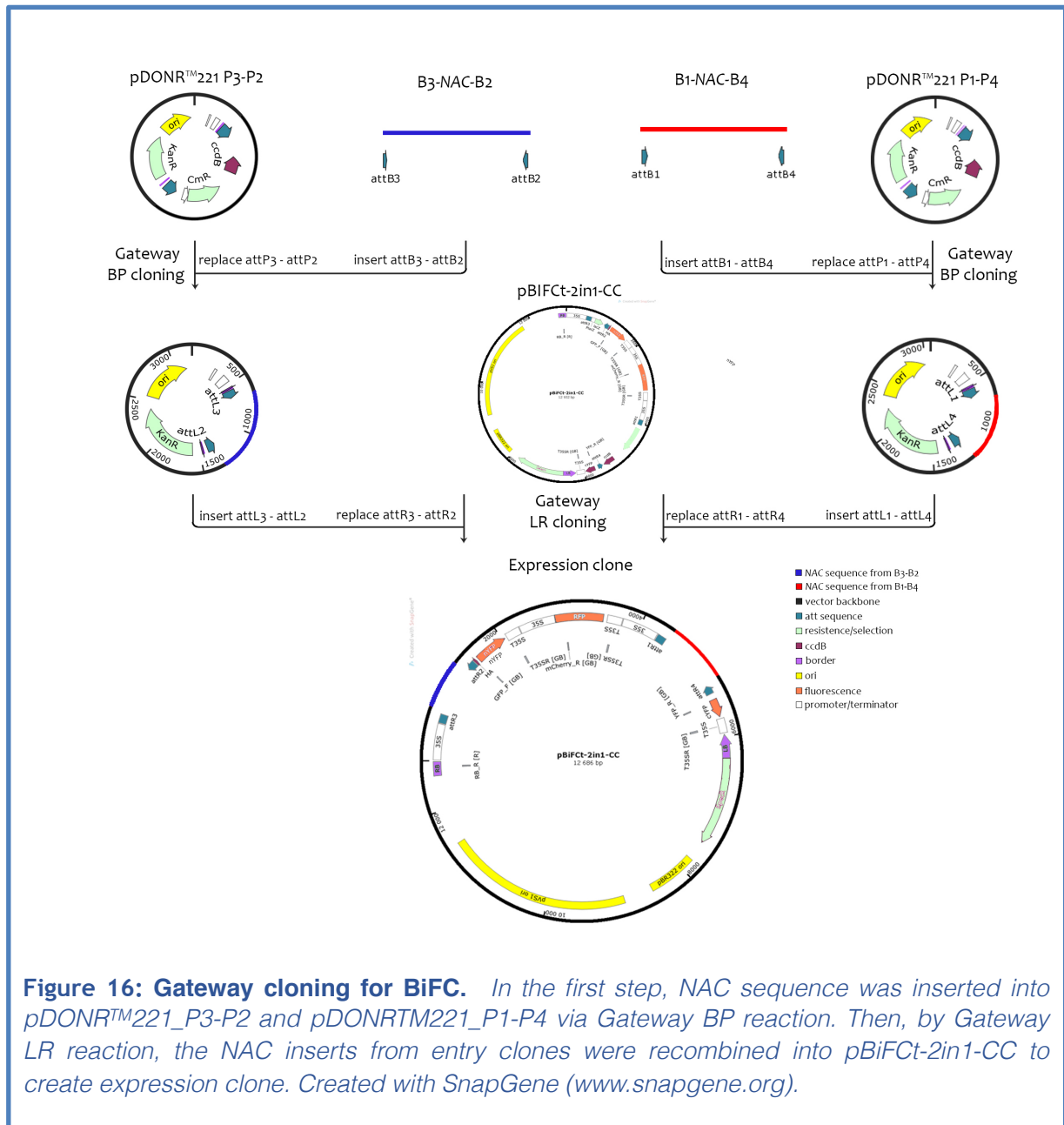
Gateway cloning

BP reaction

pDONRTM211_P3-P2 (contained attP3, and attP2 sites) and pDONRTM211_P1-P4 (contained attP1, and attP4 sites) were used as entry clones for BP reaction (fig. 16). Each gene was cloned into both entry vectors, every time with the respective attB sites, resulting in the total of 14 entry clones. The bacteria transformation, colony PCR, plasmid isolation, and its verification by Sanger sequencing were performed in the same way as above for the Y2H system. Kanamycin (50 µg.ml⁻¹) was used for selection of both entry clones.

LR reaction

Two-site destination vector BiFC-2in1-CC was used to prepare the expression clones. This vector contains two pairs of attR recombination sites - attR3 and attR2 to recombine with pDONRTM211_P3-P2, and attR1 and attR4 to recombine with pDONRTM211_P1-P4. attR3-attR2 site is in frame with nYFP sequence, and attR1-attR4 is in frame with cYFP sequence. When expressed, both halves of YFP will be fused with C-terminus of tested proteins. For the control of successful transformation, *ccdB* gene is originally inserted between attR1-attR4 sites and *lacZ* between attR3-attR2 sites. *ccdB* gene encodes toxin which acts as gyrase poison in *E. coli*, and so only cells with excised *ccdB* gene will survive. *LacZ* expression enables blue-white detection of transformants on plates containing X-gal and IPTG by forming indigo 5,5'-dibromo-4,4'-dichloro-indigo pigment, which will accumulate as a blue stain in transformed cells with interacting proteins. The vector also carries the sequence encoding red fluorescence protein (RFP) for the detection of *Agrobacterium* infiltration (fig. 16). Again, all combinations of NAC α and NAC β heterodimers were cloned resulting in 10 different expression clones. For heterodimers, NAC β sequences were cloned into P3-P2 recombination sites



accompanied by each NAC α into P1-P4 site. Only selected homodimers were used in BiFC, since no interactions were expected. NACB homodimers were cloned in three combinations - NACB1 in both recombination sites, NACB1 in P3-P2 with NACB2 in P1-P4, and NACB2 in both recombination sites. NAC α 1-NAC α 1, and NAC α 2-NAC α 3 were selected as representative pairs to test α -homodimer formation. Furthermore, the negative control for protein interaction-independent activation of YFP halves, bZIP34 (protein that should not interact with any NAC subunits) was cloned under P1-P4 sites in combination with NACB1 between the P3-P2 sites. The bacteria transformation, colony PCR, plasmid isolation, and its verification by

Sanger sequencing were performed in the same way as above for the Y2H system. LB media contained this time spectinomycin (100 μ g.ml⁻¹), X-gal (0.1 mM) and IPTG (0.5 mM).

Transformation of *Agrobacterium tumefaciens* by electroporation

200 ng of plasmid DNA was added to 50 μ l of *Agrobacterium tumefaciens* GV3101 house-made competent cells and incubated for 3 minutes on ice. The mixture was transferred into the pre-chilled electroporation cuvettes, and electroporated by Eppendorf Electroporator (Eporator®, Eppendorf, 4309000019) at 2.0 kV, resistance 200 Ω and capacity 25 μ F. Immediately, 1 ml of cold YEB media (0.6% yeast extract, 0.5% peptone from casein tryptic digest, 0.5% sucrose, 0.05% MgSO₄.7H₂O) was added, the solution was transferred into fresh Eppendorf tubes, and then incubated at 28°C for 2 hours with 180 rpm shaking. 200 μ l of each transformant was planted onto the individual YEB plates containing gentamicin 50 μ g.ml⁻¹, rifampicin 100 μ g.ml⁻¹ and spectinomycin 100 μ g.ml⁻¹. The plates were incubated at 28°C for 2 days. Then, seven colonies from each plate were streaked onto new YEB plate and let grow overnight at 28°C.

Tobacco leaf infiltration

The tobacco infiltration protocol was carried out according to Gehl et al. (Gehl *et al.*, 2009). Single colony from transformed *Agrobacterium* plate was transferred into 5 ml liquid YEB medium and cultured overnight at 28°C with 200 rpm shaking. The culture was then pelleted by the centrifugation for 5 minutes at 1620x g. The pellet was washed twice with 1 ml of infiltration medium (10mM MES (Duchefa Biochemie, M1503.0250), 10mM MgCl₂ (Merck, M8266-100G), 200 μ M acetosyringone (Merck, D134406-1G)), spun for 5 min at 1620x g and resuspended in 1 ml of infiltration medium. The solution was diluted to OD₆₀₀= 0.5. The same procedure was repeated using p19 repressor, resuspended to OD₆₀₀ = 0.05. The repressor was mixed with plasmid of interest in the equimolar ratio. The tubes were incubated for 3 hours in the dark at room temperature. The bacteria were injected into the leaf of 6-weeks-old *Nicotiana bentamiana* plants by 1 ml plastic syringe. The plants were incubated for 48 hours under long day conditions. After 2 and 3 days, the interactions in epidermal cells were observed under the confocal

microscope (Zeiss LSM 880 with Airyscan detector - Zeiss, Oberkochen, Germany). A round part of the leaf was cut from the site of infiltration and mounted into 30% glycerol. 488 nm excitation and 510 nm emission was used for YFP observation, whereas 561 nm excitation and 604 nm emission was used to visualize RFP. The photos were further processed in Fiji (Schindelin *et al.*, 2012) and Adobe Photoshop C6S (Adobe, San Jose, California, USA).

Transcriptome analysis

RNA extraction and sequencing

Four genotypes of *A. thaliana* were sown onto Jiffy tablets: Columbia-0 wild type (Col-0 WT), homozygous plants of the T-DNA insertion line SALK_043673, representing a single homozygous mutant of NACB1 (At1g73230, *nacB1*), homozygous plants of the T-DNA insertion line GK368-H02, representing a single homozygous mutant of NACB2 (At1g17880, *nacB2*), and the double homozygous plants created by the conventional crosses of the two above T-DNA insertion lines, representing the double homozygous mutant of NACB (*nacB1 nacB2*). The total RNA was extracted from harvested *A. thaliana* young flower buds in four replicas for each genotype by the RNeasy Plant Mini Kit (Qiagen, Venlo, Netherlands, 74904) according to the manufacturer's instructions. 20 mg of flower bud tissue was harvested and grinded thoroughly in liquid nitrogen by a mortar in a pestle. 450 μ l of RLT Buffer was added to the homogenized sample and transferred to a QIAshredder spin column and centrifuged at 13000 \times g for 2 min. The supernatant was transferred to a fresh Eppendorf tube and 225 μ l of 96% ethanol was added. The sample was transferred into an RNeasy Mini spin column and centrifuged at 10 000 \times g for 30 seconds. The flow-through was discarded, 700 μ l of Buffer RW1 was added to the column and spun again. The flow-through was discarded again. This step was repeated twice with 500 μ l Buffer RPE. Then the Rneasy Mini spin column was placed into a new collection tube and spun for another minute. Rneasy Mini spin column was placed into a fresh 1.5 ml Eppendorf tube and 30 μ l of RNase-free water was added to the centre of spin column membrane. The tube was centrifuged to elute the RNA, concentration of which was measured on NanoDrop™ One^c, and its integrity was checked via electrophoresis on 1.2% agarose gel in 1 \times TAE with ethidium bromide. The eluted RNA was treated with DNA-free™ DNA

Removal Kit (Thermo Fisher Scientific, Waltham, USA). 2.5 µl of 10xDNase I Buffer and 1.5 µl of rDNase I were added to 10 µg of extracted RNA and topped up to 25 µl. The mixture was incubated for 30 minutes at 37°C. 2 µl of resuspended DNase Inactivation Reagent were added and mixed. The tube was incubated for 2 minutes at room temperature and mixed occasionally. The tubes were centrifuged to pellet the DNase inactivation reagent and the solution was transferred to a fresh microtube. The purity, integrity and concentration of DNA-free RNA was measured on Bioanalyzer Nanochip (IMG-CORE-AGILENT 2100, Santa Clara, USA). The following steps including library preparation and sequencing were conducted by Macrogen Inc. (Seoul, Republic of Korea). Each library was prepared from 3 µg of the high-quality RNA. The TruSeq Stranded mRNA LT Sample Prep Kit and TruSeq Stranded Total RNA LT Sample Prep Kit (Plant) following the TruSeq Stranded mRNA Sample Preparation Guide, Part # 15031047 Rev. E and TruSeq Stranded Total RNA Sample Prep Guide, Part # 15031048 Rev. E were used for the library preparation and the libraries were sequenced on Illumina platform.

Mapping and assembly of reads

FastaQ files of raw reads obtained from the company were processed in the following manner. FastQC ver. 0.11.8 (<http://www.bioinformatics.babraham.ac.uk/projects/fastqc>) and Cutadapt ver. 1.9.1 (Martin, 2011) were run to test the quality of the pair-end raw reads and to trim technical sequences resulting with quality reads only (phred score > 20). STAR ver. 206.1a (Dobin *et al.*, 2013) was used for mapping the reads to reference genome of *A. thaliana* (ver. TAIR10) downloaded from the Araport database (https://www.araport.org/downloads/TAIR10_genome_release). Subread package ver. 1.6.3 (Liao *et al.*, 2013) and RSEM v1.3.1 (Li and Dewey, 2014) were used for reads quantification. Differential expression analyses were performed with the DESeq2 ver. 3.8 with FoldChange $\geq \pm 1.5$ and adjusted p-value < 0.05 used as thresholds for establishing significantly differentially expressed genes (DEGs) between Col-0 (WT) and *nacB1 nacB2*; Col-0 (WT) and *nacB1*; and Col-0 (WT) and *nacB2*.

Annotation and enrichment analyses

The DEG lists were functionally annotated by ThaleMine, tool of Araport website (<https://apps.araport.org/thalemine/begin.do>, ver. 1.10.4). KEGG database (<https://www.genome.jp/kegg>, Release 89.0) and Mapman software (v.: 3. 5. 1, (Thimm *et al.*, 2004) were used to identify molecular pathways affected by DEGs. For further analyses of functional significance of DEGs, biological processes, molecular function and cellular component GO enrichment analyses were performed using Panther database (<http://pantherdb.org>, annotation version: GO Ontology database Released 2018-12-01) with Fisher's exact test with false discovery rate < 0,05 as statistical significance threshold.

Confirmation of DEGs expression by qRT-PCR

Both genes encoding NAC β subunits (*NAC β 1* At1g73230 and *NAC β 2* At1g17880), all five genes encoding NAC α subunits (*NAC α 1* At3g12390, *NAC α 2* At3g49470, *NAC α 3* At5g13850, *NAC α 4* At4g10480, *NAC α 5* At1g33040) and five other differentially expressed genes (toll-interleukin-resistance (TIR) domain family protein (At2g20142), peroxidase 71 (At5g64120), trypsin inhibitor protein 1 (At2g43510), GDSL-motif esterase/acyltransferase/lipase (At1g20120), and phytoalexin deficient 4 (At3g52430)) were selected for qRT-PCR verification. Tubulin B chain 3 (*tub3*; At5g62700), and EARLY FLOWERING 4 (*eLF4*; At2G40080) were used as references. Residual RNA collected for sequencing was used for the verification in three biological replicas for each plant genotype (*WT*, *nac β 1 nac β 2*, *nac β 1*, and *nac β 2*). The reactions were performed with GoTaq® qPCR Master Mix (Promega, Madison, WI, USA) on LightCycler 480 (Roche, Basel, Switzerland) using the primer sets given in figure 17 according to the manufacturer's instructions. cT values for each sample were recorded by the LightCycler 480 Software version 1.5 (Roche, Basel, Switzerland). The same software was used to control the quality of the obtained data. Fragments per kilobase million (FPKM) values of transcript from RNA sequencing (RNA-seq) data were counted using RSEM software. Linear regression of log based FPKM and cT values was projected in MS Excel (Microsoft, Redmond, USA).

Primers used for qRT-PCR

Amplified Gene	Forward primer	Reverse primer
At3g12580	CCAACACCGTCTTCGATGC	GTTTCTCCTCTCCCTTGTTG
At2g20142	GAGTGATGAGGAGATGTTGG	GTGCAGAGGAGATCTGGTCG
At5g64120	CAGCCTGTTCTTGAGTGAG	CCGGTCCGAACCTCAATCTC
At2g43510	TGGCAAAGGCTATCGTTTCC	GGAAATATCCGAGGCGCAC
At5g52390	CTCGCCCAACATGACTGGTC	CTACTTCAACCTTGCTGCTGG
At1g33040	GAGGACGTCTGAAGTTGAAGGG	CACTCTGCTGACATCTGAGACAG
At3g12390	TTCCGCACGAATCACGAATCTC	CTTCGGGCTTATCGAGATCG
At3g49470	TCGTCACTCACCACCTCAC	GTAACCGGTGGTTGCTCAGG
At4g10480	CTCCGAAGAAGAAGATAAGAG	CGTTCTCCTTCTGGAGCTTC
At5g13850	TAGGGTTTTCGTCACTCGCC	CAAGATCGATCTTCTGCTCTCC
At1g73230	TGCTCAGAAGAGGTCGAGCG	GGGAGAGACTTTCGAGACCC
At1g17880	GCTGAGGCGGCATTACCTTC	GCGGTTCTCCTCAGACCAA

Figure 17: Set of primers used for qRT-PCR amplification.

Results

Yeast two-hybrid system

Cloning

To test specific protein-protein interaction of NAC heterodimers and homodimers in yeasts, the expression clones were firstly prepared by Gateway™ cloning. Five NAC α and two NAC β cDNA sequences were cloned into pDONR™221 to create entry clones and subsequently into two destination vectors, pDEST™32 and pDEST™22 to be co-transformed into the Yeast MaV203 strain. When expressed in yeast, the protein coded by pDEST™32 vector fused with DNA activation domain worked as bait, whereas protein coded by pDEST™22 in fusion with DNA binding domain was called as prey. For heterodimers, the transformation resulted in 20 bait-prey combinations to cover all possible heterodimers (in both prey-bait/bait-prey configurations) formed in *A. thaliana*. Homodimers were also transformed in cross-wise manner and the transformation yielded 29 different transformants. In case of protein interaction, the GAL4 DNA activating domain of prey approximated DNA binding domain of bait and three individual reporter genes were expressed and visualised via enzymatic detection or auxotrophy selection on five different media (fig. 18). Strong and weak interaction controls were included, as well as negative and auto-activation controls with one or both empty expression clones.

Interaction results

The first reporter gene was *lacZ* and its expression was monitored on YPAD medium via X-gal assay, which is a colorimetric assay for β -galactosidase activity. In case of interaction, and upon introduction of x-gal and its cleavage by β -galactosidase, blue staining of colonies with interactors was caused by accumulation of 5,5'-dibromo-4,4'-dichloro-indigo pigment. Blue staining of colonies was observed after one hour of incubation at 37°C. No further changes were monitored after longer incubation (as long as 24 hours). The results were consistent between the three individual transformations showing interaction in 10 individual pairs (first position indicates prey, second position bait): α 1-B1, α 1-B2, α 2-B1, α 2-B2, α 3-B1, α 3-B2, α 4-B2, α 5-B2, B1- α 2, B2- α 2 (fig. 18). There was no staining observed in negative controls declaring specificity of the observed interactions. Strong and weak positive interaction controls were also stained in blue verifying the interaction formation under the test conditions.

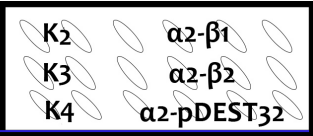
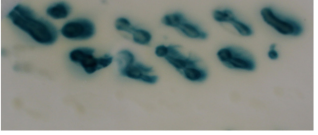
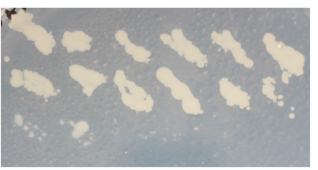
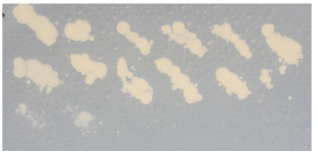
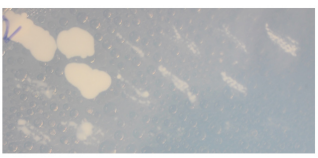
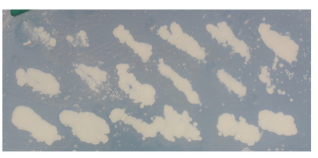
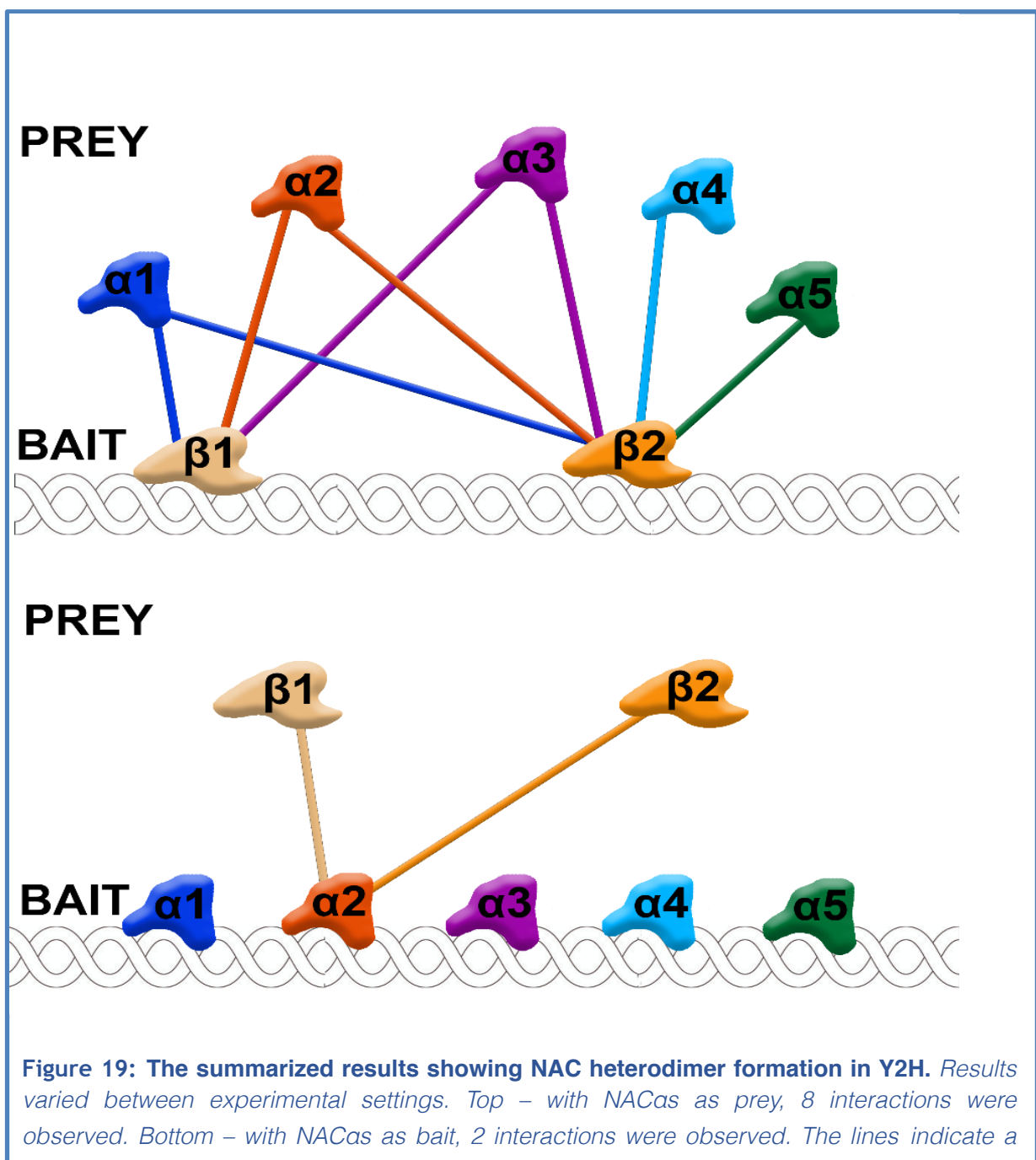
medium	reporter gene	detection of interaction	interacting NACs	interacting controls	
YPAD	<i>LacZ</i>	blue staining upon expression of β -galactosidase in x-gal assay	$\alpha 1-\beta 1$ $\alpha 1-\beta 2$ $\alpha 2-\beta 1$ $\alpha 2-\beta 2$ $\alpha 3-\beta 1$ $\alpha 3-\beta 2$ $\alpha 4-\beta 2$ $\alpha 5-\beta 2$ $\beta 1-\alpha 2$ $\beta 2-\alpha 2$	K2 - strong positive interaction K3 - weak positive interaction (partial)	
SC -Leu-Trp-His + 25mM 3AT	<i>HIS3</i>	growth of colonies	$\alpha 1-\beta 1$ $\alpha 1-\beta 2$ $\alpha 2-\beta 1$ $\alpha 2-\beta 2$ $\alpha 3-\beta 1$ $\alpha 3-\beta 2$ $\alpha 4-\beta 2$ $\alpha 5-\beta 2$ $\beta 1-\alpha 2$ $\beta 2-\alpha 2$	K2 - strong positive interaction K3 - weak positive interaction	
SC -Leu-Trp-His + 50mM 3AT	<i>HIS3</i>	growth of colonies	$\alpha 1-\beta 1$ $\alpha 1-\beta 2$ $\alpha 2-\beta 1$ $\alpha 2-\beta 2$ $\alpha 3-\beta 1$ $\alpha 3-\beta 2$ $\alpha 4-\beta 2$ $\alpha 5-\beta 2$ $\beta 1-\alpha 2$ $\beta 2-\alpha 2$	K2 - strong positive interaction K3 - weak positive interaction	
SC -Leu-Trp-Ura	<i>URA3</i>	growth of colonies	none	K2 - strong positive interaction K3 - weak positive interaction (partial)	
SC -Leu-Trp + 5FoA	<i>URA3</i>	suspension of growth	none	K2 - strong positive interaction	

Figure 18: Y2H results of NAC heterodimer formations on each selective medium with photo of the experiment in the last column.

The second reporter gene was *HIS3* and its activity was monitored via auxotrophic selection on SC-Leu-Trp-His plates containing 3AT, where only colonies with interacting proteins grew (fig. 18). 3AT specifically inhibits histidine synthesis in dose-dependent manner, thus adjusting 3AT concentration to the tolerance threshold, which can raise the sensitivity of detecting weak interactions. In this experiment 25 mM and 50mM AT concentrations were chosen for detecting the interaction, since these concentrations proved to be the most specific indicators, enabling to grow only cells with interacting proteins. The plates with 10mM AT concentration exhibited background grow of colonies without interacting proteins. On the other hand, 100mM AT concentration proved to be excessively toxic for any growing cells. According to 25 mM AT and 50 mM AT plates, 10 pairs showed interaction in at least two replicates out of three: α 1-B1, α 1-B2, α 2-B1, α 2-B2, α 3-B1, α 3-B2, α 4-B2, α 5-B2, B1- α 2, B2- α 2 (fig. 18). No negative control grew on 25mM and 50mM AT plates, proving specificity of the interactions. For positive controls, both strong and weak interaction controls grew on 3AT plates, which was in accordance with the expected results.

The third reporter gene was represented by *URA3*. Two selective media were used to monitor this auxotrophy selection. SC-Leu-Trp-Ura plates enabled the growth of colonies capable of uracil synthesis - those with interacting proteins. Nevertheless, in our experiments this medium proved to represent an excessively strong selection and no interactions were formed in any NAC combination. Moreover, only the strong positive control grew on these plates suggesting weaker interaction between NAC subunits in yeast nuclei. No growth of negative controls was observed. Similarly, no interactions were observed on the second selective media for *URA3* auxotrophy - SC-Leu-Trp-Ura containing 5-Foa. This time, in case of interaction and the induction of uracil synthesis gene, the toxic 5-fluorouracil was formed, thus only cells without interacting proteins could grow on this media. In this experiment, all negative controls and tested pairs grew, therefore showing no interaction. On the contrary, only strong interaction control did not grow, which showed that the selection was probably too strong to monitor weaker NAC interactions.

In summary, according to 3AT selection plates and X-gal assay results, heterodimer formation was observed in these NAC combinations: $\alpha 1$ - $\beta 1$, $\alpha 1$ - $\beta 2$, $\alpha 2$ - $\beta 1$, $\alpha 2$ - $\beta 2$, $\alpha 3$ - $\beta 1$, $\alpha 3$ - $\beta 2$, $\alpha 4$ - $\beta 2$, $\alpha 5$ - $\beta 2$, $\beta 1$ - $\alpha 2$, $\beta 2$ - $\alpha 2$ (fig. 18). To sum up the results from all the above reporter genes, only $\alpha 2$ interacted with both β s regardless of the experimental setting. $\alpha 4$ and $\alpha 5$ interacted only with $\beta 2$ when acting as preys, whereas $\alpha 1$ and $\alpha 3$ interacted with both β s only as preys (Fig. 19). Results from - Ura plates and +5Foa plates indicate weaker interactions of these interacting partners. For homodimer testing, no interaction was observed in any combination, showing that NAC homodimers were not formed in the environment of yeast nuclei.



Bimolecular fluorescence complementation

Construct preparation

Five NAC α genes and two NAC β genes were cloned into entry vectors pDONRTM221_P3-P2 and pDONRTM221_P1-P4 by GatewayTM BP recombination reaction. LR recombination reaction was then performed to recombine NAC sequences from entry clones to the multisite destination vector BiFC2in1-CC giving rise to expression clones containing sequences of gene pairs tested for their interaction. In this BiFC protocol, two genes from expression clone are expressed in leaves of *Nicotiana benthamiana*, each fused with half of YFP. In case of interaction, these two halves of YFP are approximated to each other to form functional YFP protein and emit fluorescence. For testing the heterodimer formation, 10 pairs of different NAC β and NAC α combinations were created.

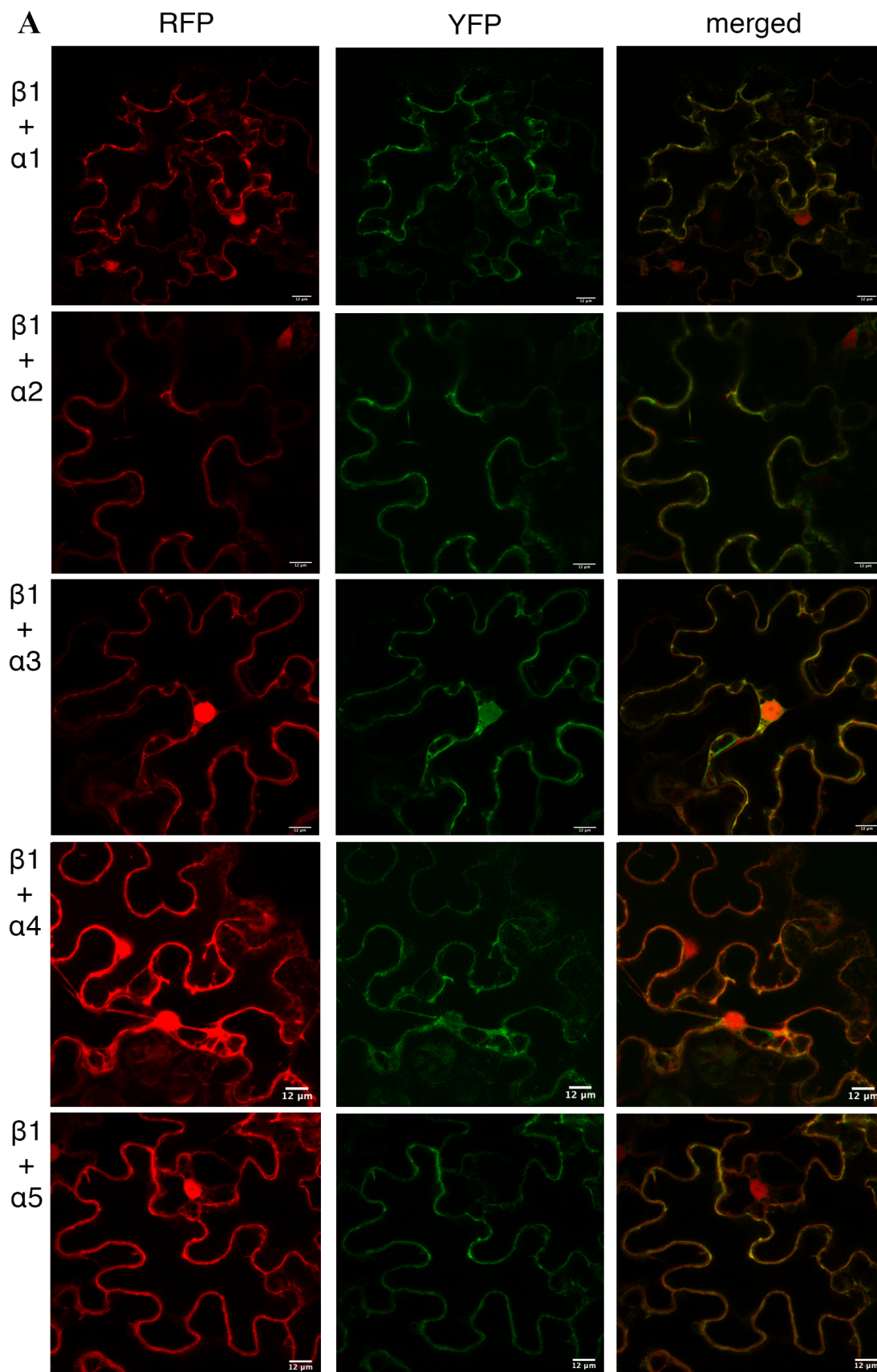
Firstly, expression clones possessing NAC β 1 sequence in the P3-P2 recombination site together with each of five NAC α s in the P1-P4 site were prepared resulting in 5 protein combinations - NAC β 1-nYFP + NAC α 1-cYFP, NAC β 1-nYFP + NAC α 2-cYFP, NAC β 1-nYFP + NAC α 3-cYFP, NAC β 1-nYFP + NAC α 4-cYFP, and NAC β 1-nYFP + NAC α 5-cYFP. Secondly, expression clones with NAC β 2 in P3-P2 site were prepared together with each NAC α in P1-P4 site - NAC β 2-nYFP + NAC α 1-cYFP, NAC β 2-nYFP + NAC α 2-cYFP, NAC β 2-nYFP + NAC α 3-cYFP, NAC β 2-nYFP + NAC α 4-cYFP, NAC β 2-nYFP + NAC α 5-cYFP. For the verification of the NAC β homodimer formation, NAC β 1 was cloned into P3-P2 site with NAC β 1 in P1-P4, NAC β 1 in P1-P4 site with NAC β 2 in P3-P2, and NAC β 2-NAC β 2 combination expression clones were also prepared, providing three protein combinations - NAC β 1-nYFP + NAC β 1-cYFP, NAC β 2-nYFP + NAC β 1-cYFP, NAC β 2-nYFP + NAC β 2-cYFP. NAC α 1 in P1-P4 with NAC α 1 in P3-P2 and NAC α 2 in P1-P4 with NAC α 3 in P3-P2 were selected as representative homodimer interaction pairs, as protein combination - NAC α 1-nYFP + NAC α 1-cYFP, NAC α 3-nYFP + NAC α 2-cYFP. For negative control, NAC β 1 in P1-P4 was cloned with bZIP34 in P3-P2 - giving rise to protein combination bZIP34-nYFP + NAC β 1-cYFP.

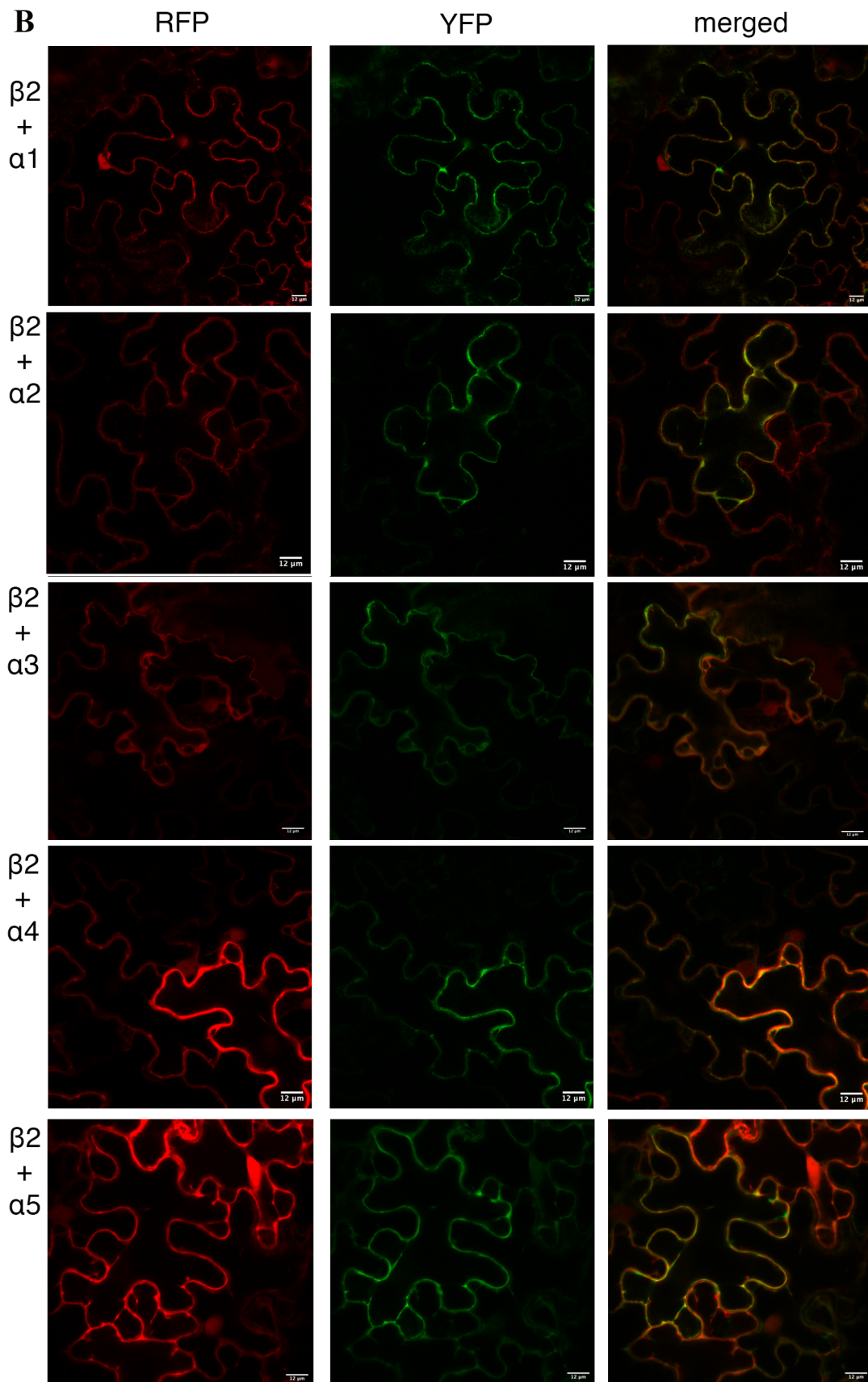
Confocal microscopy of transformed leaves

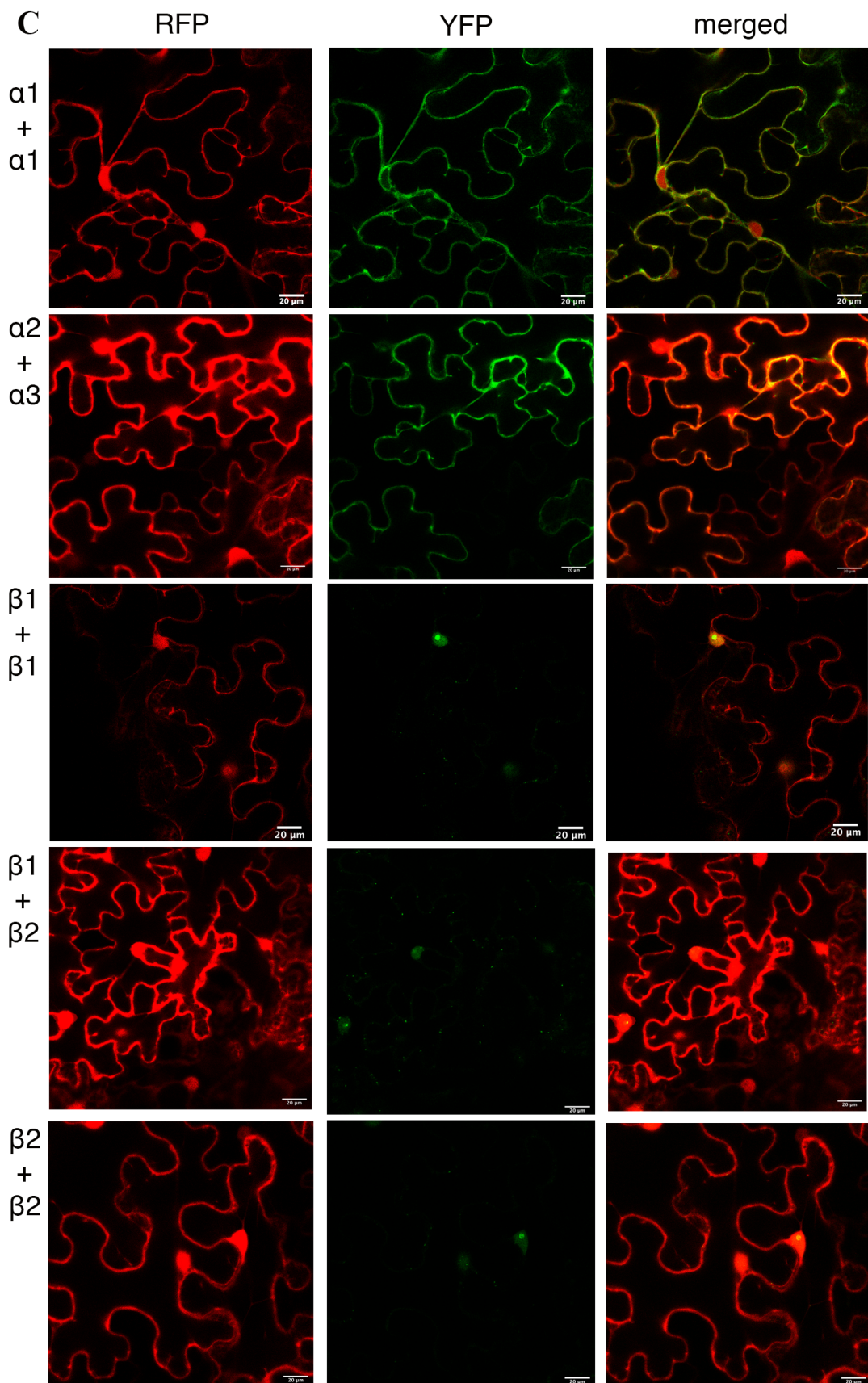
The RFP emission signalled successful infiltration of expression clones into the *N. benthamiana* epidermal cells, whereas the presence of YFP signal indicated the interaction between the two tested proteins. All observed YFP signals were

colocalized with control RFP signal, which suggested that the YFP signal originated from interacting partners and should not represent some random background signal. The interaction results were consistent in case of heterodimer formation, regardless of the tested subunit pair in two independent infiltrations after 2 and 3 days of incubation. Two different times of plant incubations were selected due to possible variations in expression time/localisation for different proteins and since some interactions could be detectable only after longer incubation time. All heterodimers localized mainly to cytoplasm and occasionally to nucleus (fig. 20 A, B) regardless of the incubation time. This observation was in accordance with the predicted β -subunit localization and with the localization of NAC β subunits fused with green fluorescence protein (GFP) (Fila et al., manuscript in preparation), which both showed cytoplasmatic and nuclear localisation. Both NAC α combinations showed homodimer formation, which was localized exclusively into cytoplasm, and was never found in nucleus after 2 and 3 days of incubation. This is also in agreement with the subcellular localization of NAC α subunits tagged with GFP, which showed only cytoplasmatic localization (Fila, unpublished data). The formation of β homodimers was also observed in all three protein combinations with localization in nucleus and in small vesicles moving rather chaotically in the cytoplasm (Fig. 20 C). No YFP signal was observed in NAC β 1 and bzip34 combination, which can be regarded as partial control for specificity of other observed interactions, since NAC β 1 and bzip34 were not predicted to interact with each other.

Figure 20: Images of BiFC interactions from confocal microscope (Zeiss LSM 880 with Airyscan detector). *A – heterodimer formation with NAC β 1. B – heterodimer formation with NAC β 2. C – homodimer formation. The first column shows RFP signal as control for successful infiltration. The second column shows YFP signal indicating interaction. The third column shows colocalization of the YFP and RFP signals indicating specificity of observed interaction. Scale bar represents 12 μ m in A, B and 20 μ m in C. (next three pages).*







Transcriptome analyses

Sample preparation and raw data processing

Observed phenotypic defects of the *nacB1 nacB2* plants were most significant in the flowers and siliques. Also *in vitro* and *in vivo* pollen cultivation data and blue dot assay proved the defects to be in both gametophytes and/or sporophyte, so flower buds (including all the mentioned tissues) were chosen for the analyses of transcripts and their expression influenced in the *nacB1 nacB2* plants. The single phenotype-less *nacB1* (At1g73230) and *nacB2* (At1g17880) mutants were also included in the analysis.

RNA was collected from flower buds of all four genotypes and after integrity and purity test, three replicas of each genotype were sequenced for RNA genome-wide transcriptional analyses on Illumina platform. Approximately 40.6 million of paired-end 101 bp reads per sample were obtained. Around 99% of reads passed the quality control test, out of which on average 94.3% of high-quality reads were uniquely mapped to *A. thaliana* reference genome (TAIR10).

Differential expression analyses

Three differential expression analyses were performed by DESeq2 package for WT vs. *nacB1 nacB2*, WT vs. *nacB1*, and WT vs. *nacB2* combinations. Several tests visualised the data consistence between replicas. For data credibility manifestation, some tests from WT vs. *nacB1 nacB2* DESeq2 pipeline are showed in figure 21. Pearson correlation coefficient, r , is used as a measure of the strength of linear correlation between two data sets and shows pairwise correlation. The coefficient r used for hierarchical clustering can determine whether the sample replicas are more similar to each other than to the distinct samples. The measure of similarity is then projected as $d = 1 - r$ (the lower the d , the more similar data). In fig 21 A, WT replicas together with *nacB1 nacB2* replicas were presented in two individual branches and showed stronger linear correlation. Another approach was represented by Principal Components Analyses (PCA), where again the variability between the samples was tested. In the plot, visualization-based clustering covering 95% of variability in two-dimension PCA is showed. From the results

comparing *nacβ1 nacβ2* with the wild type, it can be concluded that the individual samples cluster according to their original genotype (fig. 21 B). P-value for differential expression analyses was adjusted to $\alpha = 0,05$. Out of total 27055 nonzero genes, 1842 (6.8%) were upregulated and 3050 (11%) downregulated in the *nacβ1 nacβ2* flower buds. 4657 (17%) genes were removed by independent filtering due to low read count. MA plot in fig. 21 C provides a view of differential changes between two conditions with M (log ratios of fold change), and A (average expression mean). Moreover, the algorithm detects genes passing the significance threshold (p-value < 0,05), marking them in red. From this graph, a higher number of downregulated genes together with the distribution of expression values among the differentially expressed genes is clearly visible (fig. 21 C). The analyses

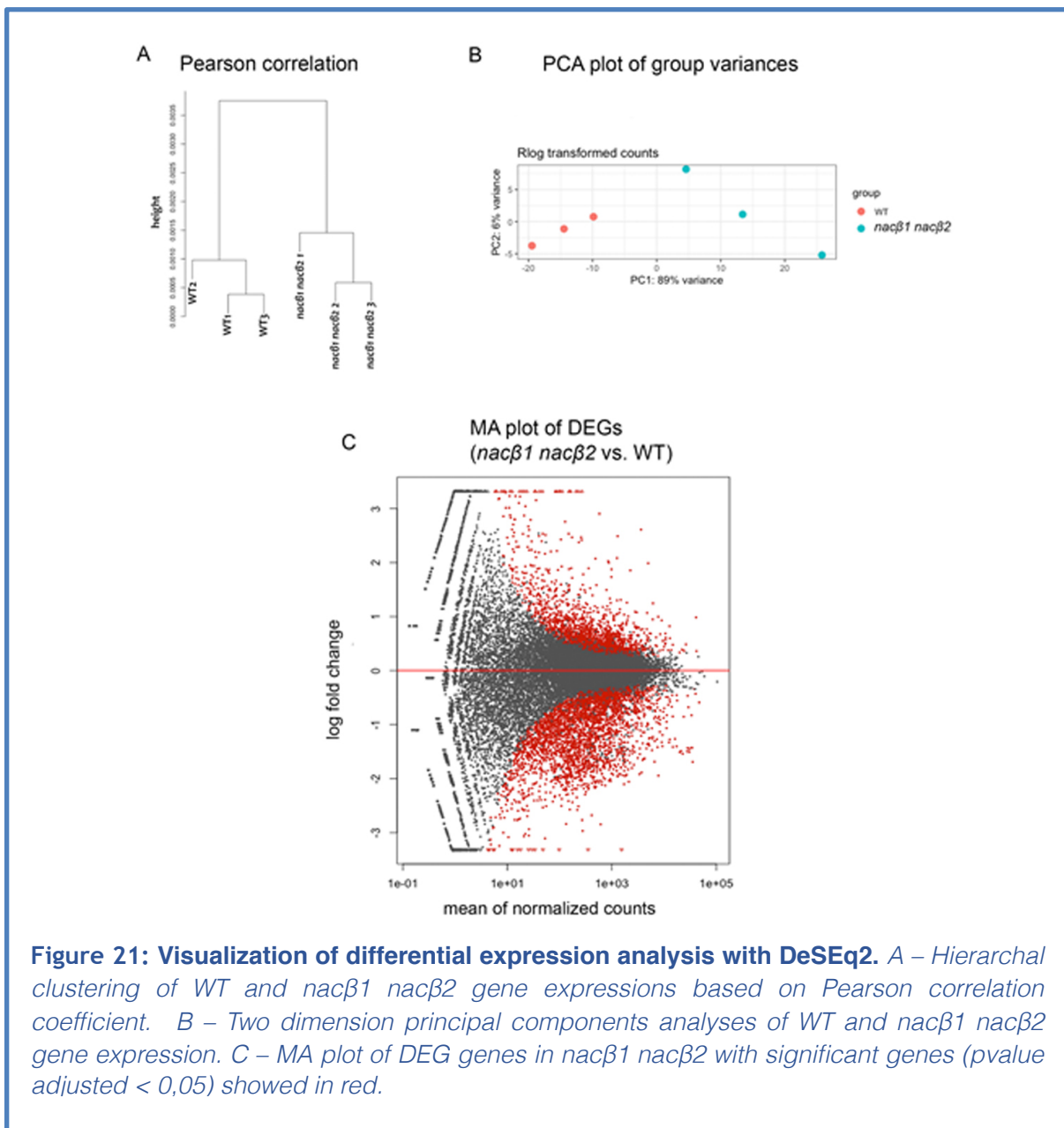


Figure 21: Visualization of differential expression analysis with DeSeq2. A – Hierarchical clustering of WT and *nacβ1 nacβ2* gene expressions based on Pearson correlation coefficient. B – Two dimension principal components analyses of WT and *nacβ1 nacβ2* gene expression. C – MA plot of DEG genes in *nacβ1 nacβ2* with significant genes (pvalue adjusted < 0,05) showed in red.

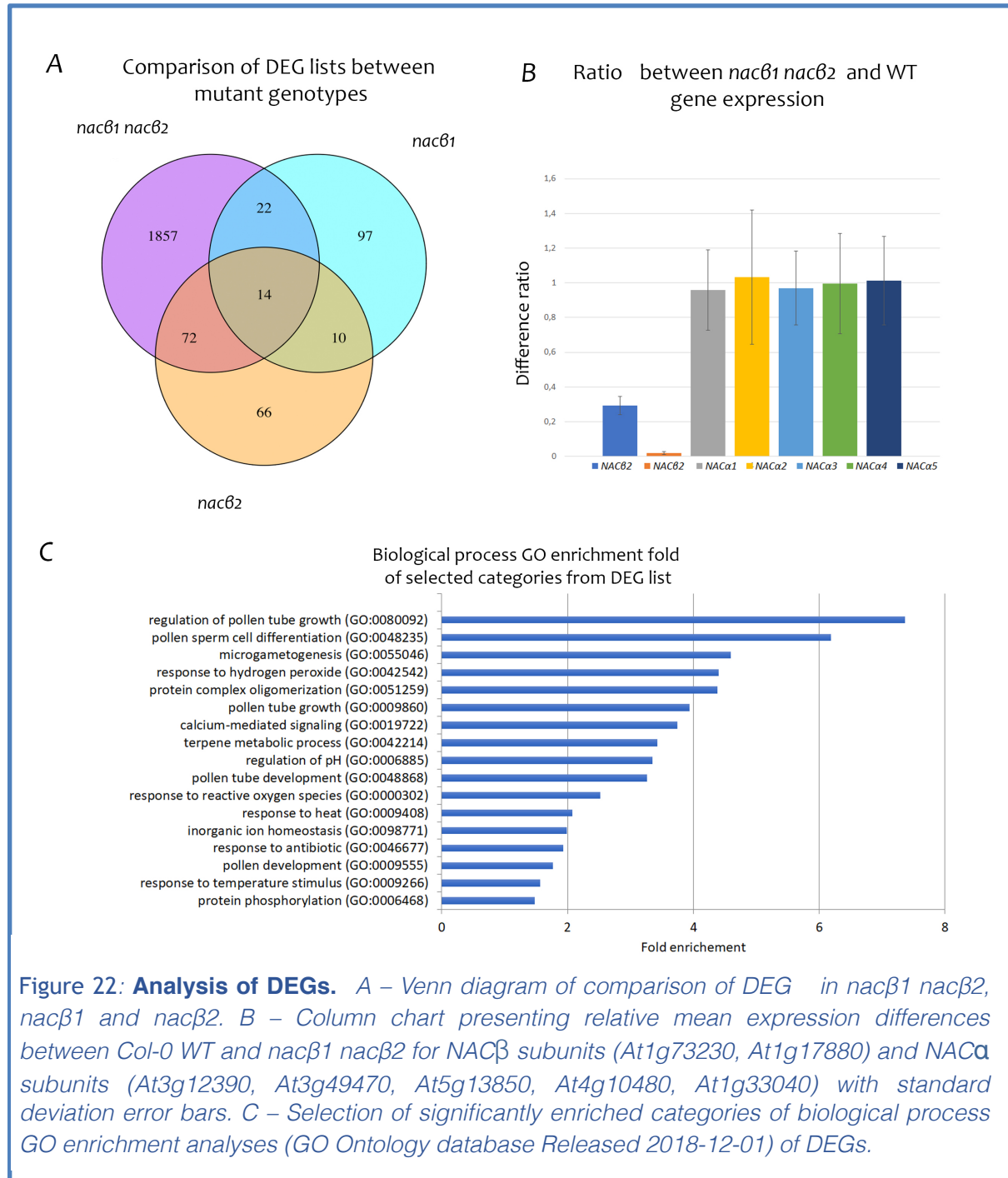
resulted in the list of gene IDs annotated with base mean (the average normalized read counts from all samples), log₂ scaled Fold Change (between the *nacB1 nacB2* and WT), lfcSE (standard error for log₂FoldChange estimate), Stat (Wald statistic - logFC divided by SE), p-value (Wald test p-value), Padj (Benjamini-Hochberg adjusted P-value) and also symbol and brief description added from Thalemine annotation website (supplement table 1). Padj < 0,05 and logFold2Change > 1 and < -1 were selected as thresholds for further analyses. The final list consisted of 1965 DEGs in the *nacB1 nacB2* with 363 upregulated and 1602 downregulated genes.

As expected from the phenotypic analyses, notably lower changes in transcription were observed in the two *nacB* single mutants resulting with only 162 and 143 DEG in *nacB1* and *nacB2*, respectively (fig. 22 A). Moreover, no significant changes in gene expression were observed in NAC α coding genes, suggesting no mutual regulation of NAC subunits on the transcriptional level (fig. 22 B). The data also show ultimate silencing of *NACB1* with expression close to 0 in the *nacB1 nacB2* and *nacB1* proving total knock-out of *NACB1*. However, the expression of *NACB2* in *nacB1 nacB2* and *nacB2* reached still approximately half of the expression from the Col-0 (WT), representing a knock-down of *NACB2*.

DEG list analyses

In the first step, the gene function of DEG list was analysed, so the transcripts were classified by molecular function, biological processes and cellular component using gene ontology (GO) enrichment analysis (test PANTHER Overrepresentation Test (Released 20190606), annotation version GO Ontology database Released 2019-02-02, PANTHER14.1). 1928 DEGs were successfully mapped by the software and underwent the enrichment analyses with Fisher's Exact test, FDR < 0.05 as significance threshold (fig. 22 C). Several GO terms involved in pollen development were positively enriched such as "pollen tube growth", "regulation of pollen tube growth" and "pollen sperm cell differentiation". Also stress related GO terms "response to heat" and "response to hydrogen peroxide", or "protein complex oligomerization", "calcium-mediated signalling" and "terpene metabolic process" categories were included. In molecular function, "pectin esterase inhibitor activity", "aspartyl esterase activity", "calcium ion binding", "hydrolase activity, hydrolyzing O-glycosyl compounds" and

“transmembrane transporter activity” categories were present. On cellular components category, there were positively enriched “pollen tube”, and specifically “pollen tube tip”, “plant-type cell wall”, and plasma membrane terms including “apical plasma membrane”, “integral component of plasma membrane”, and “anchored component of membrane”.



With the observed phenotype considered, the data analysis suggested two notable groups of genes. According to the biological process enrichment analysis,

91 genes were discovered to be connected with male germ-line development (tab. 1). The list consists of genes playing role in sperm cell differentiation and pollen tube growth and its regulation. Pollen tube expression was also observed in the cellular component enrichment analysis. As understood from molecular function enrichment analysis, several proteins were connected to pollen tube cell wall modification or calcium signalling. However, the whole list also consists of genes from functionally distant gene families with various molecular functions as commented in Discussion. The second group is represented by upregulated chaperones consisting of 18 heat shock proteins and 2 heat shock factors (tab. 2).

Table 1: List of DEGs in *nacβ1 nacβ2* mutant connected to pollen development. Annotations were extracted from Thalemine v1.10.4 (Krishnakumar et al., 2015), TAIR 2.9.0+ (www.arabidopsis.com) and Uniprot 2019_06 (www.uniprot.org). Direct target promoters of DU1 in orange. Sorted by protein function.

Gene ID	Symbol	Name	Potential function	Protein type	Mean expression			GO term				
					WT	mutant	Fold change	Pollen cell	Pollen development	PT	Regulation	
								cell	development		PT growth	
AT1G08730	XIC	Myosin family protein with DII domain-containing protein	actin organisation	myosin	719	372	0,48				✓	
AT1G54560	XIE	Myosin family protein with DII domain-containing protein	actin organisation	myosin	1200	571	0,44				✓	
AT2G35210	RPA	root and pollen arfgap	actin organisation	membrane trafficking	504	185	0,34	✓				
AT3G28630	CROLIN1	actin cross-linking protein, putative (DUF569)	actin organisation	actin binding	102	36	0,32				✓	
AT5G52360	ADF10	actin depolymerizing factor 10	actin organisation	actin binding	979	334	0,31				✓	
AT1G10770	AT1G10770	Plant invertase/pectin methyltransferase inhibitor superfamily	cell wall stability	pectin methyltransferase inhibitor	3047	1113	0,34				✓	
AT1G48020	PME11	pectin methyltransferase inhibitor 1	cell wall stability	pectin methyltransferase inhibitor	503	168	0,31				✓	
AT1G69940	PPME1	Pectin lyase-like superfamily protein	cell wall stability	pectin methyltransferase	20575	8317	0,38				✓	
AT2G41970	AT2G41970	Protein kinase superfamily protein	cell wall stability	kinase	242	68	0,26				✓	
AT2G47040	VGD1	Plant invertase/pectin methyltransferase inhibitor superfamily	cell wall stability	pectin methyltransferase	42471	16786	0,37				✓	
AT3G01700	AGP11	arabinogalactan protein 11	cell wall stability	glycoprotein	5639	1916	0,32				✓	
AT3G17220	PME12	pectin methyltransferase inhibitor 2	cell wall stability	pectin methyltransferase inhibitor	266	131	0,45				✓	
AT4G33970	LRX11	Leucine-rich repeat (LRR) family protein	cell wall stability	extensin	1194	394	0,31				✓	
AT5G14380	AGP6	arabinogalactan protein 6	cell wall stability	glycoprotein	9588	3208	0,31	✓			✓	
AT2G35300	LEA18	Late embryogenesis abundant protein, group 1 protein	drought stress	chaperone	65	14	0,20				✓	
AT5G13150	EXO70C1	exocyst subunit exo70 family protein C1	exocytosis	exocytosis	481	195	0,37				✓	
AT5G13990	EXO70C2	exocyst subunit exo70 family protein C2	exocytosis	exocytosis	1206	446	0,34				✓	
AT1G63180	UGE3	UDP-D-glucose/UDP-D-galactose 4-epimerase 3	galactose catabolism	epimerase	927	480	0,48				✓	
AT1G68610	PCR11	PLANT CADMIUM RESISTANCE 11	heavy metal efflux	plant cadmium resistance	334	110	0,31	✓			✓	
AT1G72290	AT1G72290	Kunitz family trypsin and protease inhibitor protein	herbivore resistance	herbivore resistance	2231	887	0,37				✓	
AT1G15990	CNGC7	cyclic nucleotide gated channel 7	ion transport	ion channel	105	56	0,49				✓	
AT1G19780	CNGC8	cyclic nucleotide gated channel 8	ion transport	ion channel	211	80	0,35				✓	
AT2G22950	ACA7	Cation transporter/ E1-E2 ATPase family protein	ion transport	ATPase	978	438	0,41				✓	
AT2G25600	SPIK	Shaker pollen inward K channel	ion transport	ion channel	460	191	0,39				✓	
AT3G62230	DAF1	F-box family protein	protein fate	ubiquitin ligase	3499	1299	0,35	✓			✓	
AT4G12920	UND	Eukaryotic aspartyl protease family protein	protein fate	protease	106	283	2,46				✓	
AT1G04450	RIC3	ROP-interactive CRIB motif-containing protein 3	ROP1 GTPase signalling	CRIB motif protein	415	160	0,35				✓	
AT1G50610	PRK5	Leucine-rich repeat protein kinase family protein	ROP1 GTPase signalling	kinase	230	51	0,20				✓	

Gene ID	Symbol	Name	Potential function	Protein type	Mean expression			GO term			
					WT	mutant	Fold change	Pollen cell	Pollen sperm	Regulation	PT
AT2G20430	RIC6	ROP-interactive CRIB motif-containing protein 6	ROP1 GTPase signalling	CRIB motif protein	199	68	0,31			✓	
AT2G33460	RIC1	ROP-interactive CRIB motif-containing protein 1	ROP1 GTPase signalling	CRIB motif protein	448	147	0,30			✓	
AT1G15330	AT1G15330	Cystathionine beta-synthase (CBS) protein	signalling	kinase	22	1	0,06	✓		✓	
AT1G28270	RALFL4	ralf-like 4	signalling	peptide ligand	1573	643	0,38			✓	
AT1G68090	ANN5	annexin 5	signalling	Ca binding	175	33	0,18	✓		✓	
AT1G79250	AGC1.7	AGC kinase 1.7	signalling	kinase	620	218	0,33			✓	
AT2G31500	CPK24	calcium-dependent protein kinase 24	signalling	kinase	1624	519	0,30			✓	
AT2G33775	RALFL19	ralf-like 19	signalling	peptide ligand	880	358	0,38			✓	
AT2G41210	PIP5K5	phosphatidylinositol- 4-phosphate 5-kinase 5	signalling	kinase	700	320	0,42			✓	
AT3G02810	LIP2	Lost in Pollen tube guidance 2	signalling	kinase	1160	381	0,31			✓	
AT3G04690	ANX1	Malectin/receptor-like protein kinase family protein	signalling	kinase	351	149	0,39			✓	
AT3G11330	PIRL9	plant intracellular ras group-related LRR 9	signalling		1206	639	0,48	✓			
AT3G20190	PRK4	Leucine-rich repeat protein kinase family protein	signalling	kinase	681	205	0,28			✓	
AT3G23380	RIC5	ROP-interactive CRIB motif-containing protein 5	signalling	CRIB motif protein	115	35	0,28			✓	
AT3G42880	PRK3	Leucine-rich repeat protein kinase family protein	signalling	kinase	400	137	0,32			✓	
AT3G50310	MAPKKK20	mitogen-activated protein kinase kinase kinase 20	signalling	kinase	106	43	0,37	✓		✓	
AT4G08850	AT4G08850	Leucine-rich repeat receptor-like protein kinase family	signalling	kinase	329	775	2,13			✓	
AT5G05850	PIRL1	plant intracellular ras group-related LRR 1	signalling		527	260	0,45	✓			
AT5G12180	CPK17	calcium-dependent protein kinase 17	signalling	kinase	671	182	0,26			✓	
AT5G20690	PRK6	Leucine-rich repeat protein kinase family protein	signalling	kinase	144	46	0,30			✓	
AT3G47440	TIP5;1	tonoplast intrinsic protein 5;1	tonoplast channel	aquaporin	451	153	0,31	✓		✓	
AT1G04880	AT1G04880	HMG box protein with ARID/BRIGHT DNA-binding domain	transcription regulation	transcription factor	784	408	0,47			✓	
AT1G22130	AGL104	AGAMOUS-like 104	transcription regulation	transcription factor	407	171	0,39	✓		✓	
AT1G69540	AGL94	AGAMOUS-like 94	transcription regulation	transcription factor	244	121	0,45	✓		✓	
AT1G77950	AGL67	AGAMOUS-like 67	transcription regulation	transcription factor	13	3	0,23	✓		✓	
AT1G77980	AGL66	AGAMOUS-like 66	transcription regulation	transcription factor	329	127	0,35	✓		✓	
AT2G17180	DAZ1	C2H2-like zinc finger protein	transcription regulation	transcription factor	69	27	0,36	✓		✓	
AT2G32460	MVB101	myb domain protein 101	transcription regulation	transcription factor	1121	572	0,47	✓		✓	
AT2G42380	BZIP34	Basic-leucine zipper (bZIP) family protein	transcription regulation	transcription factor	726	377	0,46	✓		✓	
AT3G10470	AT3G10470	C2H2-type zinc finger family protein	transcription regulation	transcription factor	206	59	0,27	✓		✓	
AT3G18360	AT3G18360	VQ motif-containing protein	transcription regulation		1102	533	0,44			✓	
AT3G47870	LBD27	LOB domain-containing protein 27, SIDECAR	transcription regulation	transcription factor	638	226	0,32	✓		✓	

Gene ID	Symbol	Name	Potential function	Protein type	Mean expression			GO term			
					WT	mutant	Fold change	Pollen development	Pollen cell differentiation	Pollen sperm	Regulation
AT3G60460	DUO1	myb-like HTH transcriptional regulator family protein	transcription regulation	transcription factor	55	24	0,40	✓	✓		
AT4G26440	WRKY34	WRKY DNA-binding protein 34	transcription regulation	transcription factor	164	63	0,35	✓			
AT4G35280	DAZ2	C2H2-like zinc finger protein	transcription regulation	transcription factor	61	19	0,28	✓	✓		
AT4G35700	DAZ3	zinc finger (C2H2 type) family protein	transcription regulation	transcription factor	370	130	0,33	✓	✓		
AT1G07340	STP2	sugar transporter 2	transport	transporter	1001	268	0,24	✓			
AT5G14870	CNGC18	cyclic nucleotide-gated channel 18	transport	ion channel	537	241	0,41			✓	
AT5G16530	PIN5	Auxin efflux carrier family protein	transport	transporter	42	131	2,83	✓			
AT5G28470	AT5G28470	Major facilitator superfamily protein	transport	transporter	645	336	0,48			✓	
AT5G40260	SWEET8	Nodulin MtN3 family protein	transport	transporter	1288	558	0,39	✓			
AT5G53520	OPT8	oligopeptide transporter 8	transport	transporter	56	25	0,43	✓	✓		
AT5G46220	TOD1	transmembrane protein (DUF616)	turgor regulation	ceramidase	177	80	0,40			✓	
AT1G61290	SYPI24	syntaxin of plants 124	vesicle trafficking	SNARE gene	236	68	0,26			✓	
AT3G12160	RABA4D	RAB GTPase homolog A4D	vesicle trafficking	GTPase	241	83	0,32			✓	✓
AT3G51300	ROP1	RHO-related protein from plants 1	vesicle trafficking	GTPase	138	53	0,35			✓	
AT4G13240	ROPGEF9	RHO guanyl-nucleotide exchange factor 9	vesicle trafficking	GTPase activator	253	89	0,33				✓
AT4G24580	REN1	Rho GTPase activation protein (RhoGAP) with PH domain-containing protein	vesicle trafficking	GTPase activator	1281	616	0,44			✓	
AT1G09080	BIP3	Heat shock protein 70 (Hsp 70) family protein		chaperone	38	130	3,05			✓	
AT1G19890	MGH3	male-gamete-specific histone H3		histone	277	115	0,38	✓	✓		
AT1G24520	BCP1	homolog of Brassica campestris pollen protein 1			1838	542	0,28	✓	✓		
AT1G54280	AT1G54280	ATPase E1-E2 type family protein		ATPase	564	284	0,47			✓	
AT1G63530	AT1G63530	hypothetical protein			61	26	0,38			✓	
AT1G64110	DAA1	P-loop containing nucleoside triphosphate hydrolases superfamily protein		ATPase	183	68	0,34	✓	✓		
AT3G04620	DAN1	Alba DNA/RNA-binding protein		nuclei acid binding	2656	1312	0,45	✓	✓		
AT3G23840	AT3G23840	HXXXD-type acyl-transferase family protein		transferase	3946	2075	0,47	✓			
AT3G28780	AT3G28780	transmembrane protein, putative (DUF1216)			17136	7306	0,40	✓			
AT4G29470	PLA2-DELTA	Phospholipase A2 family protein			406	123	0,28	✓		✓	
AT5G02390	DAU1	TRM32-like protein (DUF3741)			157	64	0,37	✓	✓		
AT5G19360	CPK34	calcium-dependent protein kinase 34		kinase	329	96	0,27				✓
AT5G39400	PTEN1	Calcium/lipid-binding (CaLB) phosphatase		phosphatase	774	263	0,32	✓			
AT5G39650	DAU2	transmembrane protein, putative (DUF679)			183	54	0,27	✓	✓		
AT5G46795	MSP2	microspore-specific promoter 2			373	104	0,26	✓	✓		

Table 2: List of DE heat stress genes in *nacβ1 nacβ2* mutant. Annotations were extracted from TAIR 2.9.0+ (www.arabidopsis.org). Sorted by fold change.

Gene ID	Symbol	Name	Potential function	Heat shock protein family	mean expression WT	mean expression mutant	Fold change
AT1G53540	AT1G53540	HSP20-like chaperones superfamily protein	heat stress	sHSP	1	95	7,07
AT5G12030	HSP17.6A	heat shock protein 17.6A	heat stress, protein folding	sHSP	4	426	6,86
AT4G10250	ATHSP22.0	HSP20-like chaperones superfamily protein	heat stress	sHSP	1	71	6,04
AT5G12020	HSP17.6II	17.6 kDa class II heat shock protein	heat stress	sHSP	3	196	5,91
AT4G25200	HSP23.6-MITO	mitochondrion-localized small heat shock protein 23.6	heat stress	sHSP	2	82	5,03
AT3G46230	HSP17.4	heat shock protein 17.4	heat stress	sHSP	8	165	4,19
AT2G29500	AT2G29500	HSP20-like chaperones superfamily protein	heat stress	sHSP	20	293	3,76
AT3G51910	HSFA7A	heat shock transcription factor A7A	heat stress	HSF	2	21	3,01
AT3G12580	HSP70	heat shock protein 70	heat stress, protein folding	HSP70	981	6515	2,61
AT5G52640	HSP90.1	heat shock-like protein	heat stress	HSP90.1	377	2303	2,49
AT5G51440	AT5G51440	HSP20-like chaperones superfamily protein	heat stress	sHSP	77	461	2,47
AT1G59860	AT1G59860	HSP20-like chaperones superfamily protein	heat stress, protein folding	sHSP	44	182	1,93
AT5G37670	AT5G37670	HSP20-like chaperones superfamily protein	heat stress, protein folding	sHSP	17	56	1,61
AT1G09080	BIP3	Heat shock protein 70 (Hsp 70) family protein	heat stress, protein folding	HSP70	38	130	1,61
AT1G07400	AT1G07400	HSP20-like chaperones superfamily protein	heat stress	sHSP	245	796	1,58
AT2G32120	HSP70T-2	heat-shock protein 70T-2	heat stress, protein folding	HSP70T-2	78	239	1,51
AT2G26150	HSFA2	heat shock transcription factor A2	heat stress	HSF	125	368	1,41
AT1G74310	HSP101	heat shock protein 101	heat stress	sHSP	503	1392	1,33
AT5G59720	HSP18.2	heat shock protein 18.2	heat stress	sHSP	60	139	1,06
AT1G54050	AT1G54050	HSP20-like chaperones superfamily protein	heat stress	sHSP	213	470	1,00

qRT-PCR data validation

To validate data obtained from RNAseq, RT-qPCR method provides an independent approach enabling the computation of gene expression. The log scaled FPKM values obtained from RNAseq should negatively linearly correlate with cT values obtained from RT-qPCR measurement. The higher the FPKM value, the higher is the expression of certain gene in RT-qPCR. On the other hand, the higher the cT value, the less abundant transcripts were present. To validate our transcriptomics data, the abundance of several candidate genes (in the same RNA as was sent for sequencing) was determined by quantitative RT-qPCR. There were all five genes coding for NAC α , and two NAC β genes together with other seven randomly-selected genes, namely peroxidase superfamily protein (At4g36430), toll-interleukin-resistance (TIR) domain family protein (At2g20142), peroxidase 71 (At5g64120), trypsin inhibitor protein 1 (At2g43510), GDSL-motif esterase/acyltransferase/lipase (At1g20120), phytoalexin deficient 4 (At3g52430), and PAR1 protein (At5g52390). The cT values were extracted from RT-qPCR experiment and projected in dot plot against log₂ scaled FPKM values in Microsoft Excel and correlation coefficient $R^2 = 0,7842$ was calculated (fig. 23). The linear regression trendline was added to the plot and according to the R^2 coefficient and trend visualization, the RNAseq data were successfully validated by RT-qPCR.

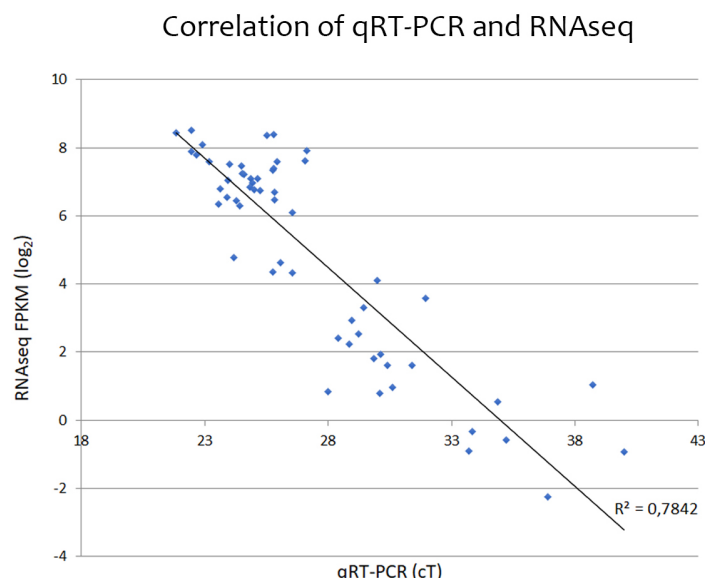


Figure 23: Linear regression of log₂FPKM values gained from RNA-seq data and cT values from RT-qPCR for each genotype for twelve DE genes in *nacβ1 nacβ2* (At1g17880, At1g73230, At2g20142, At5g64120, At2g43510, At3g12580, At5g52390, At3g12390, At3g49470, At5g13850, At4g10480, At1g33040) with correlation coefficient $R^2 = 0.7842$.

Discussion

The formation of NAC complex in plants

In plants, number of genes encoding NAC subunits varies between the species. The genome of our model plant *A. thaliana* codes for five genes of NAC α subunits and two genes of NAC β subunits. The goal of these experiments was to establish whether all subunits are capable of dimer formation and whether there are any binding preferences between them as was observed in yeasts (Ott *et al.*, 2015). This question was addressed by two methods studying protein-protein interactions (namely Y2H system and BiFC).

In Y2H system, the consistent results supported with credible controls were obtained. Heterodimer formation was observed in 10 out of 20 pairwise combinations, showing heterodimer formation and interaction preferences between individual subunits. Besides, no homodimer formation between any two NAC subunits was observed. In BiFC, the results were also consistent between the two replicas, supported with RFP and YFP signal colocalization and a negative result of non-interacting NAC β 1 and bzip34 pair. However, in BiFC, there were not observed any apparent interaction preferences, thus resulting in formation of all heterodimers. The interactions were also formed in selected homodimer pairs but showed a different localisation, as discussed in more detail later. However, before setting any conclusion, limitations of each method have to be taken into account, since both false positive and false negative results can be acquired by either of the methods.

In Y2H system, the interactions take place in yeast nucleus and each partner is fused with yeast reporter protein. This may cause steric hindrance of interaction sites on the tested partners and thus provide false negative results (Brückner *et al.*, 2009). In our experimental setting, we tried to minimize this phenomenon by testing the interactions in cross-wise manner in both prey-bait and bait-prey combinations. As expected from the reason mentioned above, the results varied between the two constellations. With NAC α s as preys, all NAC α s showed interaction with at least one of the NAC β s, whereas in case of NAC α s in the bait position, only NAC α 2 interacted with both NAC β s. This could be caused by the mentioned steric hindrance of NAC's interaction site. Why then does NAC α 2 stand out? One of possible explanations is that NAC α 2 differs in protein sequence from the other

NAC α s. The alignment of five protein sequences of NAC α showed nearly identical sequences in NAC domain sequence, but more differences were found in the N-terminal sequence. When visualized on phylogenetic tree based on protein sequence similarity, the NAC α s were separated into two clusters. NAC α 4 and NAC α 5 showed higher similarity to each other, which could explain why they interacted only with NAC β 2, proposing their potential functional specialisation. However, the relation between NAC α 1, NAC α 3 and NAC α 2 cannot be distinguished according to this analysis. Although they were still highly similar, there were apparent differences between each subunit on the level of protein sequence. If we look back to commercially available controls used in Y2H, the point mutation caused a change from a strong interaction (K2 - Krev1 and RalGDS-wt) to a weaker one (K3 - Krev1 and RalGDS-m1), and again another point mutation from a weak interaction to no interaction at all (K4 - Krev1 and RalGDS-m2). NAC heterodimers showed interaction only on 3AT plates and upon x-gal assay. On the contrary, no interaction was observed on SC-Leu-Trp-Ura and 3FoA-containing plates, indicating weaker interaction between NAC subunits. Hence, it may be possible that even the slight difference in NAC α 2 sequence and consequently its structure, ceased its interaction with the NAC β .

Although NAC domain was proposed to be responsible for NAC dimerization in *Archea* and human (Liu *et al.*, 2010; Spreter *et al.*, 2005), there was no direct evidence for plant NAC heterodimer binding site. Likewise, the interaction site hindrance could be the cause for ceased homodimer formation. Another important limitation of Y2H that could cause false negative results is the lack of modifying enzymes and other factors normally present in the natural environment of the interacting protein. On the other hand, the unnatural environment may result also in false positive results, due to the same reasons or due to overexpression of interacting partners.

In BiFC, the proteins are transiently expressed in *N. bentamiana* leaves and can be localised into various compartments. Heterodimer formation was observed between all pairs present in cytosol and partially in the nucleus. Previously, heterodimer formation was proposed to be the most abundant variation of NAC complexes with cytosolic localisation (Beatrix *et al.*, 2000). However, the authors do not exclude a potential lower portion of NAC to be present in nucleus due to

NACB conserved nuclear localisation signal. What needs to be considered when evaluating BiFC results is the overexpression of interacting proteins under 35S promoter. Therefore, overexpression of NAC heterodimer-forming subunits could lead to shift of excessive NACs to the nucleus since NAC heterodimers work in 1:1 stoichiometry with ribosomes. NAC α is in this case probably dragged to nucleus after heterodimer formation by the NLS in NACB. In case of homodimers, another fact needs to be taken into consideration. NAC heterodimer was proposed to be the main complex, yet in the character of NAC α subunits crystal structure, homodimers could still be formed between the overrepresented subunits. In this case, observed cytosolic NAC α homodimer formation could be an artefact caused by the overexpression. The cytosolic localisation was in accordance with previous GFP localisation of NACs under 35S, which showed to be only cytosolic (Fíla et al., unpublished data). Whereas GFP-fused NACBs were localised into both nucleus and cytoplasm under both 35S and its native promoters (Yang *et al.*, 2018) (Fíla, Klodová, Šesták, Honys, manuscript in preparation). In BiFC, NACB homodimers were observed in nucleus, which could be due to their proposed function as transcription regulators in plants. Also, localisation in small moving vesicular structures was observed. In the current stage of knowledge, it is hard to conclude their origin and possibly colocalization with known markers will have to be performed. Nonetheless, it could be possible, that similar signal is masked by strong cytosolic signal in the NAC heterodimer localisation and these vesical-like structures can represent natural storage bodies for NACs in plants.

Taken all interaction results together, the heterodimer formation between *A. thaliana* NAC subunits was observed. Furthermore, their localisation in cytosol was confirmed. As for homodimer formation, discordance between the two methods could be explained based on experimental artefacts causing false positive or false negative results in either of the methods. Therefore, before setting final conclusions about the composition of NAC complexes formed, the third method based on Förster resonance energy transfer (FRET) will be performed.

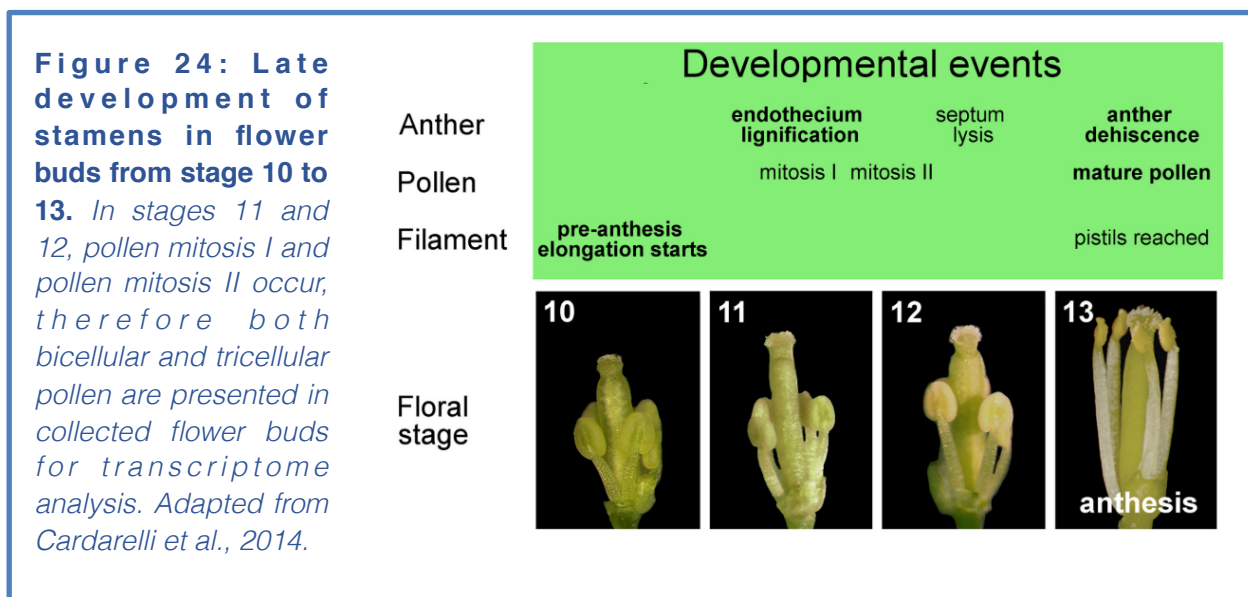
Analyses of nac β 1 nac β 2 flower bud transcriptome

NacB1 nacB2 double mutant of *A. thaliana* exhibited quite a strong phenotype for example in lower rate of pollen germination and ovule targeting capacity. Another aberration was observed in numbers of flower organs and silique

length. Thus, flower buds were selected as a representative tissue to cover both gametophyte and sporophyte tissues. To investigate the molecular mechanisms underlying these processes, RNAseq transcriptomic analyses of flower buds were carried out. Transcriptomic profile of the double homozygous mutant was compared with Col-0 WT flower bud transcriptome resulting in the list of significantly differentially expressed (DE) genes with 363 upregulated and 1602 downregulated genes. The majority of downregulated genes can be explained by the potential NACB role as transcription activator. In the RNA seq data, it was also proved that *NACB1* was a total knock-out, whereas the expression on *NACB2* was only lowered exhibiting in the *nacB1 nacB2* mutant about half of the WT expression rate. The results also did not show any differences in NAC α s expression in the mutant, implying no mutual regulation between the NAC α and NAC β subunits on the transcriptional level. The NAC single mutants were also included in the analysis, yet as expected from the phenotype-less mutants, much lower number of genes (particularly 162 and 143 genes) was differentially expressed. Such a trend implies the functional redundancy between the two β subunits. Therefore, the subsequent analyses were performed on the data acquired from the double mutant. According to the GO term enrichment analyses, two main groups emerged. The first group was represented by stress connected responses and the second one was connected to pollen development and pollen tube growth.

The silencing of *NACB* in plants usually led to lower tolerance to abiotic and biotic stresses. Similar phenomenon was observed also in our lab, when *nacB1 nacB2* showed lower germination rate and slower growth when compared to WT under salt and osmotic stress (Šesták, unpublished data). Furthermore, pollen development is accompanied with tissue dehydration comparable to drought stress conditions (Firon *et al.*, 2012). However, in the mutant, there were downregulated 18 genes encoding LEA proteins (which imply drought tolerance). On the other hand, there were notably upregulated several chaperones. For instance HSP101 (AT1G74310), HSP70 (AT3G12580), BiP2 (AT1G09080), HSP90.1 (AT5G52640), HSP70T-2 (AT2G32120), 3 small heat shock proteins (sHSP) (HSP17.4 AT3G46230, HSP17.6A AT5G12030, HSP18.2 AT5G59720), 9 HSP20-like family chaperones (AT1G53540, ATHSP22.0 AT4G10250, AT2G29500, AT5G51440, AT1G59860, AT5G37670, AT1G07400, AT1G54050, AT4G21870) and 2 heat stress factors (HSFA2

AT2G26150, HSF7A AT3G51910). HSP40 forms a dimer with HSP70 to promote protein binding, and together they play roles in stress tolerance and in solubilizing protein aggregates. BiP3 is a HSP70 chaperone expressed exclusively under stress conditions in the endoplasmic reticulum together with BiP1 and BiP2. Decreased expression of these chaperones was reported to correlate with decrease in pollen tube growth (Maruyama *et al.*, 2014). A similar function is shared by sHSP, the most abundant plant chaperone family. Apart from enhancing plant immunity and responding to heat stress, they were found to play their role in solubilization of protein aggregates. They were usually less abundant proteins and with temporally and/or spatially specific expression during the plant development. They were reported to regulate embryonic development or seed maturation. The upregulation of other chaperones in *nacB1 nacB2* and downregulation of stress response genes could be explained based on previous data acquired in yeast. The absence or lower abundance of NAC heterodimer could be mimicked by other chaperone systems.



The regulations of the genes playing role in pollen development was supported by the observed phenotype, since the mutant exhibited lower rate of pollen germination *in vitro*, slower pollen tube growth and a lower fertilization rate. 91 DEG genes (87 downregulated, 4 upregulated) were connected to male gametophyte development in different stages from sperm cell differentiation, through pollen tube development to pollen tube growth regulation. The effects in various parts of male gametophyte development originate probably from the

characteristics of flower bud tissues. The collected flower buds included flowers up to stage 12. During stages 10 to 12, pollen mitosis I and pollen mitosis II occur, meaning that pollen present inside the collected flower buds was probably a mixture of bicellular and tricellular pollen (fig. 24). The presence of pollen tube regulatory proteins can be explained by expression of their mRNAs earlier in the male gametophyte development and their storage during pollen development in the translationally-inactive complexes. This phenomenon was previously observed in other plant species such as tobacco (Honys *et al.*, 2009) or maize (Stinson *et al.*, 1987), however there is no experimental proof for such storage bodies in *A. thaliana*. Later, during the rapid pollen germination and pollen tube growth, the massive translation according to the stored mRNAs is performed (Honys *et al.*, 2009). “Male gamete development” GO group consisted of 13 genes (DMP9 AT5G39650, PCR11 AT1G68610, DAU1 AT5G02390, DAZ1 AT2G17180, DAZ2 AT4G35280, DAZ3 AT4G35700, TIP5;1 AT3G47440, DAA1 AT1G64110, DAN1 AT3G04620, AT3G62230, MGH3 AT1G19890, OPT8 AT5G53520, MPKKK20 AT3G50310), all of which were reported to be DUO1 (AT3G60460) targets according to the TAIR database (<https://www.arabidopsis.org>). DUO1 was also downregulated in the double mutant and is a MYB transcription factor responsible for sperm cell production. Specifically, it is responsible for pollen mitosis II, i.e. division of the germ cell into two sperm cells by regulating the accumulation of the mitotic cyclin CYCB1 in G2 phase (Brownfield, 2009a). As a transcription factor, DUO1 activates several genes that were discovered to be connected with male germline development (Borg *et al.*, 2011). Among the downregulated DUO1-activated genes in *nacB1 nacB2*, there was DMP9/DAU2 (AT5G39650) protein responsible for double fertilization, mutation of which led to seed abortion (Takahashi *et al.*, 2018). Three DUO1-activated zinc-finger transcription factors DAZ1, DAZ2, DAZ3 were upregulated in *nacB1 nacB2*. DAZ1/DAZ2 complex promotes transition from G2 to M phase leading to germ cell division by repression of the B1-type cyclin inhibitor (Borg *et al.*, 2014). The other DUO1-regulated genes were for instance TIP5;1, which codes for a sperm cell-specific vacuolar aquaporin important for pollen tube growth (Wudick *et al.*, 2014), and MGH3, which represents a male gametophyte-specific histone H3 gene (Okada *et al.*, 2005). Apart from DUO1-activated genes, there were four agamous-like MADS box proteins, which were down-regulated in the *nacB1 nacB2* mutant -

AGL104 (AT1G22130), AGL66 (AT1G77980), AGL67 (AT1G77950), and AGL94 (AT1G69540). MADS box are transcription factors connected with various development regulations, and agamous-like proteins form heterodimers when active. The double mutant of AGL66 and ALG104 showed a reduced pollen viability, reduced fertility, delayed pollen grain germination, and aberrant pollen tube growth (Adamczyk and Fernandez, 2009). The other downregulated genes were for instance RALF4 and RALF19, peptide ligands of BUPS1 and BUPS2 receptors. They are responsible for pollen tube integrity, they are likely competitively replaced by ovule specific RALF34, which promotes PT rupture and sperm cell release (Ge *et al.*, 2017). Several other genes connected to pollen tube growth were present. For instance, two pectinesterase inhibitors (PMEI1 AT1G48020, PMEI2 AT3G17220), and two pectinesterases (PPME1 AT1G69940, PME5 AT2G47040). Pectinesterases and pectinesterase inhibitors are important for cell wall maintenance, and specifically pollen tube cell wall rigidity and dynamics (Röckel *et al.*, 2008). Then, there was a Rab GTPase gene RABA4D responsible for vesicular trafficking in pollen tube. Mutants in these genes showed a slower rate of pollen tube growth as well as a reduced guidance capacity (Szumlanski and Nielsen, 2009). Last but not least, ANN5 is a protein highly expressed in pollen with calcium- and lipid-binding ability. Its knock-outs showed higher lethality rate, smaller pollen grains and delayed pollen tube growth (Lichocka *et al.*, 2018). Taken together, these 91 DEGs could be responsible for the observed phenotype since they show an important role in male gametophyte development.

To conclude above research with *nacB1 nacB2* mutant phenotype in consideration, NAC is probably included in regulation of various male germ-line development genes with different molecular functions. The downregulation of genes responsible for pollen tube growth and guidance, such as RALF4 and RALF19 or ANN5 could result in the observed *nacB1 nacB2* phenotype - particularly lower rate of pollen germination, slower pollen tube growth and worse targeting efficiency of pollen tubes. However, the transcriptomic results indicate possible aberration in earlier development, namely sperm cell differentiation, but no pollen nucleus phenotype (Reňák *et al.*, 2014) was observed. There could be two alternative explanations for such an observation. Either the downregulation of the responsible genes, such as DUO1, was only partial with no direct phenotypical

effect, or alternatively, the aberration resulted in quantitative effect rather than the qualitative one. It is possible that downregulation of genes responsible for regulation of such basal steps of pollen development resulted in notably lower pollen production. The possible connection between the stress and development groups can be explained by excessive protein aggregation and lower ability to resist stress such as desiccation during pollen development. Consequently, these issues can have negative effect on plant reproduction (Raja *et al.*, 2019).

The aberration of sepals and petals number in *nacB1 nacB2* could be much harder to be explained by the transcriptomics data. There are two genes from Clavata 3/ERS Related gene family - downregulated CLE19 (AT3G24225) and upregulated CLE44 (AT4G13195). CLE genes encode signal peptides with conserved 14-amino acid CLE domain and work probably as morphogenetic factors in multiple tissues. Some CLE peptides showed regulation effect on both shoot and root meristem, several of them were functionally similar to CLE3 (Yamaguchi *et al.*, 2017). CLE44 was reported to play its role in vascular development (Yamaguchi *et al.*, 2017) and CLE19 in endosperm and embryo development (Xu *et al.*, 2015), but whether they play particular role in the size regulation of shoot meristem as CLE3 remains unclear.

Overall, the knock-down of NACB subunits in *A. thaliana* led in general to upregulation of other chaperones and downregulation of genes involved in stress responses and male germ-line development. The lower abundance of NAC heterodimer could be mimicked by other chaperones as reported in yeast, and the NACB subunits by themselves could work as transcription activators of genes responsible of male gametophyte development, pollen tube growth, fertilization and probably other genes connected with reproduction. However, to elucidate these hypotheses, it will be important to perform further experiments.

Conclusion

The first and the second objective of this thesis were to verify NAC complex formation in *A. thaliana* and uncover potential binding preferences between the paralogues coding for the two subunits. Two methods were used to address these questions - Y2H and BiFC. According to these methods, NAC heterodimer formation between *A. thaliana* NAC subunits was observed. However, in case of binding preferences between various NAC subunits, the methods did not show consistent data so in order to elucidate any interaction preferences and homodimer formation, another protein-protein interaction method will have to be added.

In the third objective, the goal was to analyse flower bud transcriptome of the previously obtained *nacB1 nacB2* double homozygous mutant, which possessed quite a strong phenotype (mainly exhibited as deviations in flower organ numbers, slow growth and lower targeting efficiency of pollen tube, reduced seed set and lower chlorophyll content). The analyses resulted in 1965 DEGs and two important gene groups emerged. First, 87 down-regulated genes connected to male germ-line development, and specifically connected to sperm cell differentiation and pollen tube growth, were discovered. This group consisted of genes coding proteins with variable molecular mechanisms. For example pollen specific transcription regulator DUO1 and 13 of its effectors or RALF4 and RALF19, peptide ligands important for pollen tube integrity, were presented in the list. However, many of these genes showed a defective phenotype like *nacB1 nacB2* upon silencing. It may be thus possible, that NACB subunit played a role in transcriptional regulation of these genes. Notably, Moreover, 26 heat shock chaperones and 2 heat shock factors were upregulated in the *nacB1 nacB2* mutant possibly enabling to cover the NAC heterodimer absence. This observation indicated the NAC role in plant chaperone system. Finally, several stress-connected gene families were included in the list. As previously reported in plants, these genes could be influenced by NACB transcription regulation.

Citations

- Adamczyk, B.J. and Fernandez, D.E. (2009)** MIKC* MADS Domain Heterodimers Are Required for Pollen Maturation and Tube Growth in Arabidopsis. *Plant Physiol.*, **149**, 1713-1723.
- Aida, M., Ishida, T., Fukaki, H., Fujisawa, H. and Tasaka, M. (1997)** Genes Involved in Organ Separation in Arabidopsis: An Analysis of the cup-shaped cotyledon Mutant. , **9**, 841-857.
- Alamo, M. del, Hogan, D.J., Pechmann, S., Albanese, V., Brown, P.O. and Frydman, J. (2011)** Defining the specificity of cotranslationally acting chaperones by systematic analysis of mRNAs associated with ribosome-nascent chain complexes. *PLoS Biol.*, **9**.
- Albanèse, V., Yam, A.Y.W., Baughman, J., Parnot, C. and Frydman, J. (2006)** Systems analyses reveal two chaperone networks with distinct functions in eukaryotic cells. *Cell*, **124**, 75-88.
- Beatrix, B., Sakai, H. and Wiedmann, M. (2000)** The α and β subunit of the nascent polypeptide-associated complex have distinct functions. *J. Biol. Chem.*, **275**, 37838-37845.
- Bloss, T.A., Witze, E.S. and Rothman, J.H. (2003)** Suppression of CED-3-independent apoptosis by mitochondrial BNAC in *Caenorhabditis elegans*. *Nature*, **424**, 1066-1071.
- Borg, M., Brownfield, L., Khatab, H., Sidorova, A., Lingaya, M. and Twell, D. (2011)** The R2R3 MYB Transcription Factor DUO1 Activates a Male Germline-Specific Regulon Essential for Sperm Cell Differentiation in Arabidopsis . *Plant Cell*, **23**, 534-549.
- Borg, M., Rutley, N., Kagale, S., et al. (2014)** An EAR-Dependent Regulatory Module Promotes Male Germ Cell Division and Sperm Fertility in Arabidopsis. *Plant Cell*, **26**, 2098-2113.
- Brückner, A., Polge, C., Lentze, N., Auerbach, D. and Schlattner, U. (2009)** Yeast two-hybrid, a powerful tool for systems biology. *Int. J. Mol. Sci.*, **10**, 2763-2788.
- Cardarelli, M. and Cecchetti, V. (2014)** Auxin polar transport in stamen formation and development: how many actors? *Front. Plant Sci.*, **5**, 1-13.
- Creagh, E.M., Brumatti, G., Sheridan, C., Duriez, P.J., Taylor, R.C., Cullen, S.P.,**

- Adrain, C. and Martin, S.J.** (2009) Bicaudal Is a Conserved Substrate for Drosophila and Mammalian Caspases and Is Essential for Cell Survival. , **4**.
- Deng, J.M. and Behringer, R.R.** (1995) An insertional mutation in the BTF3 transcription factor gene leads to an early postimplantation lethality in mice. *Transgenic Res.*, **4**, 264-269.
- Deuerling, E., Schulze-Specking, A., Tomoyasu, T., Mogk, A. and Bukau, B.** (1999) Trigger factor and DnaK cooperate in folding of newly synthesized proteins. *Nature*, **400**, 693-696.
- Deuerling, E., Gamerdinger, M. and Kreft, S.G.** (2019) Chaperone Interactions at the Ribosome. *Cold Spring Harb. Perspect. Biol.*
- Dobin, A., Davis, C.A., Schlesinger, F., Drenkow, J., Zaleski, C., Jha, S., Batut, P., Chaisson, M. and Gingeras, T.R.** (2013) STAR: Ultrafast universal RNA-seq aligner. *Bioinformatics*, **29**, 15-21.
- Duttler, S., Pechmann, S. and Frydman, J.** (2013) Principles of cotranslational ubiquitination and quality control at the ribosome. *Mol. Cell*, **50**, 379-393.
- Fíla, J., Radau, S., Matros, A., et al.** (2016) Phosphoproteomics Profiling of Tobacco Mature Pollen and Pollen Activated in vitro . *Mol. Cell. Proteomics*, **15**, 1338-1350.
- Firon, N., Nepi, M. and Pacini, E.** (2012) Water status and associated processes mark critical stages in pollen development and functioning. *Ann. Bot.*, **109(7)**, 1201-1213.
- Freire, M.A.** (2005) Translation initiation factor (iso) 4E interacts with BTF3, the β subunit of the nascent polypeptide-associated complex. *Gene*, **345**, 271-277.
- Gamerdinger, MA, H., T, F. and E, D.** (2015) The principle of antagonism ensures protein targeting specificity at the endoplasmic reticulum. *Science (80-.)*, **348**, 201-7.
- Ge, Z., Bergonci, T., Zhao, Y., et al.** (2017) Arabidopsis pollen tube integrity and sperm release are regulated by RALF-mediated signaling. *Science*, **358**, 1596-1600.
- Gehl, C., Waadt, R., Kudla, J., Mendel, R.R. and Hänsch, R.** (2009) New GATEWAY vectors for high throughput analyses of protein-protein interactions by bimolecular fluorescence complementation. *Mol. Plant*, **2**, 1051-1058.
- Genevaux, P., Keppel, F., Schwager, F., Langendijk-Genevaux, P.S., Hartl, F.U.**

- and Georgopoulos, C. (2004) In vivo analysis of the overlapping functions of DnaK and trigger factor. *EMBO Rep.*, **5**, 195-200.
- Hiraishi, H., Shimada, T., Ohtsu, I., Sato, T.A. and Takagi, H. (2009) The yeast ubiquitin ligase Rsp5 downregulates the alpha subunit of nascent polypeptide-associated complex Egd2 under stress conditions. *FEBS J.*, **276**, 5287-5297.
- Honys, D., Renak, D., Fecikova, J., Jedelsky, P.L., Nebesarova, J., Dobrev, P. and Capkova, V. (2009) Cytoskeleton-associated large RNP complexes in tobacco male gametophyte (EPPs) are associated with ribosomes and are involved in protein synthesis, processing, and localization. *J. Proteome Res.*, **8**, 2015-2031.
- Huh, S.U., Kim, K.J. and Paek, K.H. (2012) Capsicum annum basic transcription factor 3 (CaBtf3) regulates transcription of pathogenesis-related genes during hypersensitive response upon Tobacco mosaic virus infection. *Biochem. Biophys. Res. Commun.*, **417**, 910-917.
- Jaiswal, H., Conz, C., Otto, H., Wolfle, T., Fitzke, E., Mayer, M.P. and Rospert, S. (2011) The Chaperone Network Connected to Human Ribosome-Associated Complex. *Mol. Cell. Biol.*, **31**, 1160-1173.
- Jamil, M., Wang, W., Xu, M. and Tu, J. (2015) Exploring the roles of basal transcription factor 3 in eukaryotic growth and development. *Biotechnol. Genet. Eng. Rev.*, **31**, 21-45.
- Kang, G., Li, G., Ma, H., Wang, C. and Guo, T. (2013) Proteomic analysis on the leaves of TaBTF3 gene virus-induced silenced wheat plants may reveal its regulatory mechanism. *J. Proteomics*, **83**, 130-143.
- Kang, G., Ma, H., Liu, G., Han, Q., Li, C. and Guo, T. (2013) Silencing of TaBTF3 gene impairs tolerance to freezing and drought stresses in wheat. *Mol. Genet. Genomics*, **288**, 591-599.
- Karan, R. and Subudhi, P.K. (2012) Overexpression of a nascent polypeptide associated complex gene (SaβNAC) of *Spartina alterniflora* improves tolerance to salinity and drought in transgenic *Arabidopsis*. *Biochem. Biophys. Res. Commun.*, **424**, 747-752.
- Kogan, G.L. and Gvozdev, V.A. (2014) Multifunctional nascent polypeptide-associated complex (NAC). *Mol. Biol.*, **48**, 189-196.
- Koplin, A., Preissler, S., Llina, Y., Koch, M., Scior, A., Erhardt, M. and Deuerling,

- E. (2010) A dual function for chaperones SSB-RAC and the NAC nascent polypeptide-associated complex on ribosomes. *J. Cell Biol.*, **189**, 57-68.
- Krishnakumar, V., Hanlon, M.R., Contrino, S., et al. (2015) Araport: The Arabidopsis Information Portal. *Nucleic Acids Res.*, **43**, D1003-D1009.
- Lesnik, C., Cohen, Y., Atir-Lande, A., Schuldiner, M. and Arava, Y. (2014) OM14 is a mitochondrial receptor for cytosolic ribosomes that supports co-translational import into mitochondria. *Nat. Commun.*, **5**, 1-10.
- Li, B. and Dewey, C.N. (2014) RSEM: Accurate transcript quantification from RNA-seq data with or without a reference genome. *Bioinforma. Impact Accurate Quantif. Proteomic Genet. Anal. Res.*, **12**, 41-74.
- Liao, Y., Smyth, G.K. and Shi, W. (2013) The Subread aligner: Fast, accurate and scalable read mapping by seed-and-vote. *Nucleic Acids Res.*, **41**.
- Lichocka, M., Rymaszewski, W., Morgiewicz, K., et al. (2018) Nucleus- and plastid-targeted annexin 5 promotes reproductive development in Arabidopsis and is essential for pollen and embryo formation. *BMC Plant Biol.*, **18**, 1-15.
- Liu, Y., Hu, Y., Li, X., Niu, L. and Teng, M. (2010) The crystal structure of the human nascent polypeptide-associated complex domain reveals a nucleic acid-binding region on the NACA subunit. *Biochemistry*, **49**, 2890-2896.
- Lopez, S., Stuhl, L., Fichelson, S., et al. (2005) NACA is a positive regulator of human erythroid-cell differentiation. *J. Cell Sci.*, **118**, 1595-605.
- Ma, H.-Z., Liu, G.-Q., Li, C.-W., Kang, G.-Z. and Guo, T.-C. (2012) *Identification of the TaBTF3 gene in wheat (Triticum aestivum L.) and the effect of its silencing on wheat chloroplast, mitochondria and mesophyll cell development.* *Biochem. Biophys. Res. Commun*, **426**, 608-614.
- Macario, A.J. and Conway De Macario, E. (2001) The molecular chaperone system and other anti-stress mechanisms in archaea. *Front. Biosci.*, **6**, D262-83.
- Makarova, K.S., Aravind, L., Galperin, M.Y., Grishin, N. V, Tatusov, R.L., Wolf, Y.I. and Koonin, E. V (1999) Comparative Genomics of the Archaea (Euryarchaeota): Evolution of Conserved Protein Families , the Stable Core , and the Variable Shell. *Genome Res.*, **9**, 608-628.
- Markesich, D.C., Gajewski, K.M., Nazimiec, M.E. and Beckingham, K. (2000) bicaudal encodes the Drosophila beta NAC homolog, a component of the ribosomal translational machinery*. *Development*, **127**, 559-72.

- Martin, M. (2011) Cutadapt removes adapter sequences from high-throughput sequencing reads. *EMBnet. J.*, **17**, 10-12.
- Maruyama, D., Sugiyama, T., Endo, T. and Nishikawa, S.I. (2014) Multiple BiP genes of *Arabidopsis thaliana* are required for male gametogenesis and pollen competitiveness. *Plant Cell Physiol.*, **55**, 801-810.
- Nyathi, Y. and Pool, M.R. (2015) Analysis of the interplay of protein biogenesis factors at the ribosome exit site reveals new role for NAC. *J. Cell Biol.*, **210**, 287-301.
- Okada, T., Endo, M., Singh, M.B. and Bhalla, P.L. (2005) Analysis of the histone H3 gene family in *Arabidopsis* and identification of the male-gamete-specific variant AtMGH3. *Plant J.*, **44**, 557-568.
- Ott, A.K., Locher, L., Koch, M. and Deuerling, E. (2015) Functional dissection of the nascent polypeptide-associated complex in *Saccharomyces cerevisiae*. *PLoS One*, **10**, 1-19.
- Patzelt, H., Kramer, G., Rauch, T., Schonfeld, H.-J., Bukau, B. and Deuerling, E. (2002) Three-state equilibrium of *Escherichia coli* trigger factor. *Biol. Chem.*, **383**, 1611-1619.
- Pech, M., Spreter, T., Beckmann, R. and Beatrix, B. (2010) Dual binding mode of the nascent polypeptide-associated complex reveals a novel universal adapter site on the ribosome. *J. Biol. Chem.*, **285**, 19679-19687.
- Peng, X., Wang, Q., Liu, H. and Shen, S. (2017) Phylogenetic and functional analysis of the basic transcription factor gene BTF3 from *Jatropha curcas*. *Plant Growth Regul.*, **82**, 247-257.
- Ponce-Rojas, J.C., Avendaño-Monsalve, M.C., Yañez-Falcón, A.R., Jaimes-Miranda, F., Garay, E., Torres-Quiroz, F., DeLuna, A. and Funes, S. (2017) $\alpha\beta$ -NAC cooperates with Sam37 to mediate early stages of mitochondrial protein import. *FEBS J.*, **284**, 814-830.
- Preissler, S. and Deuerling, E. (2012) Ribosome-associated chaperones as key players in proteostasis. *Trends Biochem. Sci.*, **37**, 274-283.
- Pruthvi, V., Rama, N., Parvathi, M.S. and Nataraja, K.N. (2017) Transgenic tobacco plants constitutively expressing peanut BTF3 exhibit increased growth and tolerance to abiotic stresses. *Plant Biol.*, **19**, 377-385.
- Raja, M.M., Vijayalakshmi, G., Naik, M.L., Basha, P.O., Sergeant, K., Hausman,

- J.F. and Khan, P.S.S.V. (2019) Pollen development and function under heat stress: from effects to responses. *Acta Physiol. Plant.*, **41**, 1967-1976.
- Reimann, B., Bradsher, J., Franke, J., Hartmann, E., Wiedmann, M., Prehn, S. and Wiedmann, B. (1999) Initial characterization of the nascent polypeptide-associated complex in yeast. *Yeast*, **15**, 397-407.
- Reňák, D., Gibalová, A., Šolcová, K. and Honys, D. (2014) A new link between stress response and nucleolar function during pollen development in *Arabidopsis* mediated by AtREN1 protein. *Plant, Cell Environ.*, **37**, 670-683.
- Röckel, N., Wolf, S., Kost, B., Rausch, T. and Greiner, S. (2008) Elaborate spatial patterning of cell-wall PME and PME1 at the pollen tube tip involves PME1 endocytosis, and reflects the distribution of esterified and de-esterified pectins. *Plant J.*, **53**, 133-143.
- Rospert, S., Dubaquié, Y. and Gautschi, M. (2002) Nascent-polypeptide-associated complex. *Cell. Mol. Life Sci.*, **59**, 1632-1639.
- Schindelin, J., Arganda-Carreras, I., Frise, E., et al. (2012) Fiji: an open-source platform for biological-image analysis. *Nat. Methods*, **9**, 676.
- Shi, X., Parthun, M.R. and Jaehning, J.A. (1995) The yeast EGD2 gene encodes a homologue of the alpha NAC subunit of the human nascent-polypeptide-associated complex. *Gene*, **165**, 199-202.
- Spreter, T., Pech, M. and Beatrix, B. (2005) The crystal structure of archaeal nascent polypeptide-associated complex (NAC) reveals a unique fold and the presence of a ubiquitin-associated domain. *J. Biol. Chem.*, **280**, 15849-15854.
- Stinson, J.R., Eisenberg, A.J., Willing, R.P., Pe, M.E., Hanson, D.D. and Mascarenhas, J.P. (1987) Genes Expressed in the Male Gametophyte of Flowering Plants and Their Isolation. *Plant Physiol.*, **83**, 442-447.
- Szumanski, A.L. and Nielsen, E. (2009) The Rab GTPase RabA4d Regulates Pollen Tube Tip Growth in *Arabidopsis thaliana*. *Plant Cell*, **21**, 526-544.
- Takahashi, T., Mori, T., Ueda, K., Yamada, L., Nagahara, S., Higashiyama, T., Sawada, H. and Igawa, T. (2018) The male gamete membrane protein DMP9/DAU2 is required for double fertilization in flowering plants. *Development*, **145**, dev170076.
- Teter, S.A., Houry, W.A., Ang, D., Tradler, T., Rockabrand, D., Fischer, G., Blum, P., Georgopoulos, C. and Hartl, F.U. (1999) Polypeptide flux through bacterial

- Hsp70: DnaK cooperates with trigger factor in chaperoning nascent chains. *Cell*, **97**, 755-765.
- Thimm, O., Bläsing, O., Gibon, Y., et al. (2004) MAPMAN: A user-driven tool to display genomics data sets onto diagrams of metabolic pathways and other biological processes. *Plant J.*, **37**, 914-939.
- Vorderwülbecke, S., Kramer, G., Merz, F., Kurz, T.A., Rauch, T., Zachmann-Brand, B., Bukau, B. and Deuerling, E. (2004) Low temperature or GroEL/ES overproduction permits growth of *Escherichia coli* cells lacking trigger factor and DnaK. *FEBS Lett.*, **559**, 181-187.
- Walsh, P., George, R., Lithgow, T. and Beddoe, T. (2002) The nascent polypeptide-associated complex (NAC) promotes interaction of ribosomes with the mitochondrial surface in vivo. *FEBS Lett.*, **516**, 213-6.
- Wang, Lanfeng, Zhang, W., Wang, Lu, Zhang, X.C., Li, X. and Rao, Z. (2010) Crystal structures of NAC domains of human nascent polypeptide-associated complex (NAC) and its α NAC subunit. *Protein Cell*, **1**, 406-416.
- Wang, W., Xu, M., Wang, Y. and Jamil, M. (2014) Basal transcription factor 3 plays an important role in seed germination and seedling growth of rice. *Biomed Res. Int.*, **2014**.
- Wang, Y., Zhang, X., Lu, S., et al. (2012) Inhibition of a basal transcription factor 3-like gene Osj10gBTF3 in rice results in significant plant miniaturization and typical pollen abortion. *Plant Cell Physiol.*, **53**, 2073-2089.
- Wegrzyn, R.D., Hofmann, D., Merz, F., Nikolay, R., Rauch, T., Graf, C. and Deuerling, E. (2006) A conserved motif is prerequisite for the interaction of NAC with ribosomal protein L23 and nascent chains. *J. Biol. Chem.*, **281**, 2847-2857.
- Wiedmann, B., Sakai, H., Davis, T.A. and Wiedmann, M. (1994) A protein complex required for signal-sequence-specific sorting and translocation. *Nature*, **370**, 434-440.
- Wudick, M.M., Luu, D.-T., Tournaire-Roux, C., Sakamoto, W. and Maurel, C. (2014) Vegetative and Sperm Cell-Specific Aquaporins of Arabidopsis Highlight the Vacuolar Equipment of Pollen and Contribute to Plant Reproduction. *Plant Physiol.*, **164**, 1697-1706.
- Xu, T.T., Ren, S.C., Song, X.F. and Liu, C.M. (2015) CLE19 expressed in the

- embryo regulates both cotyledon establishment and endosperm development in Arabidopsis. *J. Exp. Bot.*, **66**, 5217-5227.
- Yamaguchi, Y.L., Ishida, T., Yoshimura, M., Imamura, Y., Shimaoka, C. and Sawa, S. (2017) A Collection of Mutants for CLE-Peptide-Encoding Genes in Arabidopsis Generated by CRISPR/Cas9-Mediated Gene Targeting. *Plant Cell Physiol.*, **58**, 1848-1856.
- Yang, K.S., Kim, H.S., Jin, U.H., Lee, S.S., Park, J.A., Lim, Y.P. and Pai, H.S. (2007) Silencing of NbBTF3 results in developmental defects and disturbed gene expression in chloroplasts and mitochondria of higher plants. *Planta*, **225**, 1459-1469.
- Yang, S., Song, C., Zhang, X., Jia, Y., Shi, Y., Ding, Y. and Gong, Z. (2018) OST1-mediated BTF3L phosphorylation positively regulates CBFs during plant cold responses. *EMBO J.*, **37**, e98228.
- Yotov, W. V. and St-Arnaud, R. (1996) Differential splicing-in of a proline-rich exon converts α NAC into a muscle-specific transcription factor. *Genes Dev.*, **10**, 1763-1772.
- Zheng, X.M., Moncollin, V., Egly, J.M. and Chambon, P. (1987) A general transcription factor forms a stable complex with RNA polymerase B (II). *Cell*, **50**, 361-368.
- Zimmermann, R., Möller, I., Jung, M., Beatrix, B., Levy, R., Kreibich, G., Wiedmann, M. and Luring, B. (1998) A general mechanism for regulation of access to the translocon: competition for a membrane attachment site on ribosomes. *Proc. Natl. Acad. Sci. U. S. A.*, **95**, 13425-13430.

Supplement

Supplement file 1: Table of 1965 statistically significant DEGs in *nacB1 nacB2* including gene IDs annotated with base mean (the average normalized read counts from all samples), log₂ scaled Fold Change (between the *nacB1 nacB2* and WT), lfcSE (standart error for log₂FoldChange estimate), Stat (Wald statistic - logFC divided by SE), p-value (Wald test p-value), Padj (Benjamini-Hochberg adjusted P-value) and also symbol and brief description added from Thalemine annotation website. Log fold change threshold set to 1.